Focused Ultrasound Mediated Blood-Brain Barrier Opening in Non-Human Primates: Safety, Efficacy and Drug Delivery

Matthew Downs

Submitted in partial fulfillment of the
requirements for the degree of
Doctor of Philosophy
in the Graduate School of Arts and Sciences

Columbia University

2015

Abstract

Focused Ultrasound Mediated Blood-Brain Barrier Opening in Non-Human Primates: Safety, Efficacy and Drug Delivery

Matthew Downs

The blood-brain barrier (BBB) is physiologically essential for brain homeostasis. While it protects the brain from noxious agents, it prevents almost all currently available drugs from crossing to the parenchyma. This greatly hinders drug delivery for the treatment of neurological diseases and disorders such as Parkinson's, Alzheimer's and Huntington's, as well as the development of drugs for the treatment of such diseases. Current drug delivery techniques to the brain are either invasive and target specific, or non-invasive with low special specificity. Neither group of techniques are optimal for long term treatment of patients with neurological diseases or disorders. Focused ultrasound coupled with intravenous administration of microbubbles (FUS) has been proven as an effective technique to selectively and noninvasively open the BBB in multiple *in vivo* models including non-human primates (NHP). Although this technique has promising potential for clinical outpatient procedures, as well as a powerful tool in the lab, the safety and potential neurological effects of this technique need to be further investigated. This thesis focuses on validating the safety and efficacy of using the FUS technique to open the BBB in NHP as well as the ability of the technique to facility drug delivery. First, a longitudinal study of repeatedly applying the FUS technique targeting the basal ganglia region in four NHP was conducted to determine any potential long-term adverse side effects over a duration of 4-20 months. The safety of the technique was evaluated using both MRI as well as behavioral testing. Results demonstrated that repeated application of the FUS technique to the basal ganglia in NHP did not generate permanent side effects, nor did it induce a permanent

opening of the BBB in the targeted region. The second study investigated the potential of the FUS technique as a method to deliver drugs, such as a low dose of haloperidol, to the basal ganglia in NHP and mice to elicit pharmacodynamical effects on responses to behavioral tasks. After opening the BBB in the basal ganglia of mice and NHP, a low dose of haloperidol was successfully delivered generating significant changes in their baseline motor responses to behavioral tasks. Domperidone was also successfully delivered to the caudate of NHP after opening the BBB and induced transient hemilateral neglect. In the final section of this thesis, the safety and efficacy of the FUS technique was evaluated in fully alert NHP. The FUS technique was successful in generating BBB opening volumes larger on average to that of the BBB opening volumes in anesthetized experiments. Safety results through MRI verification as well as behavioral testing during application of the technique demonstrated that the FUS technique did not generate adverse neurological effects. Conversely, the FUS technique was found to induce slight positive effects on the response of the NHP to the behavioral task. Collectively, the work presented in this thesis demonstrates the safety and effectiveness of the FUS technique to open the BBB and deliver neuroactive drugs in the NHP.

Table of Contents

Index of Figures v

Abbreviations viii

Acknowledgements x

Chapter 1: Introduction & Specific Aims

1.1 Introduction 1

1.2 Specific Aims 3

1.3 Longitudinal Study of the Effects from Focused Ultrasound Through the Microbubble-Mediated Blood-Brain Barrier Opening in the Non-Human Primate Brain (Specific Aim 1, Chapter 3) 4

1.4 Drug Delivery to the Basal Ganglia via Focused Ultrasound with Microbubbles Blood-Brain Barrier Opening in *in vivo* Subjects (Specific Aim 2, Chapter 4) 5

1.5 Safety and Efficacy of Blood-Brain Barrier Opening via Focused Ultrasound with Microbubbles in Alert Non-Human Primates (Specific Aim 3, Chapter 5) 6

Chapter 2: Background & Motivation

2.1 Blood-Brain Barrier 9

2.2 Current Blood-Brain Barrier Disruption and Drug Delivery Techniques 10

2.2.1 Drug Modifications 11

2.2.2 Invasive Techniques 12

2.2.3 Non-Invasive Techniques 13

2.3 Ultrasound 15

2.3.1 Focused Ultrasound with Microbubbles 16

2.3.2 Cellular Mechanisms of Blood-Brain Barrier Opening 17

2.3.3 Monitoring and Assessment of Blood-Brain Barrier Opening . . . 18

2.4 Drug Delivery via Focused Ultrasound with Microbubbles

2.4.1 Treatment of Neurological Diseases 20

2.4.2 Pharmacodynamical Behavior Modulation 20

2.5 Brain Regions for Targeted Drug Delivery

2.5.1 Basal Ganglia 21

2.5.2 Thalamus 22

2.6 Behavioral Tasks

2.6.1 Reward Magnitude Bias 23

2.6.2 Random Dot Motion 24

Chapter 3: Longitudinal Study of the Effects from Focused Ultrasound with Microbubble Mediated Blood-Brain Barrier Opening in the Non-Human Primate Brain

3.1 Abstract 25

3.2 Introduction and Study Design 26

3.3 Materials and Methods 28

3.4 Results 37

3.5 Discussion 55

3.6 Conclusions 62

3.7 Contributions 62

Chapter 4: Drug Delivery to the Basal Ganglia via Focused Ultrasound with Microbubble Blood-Brain Barrier Opening in *in vivo* Subjects

4.1 Abstract 64

4.2 Introduction and Study Design 65

4.3 Materials and Methods 68

4.4 Results

4.4.1 Low Dose Haloperidol in NHP 74

4.4.2 Low Dose Haloperidol in Mice 81

4.4.3 Domperidone in NHP 83

4.5 Discussion 85

4.6 Conclusions 89

4.7 Contributions 89

Chapter 5: Safety and Efficacy of Blood-Brain barrier Opening via Focused Ultrasound with Microbubbles in Alert Non-Human Primates

5.1 Abstract 91

5.2 Introduction and Study Design 92

5.3 Materials and Methods 94

5.4 Results 101

5.5 Discussion 113

5.6 Conclusions 115

5.7 Contributions 116

Chapter 6: Impact

6.1 Conclusions 117

6.2 Future Work 120

References 121

Appendix 1: List of Publications and Conference Presentations/Proceedings . . 136

Index of Figures

1. Specific Aims 4

2. The Blood-Brain Barrier 10

3. Microbubble-Focused Ultrasound Interactions 18

4. Passive Cavitation Detection 19

5. Targeted Brain Regions in the NHP 23

6. Blood-Brain Barrier Opening Post-Processing Pipeline 33

7. Random Dot Motion and Reward Magnitude Bias Task 34

8. Vital Monitoring 38

9. Contrast Enhanced Blood-Brain Barrier Opening 39

10. T2-weighted MRI and SWI scans of NHP N and A 40

11. Raw Reaction Time and Touch Error to Initial Cue (left column), and to the Correct Target (right column) 42

12. Average Reaction Time to Initial Cue (left column) and to the Correct Target (right column) 43

13. Average Touch Error to Initial Cue (left column), and to the Correct Target (right column) 45

14. Difference in Average Reaction Time between the Ipsilateral and Contralateral Hands as a Function of day Relative to the Day of the FUS Procedure. 46

15. Difference in Average Touch Error Between Ipsilateral and Contralateral Hands as a Function of Day Relative to the Day of the FUS Procedure. 48

16. Difference in Average Reaction Time Between Low and High Reward as a Function of Day Relative to the Day of the FUS. 49

17. Difference in Average Touch Error Between Low and High Reward as a Function of Day Relative to the Day of the FUS Procedure. 51

18. Naka-Rushton Model Fits of Accuracy Against Coherence for the RDM Task Completed by NHP N. 53

19. Raw Reaction Time Data for Alert Behavioral Testing for NHP A 54

20. Contrast Enhanced Blood Brain Barrier Opening for the Drug Study 74

21. T2-Weighted and SWI Scans for the Haloperidol Non-Human Primate Study. 75

22. Case of Hyperintense Voxels for the Haloperidol Non-Human Primate Study 76

23. Normalized Reaction Times to Cue and Target Stimuli Following Threshold Haloperidol Administration. 77

24. Naka-Rushton Model Fits of Accuracy to Coherence for the Random Dot Motion Task. 81

25. MRI Blood-Brain Barrier Opening and Safety Validation for the Mice Study. . 82

26. Distance Traveled During an Open Field Test 82

27. T2-Weighted and SWI Scans after Domperidone Administration with Blood-Brain Barrier Opening. 84

28. Alert Focused Ultrasound Behavioral Setup 97

29. Raw Reaction Time Data for Alert Behavioral Testing 99

30. EMG Recordings 103

31. MRI Safety Verification in Alert Non-Human Primates 105

32. Blood-Brain Barrier Opening Verification in Alert Non-Human Primates . . . 107

33. Alert vs Anesthetized Blood-Brain Barrier Volume 108

34. Cavitation Doses for Alert and Anesthetized Non-Human Primates 108

35. Behavioral Results after Focused Ultrasound Procedures in Alert Non-Human Primates. 111

Abbreviations

AAV:	Adeno-Associated Virus
AZ:	Alzheimer's disease
BBB:	Blood Brain Barrier
BET:	Brain Extraction Toolbox
CMT:	Carrier-Mediated Transport
DMSO:	Dimethyl Sulfoxide
EMG:	Electromyography
EMP:	Evoked Motor Potential
FUS:	Focused Ultrasound with microbubbles
ICV:	Intracerebroventricular
IM:	Intramuscular
IP:	Intra-peritoneal
IV:	Intravenous
MB:	Microbubble
MRI:	Magnetic Resonance Imaging
MW:	Molecular Weight
NHP:	Non-human Primate
PCD:	Passive Cavitation Detection
PD:	Parkinson's disease
PKC:	Protein Kinase C
PRF:	Pulse Repetition Frequency
RDM:	Random Dot Motion
RMB:	Reward Magnitude Bias
RMT:	Receptor-Mediated Transport

RT:	Reaction Time
SDS:	Sodium Dodecyl Sulfate
SWI:	Susceptibility Weighted Imaging
TE:	Touch Error
tFUS:	Transcranial Focused Ultrasound
TMS:	Transcranial Magnetic Stimulation

Acknowledgements

There have been many people who have assisted me through the journey of this PhD. Foremost, I'd like to thank Dr. Konofagou and Dr. Ferrera for providing not only guidance and assistance throughout my experiments, but also originally an opportunity to conduct research in their lab which I am forever grateful for.

My work here has been aided by numerous members from both labs. I'd specifically like to thank Dr. Teichert for acquainting me with the vast world of monkey behavioral experiments, and my right and left hands the last few years, Amanda and Marilena, for always assisting with experiments that typically ran late into the night

I'd like to thank the veterinary staff at NYSPI, Amy and Girma, for taking the time to teach me the fine art of lulling monkeys to sleep, and making sure they wake back up again.

A special thanks for people who kindled my passion for research. My parents always encouraged my curiosity from a young age, and have always supported my exploration in both the science and natural world. And Dr. Hess, who almost a decade ago gave me a project in his lab and started me down the road of academic research.

Last, I'd like to thank and recognize all the furry guys who made the rough days in lab bearable, N, O, Ob, A, Z, B, F, H, L, M, P, Ma, C, R, G, and T. All the bananas for you guys.

Chapter 1

Introduction & Specific Aims

1.1 Introduction

The blood-brain barrier (BBB) is a highly selective biological system facilitating both brain homeostasis and prevention of noxious or infectious agents reaching the brain parenchyma [1]. As with many efficient systems, there is a downside as the BBB prevents 99% of currently available small molecules (> 400 Da), and almost all large molecule drugs crossing into the brain [2]. This creates a difficult challenge for the clinical treatment of neurological and psychiatric diseases based on existing or pipeline drugs [3, 4]. Current techniques for drug delivery through the BBB such as intracranial injection are invasive and localized while others methods employing endogenous transporters are non-invasive with nonspecific delivery [5, 6, 7]. With an estimated 6.4% of the world's population expected to have a neurological disease or disorder by the end of 2015, there is a need for novel methods of treatment for diseases such as Alzheimer's, Parkinson's (PD) and Huntington's [8]. An optimal system for drug delivery through the BBB would be non-invasive, have high spatial specificity and be reproducible without any permanent long-term side effects.

Focused ultrasound coupled with intravenous (IV) administration of microbubbles (FUS) has been shown to be an effective method to open the BBB in multiple *in vivo* models for fourteen years [9, 10, 11, 12]. The FUS excites the circulating MB in the focal area of the transducer, resulting in the MB applying mechanical forces on the endothelial cells that form the BBB [13]. This technique is non-invasive and the opening of the BBB in the targeted region is reversible within hours to days tailored by the parameters employed [11, 14, 15]. Our group and others have shown the FUS technique to be successful at targeting and opening the BBB in specific brain regions of

anesthetized NHP [13, 15, 16]. The targeting of the brain structures can be achieved through either MRI guidance or stereotactical positioning [15, 16]. All *in vivo* applications of the FUS technique have been conducted with anesthetized animals [9, 10, 11, 12, 13, 14, 15, 16, 17, 18, 19]. There has been no study to date investigating the potential neurological effects of applying the FUS technique on fully alert subjects.

Although the FUS technique has been applied with multiple *in vivo* models, few studies have been conducted specifically investigating the safety of the technique on brain structure and function. One prior study investigated the safety of short-term repeated FUS BBB opening in the visual cortex of NHP and found minor damage with the parameters they used through T2-weighted MRI scans and from histological examination [16]. Aside from the short-term applications for treatment of tumors, the FUS technique in the clinic would be applied over multiple years. For treatment of neurological diseases such as PD and Alzheimer's disease, specific brain regions may need to be repeatedly targeted to facilitate drug delivery. A longitudinal study applying the FUS technique to the striatum in mice revealed no long-term adverse effects [20]. While the results from these studies are positive, the safety of a long-term application of the FUS technique in NHP requires further investigation.

Multiple groups have utilized the FUS technique to open the BBB facilitating treatment of brain tumors or to deliver therapeutic agents. To date, there have been no studies investigating drug delivery for eliciting a pharmacodynamical effect modulating behavioral responses to external stimuli [21, 22, 23]. Parkinson's disease is a complex disease affecting many neurological functions with motor deficits being the most noticeable. Parkinson's can also have neuropsychiatric effects causing difficulty with speech, decision-making, and memory [24, 25]. Potential drug therapies for PD could alter both the motor and decision making circuits in the basal ganglia and the

cerebellum [26]. It is a necessity that the pharmacodynamic effects of drugs delivered via the FUS be investigated in NHP before clinical and laboratory applications can be implemented.

The main goal of this dissertation is the evaluation of the safety and efficacy of the FUS technique in NHP. This goal was divided to three main objectives. The first investigated the safety and efficacy of the FUS technique when applied to anesthetized NHP over a duration 4-20 months (Chapter 3). Results from this study demonstrated that repeated application of the FUS to the basal ganglia in NHP did not have significant long-term effect on the targeted brain region, nor affect the responses of the NHP to a visuomotor task. Second, the FUS BBB opening technique was utilized to facilitate the delivery of haloperidol and domperidone to the basal ganglia in NHP and mice (Chapter 4). Successful delivery of the D2-antagonists resulted in pharmacodynamical modulation of the animals' behavioral responses to visuomotor or simple motor tasks. The last objective demonstrated the safety and efficacy of the FUS technique in alert subjects by opening the BBB at the caudate, thalamus and putamen regions of fully alert NHP while they completed a visuomotor task (Chapter 5). Results from this study were the first to verify the technique can be successfully applied to fully alert subjects without eliciting negative side effects.

Specific Aims

1.2 Specific Aims

This thesis has three specific aims addressing the safety and efficacy of opening the BBB with FUS in NHP. A flowchart of the individual aims is shown in Figure 1. The first specific aim focused on determining if there were detectable physiological or neurological effects of long-term application of the FUS technique to the basal ganglia in

anesthetized NHP. The second specific aim incorporated the results from the first specific aim and utilized the FUS technique to deliver D2 antagonist to the basal ganglia in NHP and mice. These two initial specific aims addressed the long-term effects, and the applicability of the FUS technique for drug delivery in anesthetized NHP. The third specific aim was necessary for pre-clinical translation of the technique and entailed applying the FUS technique to fully alert NHP investigating the safety and efficacy of the procedure.

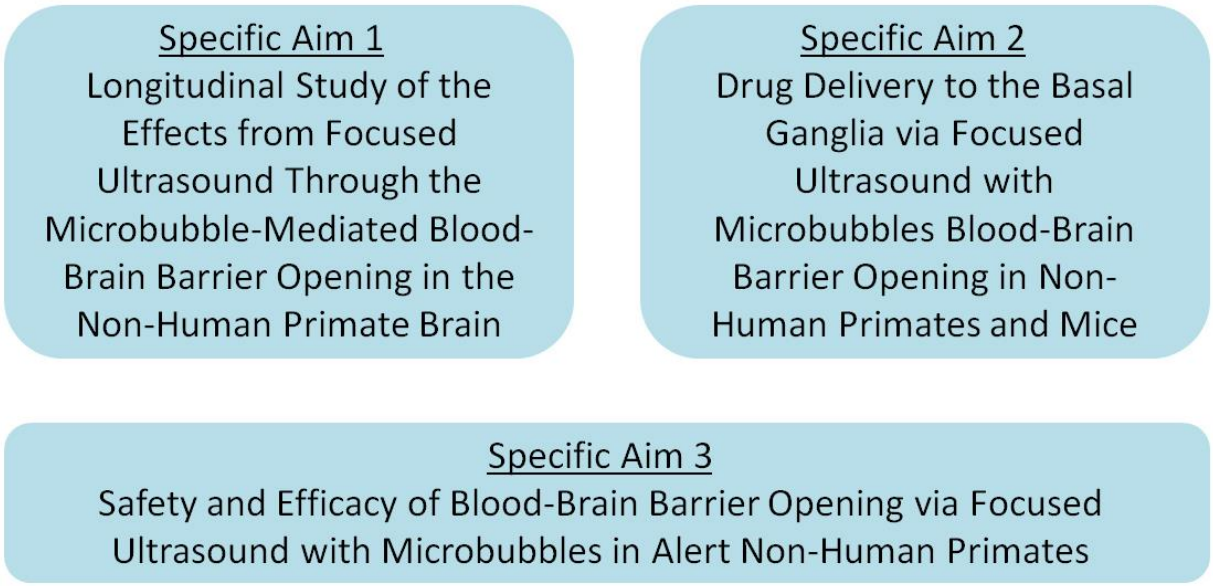

Figure 1. Specific Aims

1.3 Longitudinal Study of the Effects from Focused Ultrasound Through the Microbubble-Mediated Blood-Brain Barrier Opening in the Non-Human Primate Brain (Specific Aim 1, Chapter 3)

The purpose of this aim was to investigate the potential side effects from applying the FUS technique to the basal ganglia in anesthetized NHP over a period of 4-20 months. Specific aim 1 also developed analysis pipelines that would be implemented in the subsequent specific aims such as:

1. A brain region specific post-processing pipeline of MRI data for verification of BBB opening and safety of the procedure
2. A behavioral analysis pipeline for evaluating the potential neurological effects of the FUS technique.

To reach the goal of clinical application with the FUS technique, the removal of personal bias is required to achieve the same planning, and analysis of the procedure regardless of the user. The first section of specific aim 1 introduces a user-independent BBB opening analysis that produced results independent of personal interpretation.

For evaluation of neurological effects of chronic FUS procedures, and to determine the efficacy of drug delivery via BBB opening in specific aim 2, a behavioral analysis pipeline was created. The behavioral analysis pipeline was developed for two behavioral tasks, a reward magnitude bias (RMB) task and a RMB + random dot motion task (RDM). The behavioral analysis pipeline developed in specific aim 1 was implemented with all subsequent specific aims.

Utilizing the opening verification and behavioral analysis pipelines, a longitudinal study of repeated FUS application in anesthetized NHP was conducted. It was hypothesized that chronic application of FUS in the basal ganglia would not have an effect on decision or motor responses when conducting a behavioral task after BBB opening, nor any permanent damage to the brain (edema, microhemorrhage). Results indicated that chronic (4 months minimum, 20 months maximum) FUS BBB opening in the putamen and caudate structures of the basal ganglia in three NHP did not induce any observable long-term effects on the recorded behavioral results. The majority of the FUS procedures were without any detectable edema or microhemorrhage on T2-weighted or susceptibility weighted imaging (SWI). Overall, the results demonstrated the FUS technique is a safe and effective procedure for repeatedly opening the BBB in the basal ganglia of NHP with the parameters employed.

1.4 Drug Delivery to the Basal Ganglia via Focused Ultrasound with Microbubbles Blood-Brain Barrier Opening in Non-Human Primates and Mice (Specific Aim 2, Chapter 4)

The goal of this specific aim was to determine the efficacy of both large molecule and low dose drug delivery to the basal ganglia region in the NHP and mice brains after opening the BBB with the FUS technique.

One major benefit of opening the BBB at target specific regions is to allow large molecule drugs that normally cannot cross the native BBB to access the brain parenchyma. The FUS BBB opening technique could also be utilized to lower the administered dosage of currently available drugs that cross the intact BBB. Opening the BBB at the specific region of interest for drug effects could allow for the same desired therapeutic effect of a full dose of the drug with a lower chance of potential side effects [27]. Many neuroactive drugs have adverse side effects that could be reduced or negated with lower doses [28, 29]. This would greatly benefit Parkinson's disease patients that require daily doses of levodopa by reducing the unwanted side effects such as dyskinesia [30].

The hypothesis was the FUS technique could allow for lower doses of drugs to reach specific brain regions and elicit similar behavioral responses as a full dose of the drug. Haloperidol and domperidone, two D2- antagonists, were selected as the drugs. The first part of this aim investigated the behavioral effects of low dose haloperidol on NHP and mice after opening the BBB in the putamen and caudate-putamen regions respectively. While haloperidol normally crosses the intact BBB, a threshold IM administered dosage (0.01mg/kg) that did not affect the behavioral results while the BBB was intact was determined and applied throughout the experiment. For both animal groups, there were significant changes in the results of behavioral testing with a low dose of haloperidol after the BBB was opened, compared to behavioral results

when the BBB was intact. For the second part of this specific aim, domperidone, which cannot normally cross the BBB, was administered to four NHP after opening the BBB in the caudate. Two of the NHP displayed strong signs of hemilateral neglect, indicate that the domperidone had successfully crossed the BBB into the caudate. The drug delivery study in specific aim 2 confirmed that the FUS technique could be employed to deliver either large molecules or low drug dose to the basal ganglia and elicit pharmacodynamical effects on responses to behavioral testing.

1.5 Safety and efficacy of Blood-Brain Barrier Opening via Focused Ultrasound with Microbubbles in Alert Non-Human Primates (Specific Aim 3, Chapter 5)

Specific aim 3 determined the safety and efficacy of the FUS technique in alert NHP via MRI verification and behavioral testing.

For the FUS technique to become an outpatient procedure in the clinic, as well as a non-invasive and time efficient technique for targeted drug delivery allowing pharmacodynamical behavior modulation in the lab, the safety and efficacy of the procedure in alert subjects needed to be verified. Some groups have reported neuromodulation in alert NHP and in humans using transcranial focused ultrasound (tFUS) without MB administration [31, 32]. To modulate brain activity, both groups used acoustic pressures up to two times larger than employed in this specific aim.

The hypothesis was that the FUS technique would be both a safe and effective method to open the BBB in alert NHP. Results showed the average volume of BBB opening was slightly larger in alert compared to anesthetized animals. There was also a decrease in the occurrence of edema for the alert FUS procedures compared with the anesthetized procedures. Behavioral testing revealed a small non-significant decrease in the average reaction time to visually presented stimuli after sonication. There was also a

significant decrease in touch error while the sonication was occurring suggesting the technique could provide a small beneficial effect to motor function when targeting the basal ganglia and thalamus regions in alert NHP.

Chapter Two

Background & Motivation

2.1 Blood-brain barrier

The blood brain barrier (BBB) is a selective barrier comprising of the tight junctions between endothelial cells that line the cerebral vasculature [33]. Figure 2 shows an illustration of the BBB and surrounding neuronal cells. This barrier controls the influx and efflux of molecules and nutrients from the lumen to the parenchyma enabling brain homeostasis for neuronal activity [34, 35]. The tight junctions between endothelial cells act as a physical and metabolic barrier excluding molecules with a molecular weight greater than 400-600 Da that are not lipid soluble [4, 36]. The only other means of transport across the native BBB is through paracellular or transcellular pathways [37]. Due to the selectivity of the BBB, 99% of small molecule and almost all large molecule drugs and molecules (proteins, enzymes) cannot cross the intact BBB [38]. The selectivity of the BBB prevents many drugs from being utilized as therapeutic treatments for neurological diseases.

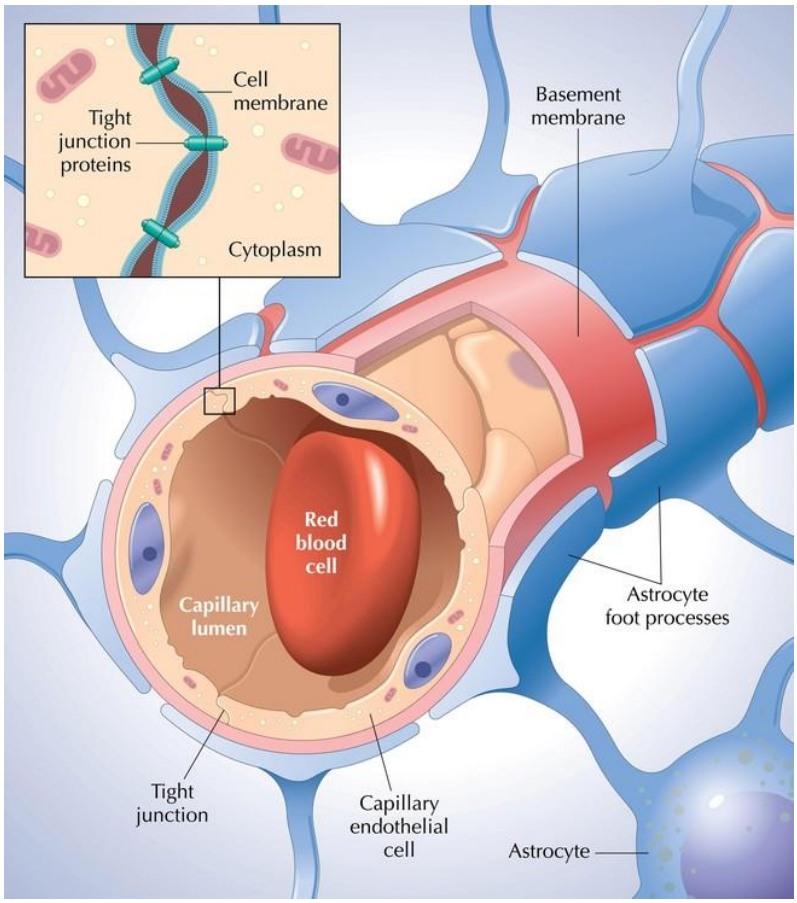

Figure 2: The Blood-Brain Barrier. Capillary endothelial cells lining the vasculature form tight junctions between cells bound by proteins creating a diffusion barrier. The astrocyte feet processes are critical for this tight junction upkeep. (Source: Netter's Atlas of Human Anatomy, 1st edition)

2.2 Current Blood-Brain Barrier Disruption and Drug Delivery Techniques

Due to the BBB being a limiting factor for the treatment of most neurological diseases and disorders, multiple techniques have been developed to circumvent it. These techniques include modifying the composition of the drugs to facilitate uptake through the BBB [39, 40, 41], physically bypassing the barrier through surgical

procedures [38, 42] and using chemical, biological or physical mechanisms to open the BBB and deliver the drug [43, 44, 45, 46, 47, 48, 49, 50, 51, 52, 53].

2.2.1 Drug Modifications

The characteristics of some drugs can be modified to increase the delivery efficiency across the BBB. These characteristics include the molecular weight, permeability as well as solubility. As mentioned in section 2.1, drugs need to be lipid soluble to cross the BBB, hence one of the main drug modification techniques is "lipidization." This process converts non-polar functional groups into polar groups increasing the ability of the drug to cross the BBB [40]. Modifying the drugs to target endogenous transport is another technique to increase drug permeability across the BBB [39]. The two main common techniques include carrier-mediated transport (CMT) and receptor-mediated transport (RMT). The implementation of these techniques is dependent on the specific drug being transported across the BBB. CMT is designed to transport hormones, nutrients and proteins across the BBB. Small molecules with MW < 600 Da that can modify their structure to mimic commonly transported molecules such as glucose or neutral amino acid are prime candidates for utilizing CMT to deliver drugs across the BBB [41]. If the drug molecule is too large, RMT could be utilized by modifying the drug to bind to the insulin receptor, insulin-like growth factor receptor or the transferrin receptors. This utilizes the endocytotic processes to deliver the drug to the brain parenchyma [54, 55].

The limitation of these drug modification techniques is that only a certain amount of drugs are able be modified to fit transport criteria, and the delivery through the BBB is not region specific [56].

2.2.2 Invasive Techniques

Invasive procedures include direct transcranial or intraventricular injections with pump infusions as well as convection-enhanced delivery [38, 42]. These techniques allow for precise delivery of the drug to the region intended for brain-drug interaction.

The main invasive technique is transcranial injection that may be either intracerebral or intracebroventricular. These are the current gold standard for invasive drug delivery to the brain as the full dose of the drug is delivered to the intended region for brain-drug interaction [57]. The limitations with this technique are that the treatment area is constrained by the diffusion of the drug (usually only a few millimeters around the injection location) and backflow of the drug into the needle and path of the needle during removal can reduce drug delivery efficiency [38].

Convection-enhanced drug delivery is another invasive technique and as with the transcranial injections physically bypasses the BBB with a catheter. Here the drug is delivered via positive hydrostatic pressure for infusion of the drug to the targeted region allowing a larger treatment area than with the transcranial injections [58]. Due to the use of the hydrostatic pressure, drug delivery efficiency is also increased over transcranial injections.

The major limitations for the two invasive techniques are that they require surgical procedures that have the potential for adverse complications and some patients may not be good candidates for sedation with anesthesia. Structural damage to the brain due to either the needle or catheter placement for the delivery of drugs is also a drawback from using invasive techniques for drug delivery across the BBB.

2.2.3 Non-Invasive Techniques

Numerous non-invasive methods have been developed for opening the BBB for drug delivery. These are divided into three groups; chemical, biological and physical. These techniques primarily disrupt the BBB, increasing the permeability of the barrier and allowing the drugs to be administered via traditional methods (orally, IV) and achieve successful therapeutic doses in the brain parenchyma.

Chemical techniques to open the BBB include administration of solvents such as Dimethyl Sulfoxide (DMSO), or surfactants such as sodium dodecyl sulfate (SDS) and Tween 80 [43, 44, 45]. The mechanism of increasing the BBB permeability with the DMSO technique involves disrupting the tight junctions between the endothelial cells that comprise the BBB [43]. Administering SDS or Tween 80 modifies protein kinase C (PKC) signaling in the endothelial cells that comprise the BBB [44, 45]. PKC is associated with the regulation, assembly and permeability of the tight junctions formed by the endothelial cells lining the cerebral vasculature [59]. This modulation of the PKC signaling increases the permeability of the BBB allowing for drugs to diffuse across into the brain parenchyma.

Biological techniques employ mannitol, adeno-associated viruses (AAV), interleukin-1 β, and RMP-7 to open the BBB as well as drug loaded macrophages and peptides as a Trojan horse drug delivery method [46, 47, 48, 49, 50, 60]. Mannitol is the most widely studied method of opening the BBB and functions by shrinking the endothelial cells and opening the tight junctions [46]. Both the AAV and interleukin-1 β method utilize cytokines which trigger an immune response to the location of delivery inducing a breakdown of the BBB [47, 60]. RMP-7 functions more similar to the chemical solvents as it opens the tight junctions between the endothelial cells lining the cerebral vasculature[50, 61, 62]. The macrophage method utilizes drug loaded

macrophages that can freely cross the BBB to deliver the drug into the brain parenchyma [49]. The macrophage method is most advantageous for treatment of neurological diseases that would incur an immune response and has been shown successful for treating HIV. Peptides, short amino acids chains with the ability to pass through lipid bilayers, are ideal for delivering biologically active molecules as they are positively charged and highly lipid-soluble [48, 63, 64]. Multiple peptides have been shown successful as a method for drug delivery to the brain, but the most successful ones are the most lipophilic which was discussed as a drug delivery technique in section 2.2.1.

Physical techniques to open BBB include using microwave, electromagnetic fields and ultrasound [51, 52, 53]. The microwave technique utilizes placement of an antenna in the skull operating at 2450 MHz and induces hyperthermia (44.3 ˚C for 30 minutes) at targeted regions [51]. This hyperthermia induces BBB openings in the targeted regions [65]. The electromagnetic fields method employs high voltage (200 kV/M) EMP pulses to activate the PKC signaling in the endothelial cells lining the cerebral vasculature, similar to the chemical surfactant method [52, 66]. This activation of the PKC signaling produced significant BBB opening after 3 hours. The ultrasound method utilizes microbubbles, an ultrasound contrast agent, coupled with a focused ultrasound transducer to accurately target specific brain regions for BBB opening [53, 67]. This technique will be covered more thoroughly in sections 2.2.1

The limitation with the majority of the aforementioned non-invasive chemical, biological and physical techniques are that they are primarily non-target specific. While both the physical techniques provide some special specificity, the microwave radiation requires the antenna be drilled into the skull, while the electromagnetic fields can only target a large area (30 x 30 cm) [51, 52]. The only technique to open the BBB that provides both special specificity and is non-invasive is the ultrasound technique.

2.3 Ultrasound

Clinical ultrasound has two main applications, diagnostic and therapeutic. Both applications utilize transducers, a device containing at minimum one piezoelectric component that produces acoustic pressure waves when voltage is applied [68]. These waves then propagate through the tissue resulting in some waves being absorbed and some reflected back to the transducer where either a different, or the same piezoelectric component detects the reflected waves and converts them to voltage for either visual interpretation or data analysis [68].

Diagnostic ultrasound typically employs B-mode, M-mode or Doppler for imaging target areas within patients such as fetuses. It can also be used to image heart motion and blood flow [69, 70, 71]. Transducers employed for diagnostic purposes typically operate with higher frequencies ranging between 2-12 MHz, have a short duty cycle (fraction of time when the transducer emits the acoustic wave relative to the full duration of the procedure) and lower acoustic pressures resulting in overall lower acoustic intensities (1.0 W/cm^2 or less). These parameters reduce the potential of damage to the tissue being imaged.

Therapeutic ultrasound utilizes specialized transducers that typically operate at higher intensities and lower frequencies. The acoustic waves generated from these transducers can cause two different effects, thermal and non-thermal [72]. Thermal effects occur with high duty cycles or continuous wave ultrasound in conjunction with higher acoustic pressures. These parameters cause the temperature of the targeted tissue to increase and can cause the tissue to become thermally ablated. Therapeutic ultrasound techniques that utilize thermal effects include high intensity focused ultrasound (HIFU) and lithotripsy [73, 74]. HIFU is utilized to ablate tissue while lithotripsy is primarily used to destroy kidney stones.

The non-thermal applications utilize transducers with lower duty cycles and lower frequencies around 0.5-1.5 MHz, but similar high acoustic pressures. Multiple therapeutic ultrasound techniques utilize non-thermal effects such as sonoporation, histotripsy and FUS mediated BBB opening [53, 75, 76]. The main non-thermal effect is cavitation, or the generation of microbubbles from nucleation sites in the tissue where small pockets of gas exist, and the interaction of the generated microbubbles with the acoustical waves [77, 78]. These microbubbles can oscillate and grow within the acoustic waves and have the potential to implode. The generation and manipulation of these bubbles can lead to different therapeutic effects. Sonoporation generates temporary pores in cell membranes induced by ultrasound to facilitate the uptake of specific drugs, while histotripsy utilizes cavitation to non-thermally destroy tissue [75, 76, 79, 80]. FUS mediated BBB opening utilizes cavitation as a mechanism to open the BBB, but in a safer, more controlled method by administering ultrasound contrast agent (microbubbles) before sonicating the target regions [53]. This allows for the disruption of the BBB with minimal damage depending on the parameters employed.

2.3.1 Focused Ultrasound with Microbubbles

Multiple groups have utilized FUS with systemically administered microbubbles (MB) to open the BBB with *in vivo* animal models such as rabbits, mice, pigs, and non-human primates (NHP) [9, 10, 11, 12]. The FUS is an acoustic transducer comprised of a piezoelectric element which when driven with an electric current, generates an acoustic pressure wave. This acoustic wave is able to propagate through the skin, skull and tissue, enabling the targeting of subcortical regions of the brain [15, 19]. The focal area of the FUS has an inverse relationship to the center frequency of the FUS. As the center frequency increases, the focal area decreases. Combining the application of FUS with systemically administered MB for BBB opening is unique as it allows for target specific opening of the BBB, the procedure is non-invasive, and the opening is transient [13,14].

Acoustic waves from the FUS transducer interact with the circulating microbubbles at the focal zone and cause short-term disruption of the tight junction complexes between the endothelial cells that form the BBB [84]. The FUS technique has been shown effective in NHP and mice over a range of ultrasound parameters and MB sizes [13, 15, 16].

2.3.2 Cellular Mechanisms of Blood-Brain Barrier Opening

The exact mechanism of BBB opening is unknown, but acoustic cavitation of the MB in the focal area of the FUS has been determined as a major factor [36]. The two central components of the acoustic cavitation have been identified as stable and inertial cavitation (Figure 3) [85, 86]. Stable cavitation is comprised of both harmonic and ultraharmonic oscillations of the MB and has been reported to be safe for *in vivo* animal models [15, 17, 87]. Inertial cavitation is defined as the broadband signal from the MB in the focal area of the FUS [17]. Inertial cavitation usually occurs at higher acoustic pressures generated by the FUS transducer and causes the MB to collapse violently [88]. These collapses have been correlated with create high-energy microjets, which can cause damage to the surrounding tissue (Figure 2 B) [85, 88]. The interactions of the MB on the vascular walls are also dependent on the size of the MB and the diameter of the vessels [88]. If the MB is smaller than the surrounding vessel, then inertial cavitation is the dominant mechanism. If the MB and the diameter of the vessel are comparable, then stable cavitation is the dominant mechanism for BBB opening. The BBB opening from the FUS technique is transient and closes between 3 and 72 h depending on the experimental parameters used (i.e. MB size, pressure applied, sonication time) [13,14].

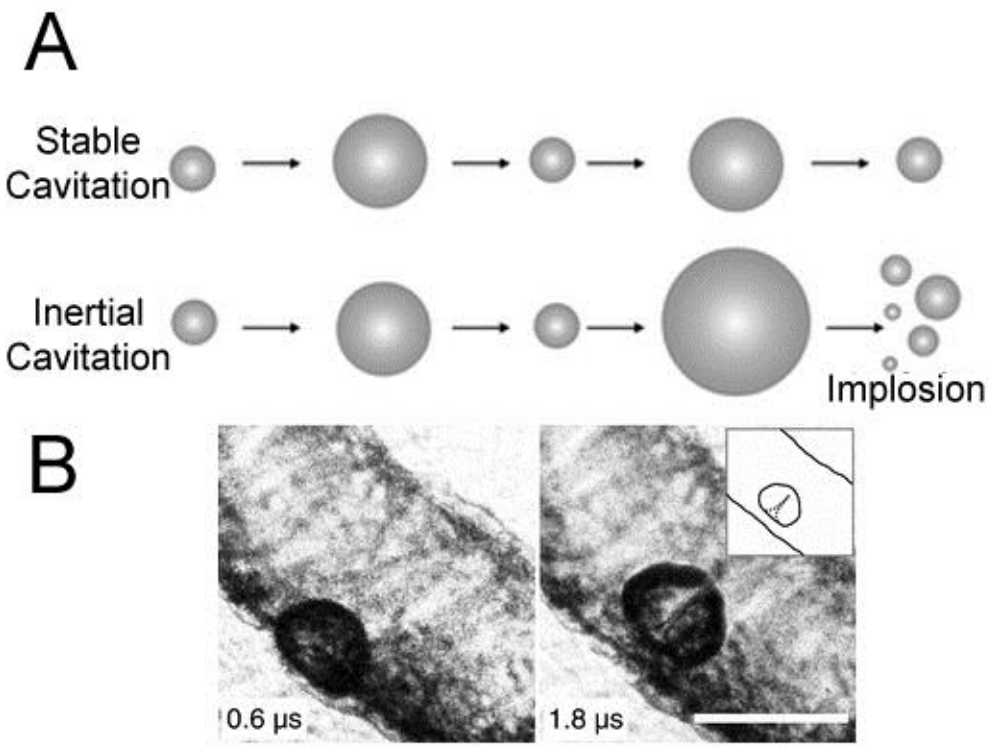

Figure 3: Microbubble-Focused Ultrasound Interactions. A) Illustrates the two dominant mechanisms of microbubble oscillation within the focal area of the focused ultrasound beam: inertial and stable cavitation. B) Shows a microbubble undergoing inertial cavitation resulting in the formation of a microjet next to the vessel wall. (Sources: (A) Lentacker I *et al.* Soft Matter, 2009, (B) Chen H. *et al.* PRL, 2011)

2.3.3 Monitoring and Assessment of Blood-Brain Barrier opening

As mentioned in chapter 2.2.2, microbubble cavitation is the main mechanism for BBB opening. The acoustic emissions from this cavitation can be monitored through passive cavitation detection (PCD). The acoustic emissions from the bubbles are detected with a hydrophone and the signals processed to determine the stable and inertial cavitation doses [18, 86, 87]. This study utilized real-time PCD to verify the microbubble dose was administered correctly and had reached the focal area of the FUS transducer (Figure 4) [18].

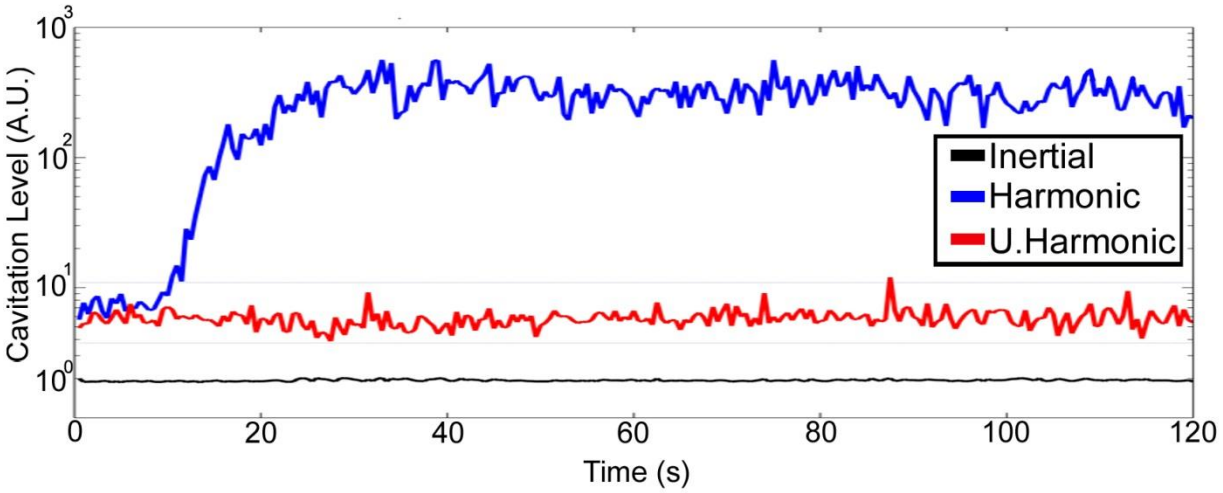

Figure 4: Passive Cavitation Detection. The acoustic emissions from the MB are constantly monitored throughout the application of the FUS technique. There is typically a 10-second lag before the harmonic signal increases past baseline. This is the time period of the MB being injected and circulating before reaching the focal area of the FUS.

The blood-brain barrier opening is currently verified using three imaging modalities, SPECT/CT, microscopy and MRI [15, 89, 90]. The only method of the three to verify BBB opening *in vivo* with both high spatial and temporal resolution is MRI. The MRI can also provide functional and anatomical information that the other modalities cannot. Contrast enhanced T1-weighted MRI sequences can indicate the location of the BBB opening and is the most common technique for BBB opening verification [9, 13, 14, 15, 16]. Gadodiamide, a contrast agent with a molecular weight (MW) of 573.66 Da that normally cannot cross the BBB is typically utilized as an indicator of BBB opening. If the FUS procedure was successful and the BBB was opened, the contrast agent will cross into the brain parenchyma. The area where the contrast agent crossed increases the intensity of the voxels for T1-weighted MRI sequences indicating the area of BBB opening. This contrast-enhanced area is then quantified in post-processing to determine the volume of opening [15]. T2-weighted and Susceptibility Weighted Imaging (SWI) can be used to detect damage such as edema, lesions, or hemorrhage [36]. Abnormal hyperintense voxels on T2-weighted scans can

indicate edema, while abnormal hypointense voxels on the SWI scans can indicate microhemorrhage [91, 92]. MRI analysis is an important multifunctional tool as other methods of measuring potential damage such as histology require the subject to be sacrificed.

2.4 Drug Delivery via Focused Ultrasound with Microbubbles

2.4.1 Treatment of Neurological Diseases

As previously mentioned current methods of drug delivery across the BBB are either non-invasive and non-specific, or target specific requiring an invasive procedure [38, 81, 82]. The FUS technique for BBB opening is a promising technique for facilitating drug delivery that combines the positive attributes from current drug delivery modalities. The FUS technique has been shown to allow the delivery of various molecules across the BBB including therapeutic antibodies (Anti-$\alpha\beta$ antibodies, endogenous antibodies, Herceptin), anti-cancer drugs (Cytarabine, Doxorubicin, Trastuzumab), Adeno-Associated Virus (AAV), nanoparticles, neurotrophic factors (BDNF, GDNF), and neural stem cells [21, 22, 23, 93, 94, 95, 96, 97, 98, 99, 100, 101, 102, 103, 104]. While delivery of these molecules only occurs with an open BBB, it is unknown if a drug that normally crosses the native barrier can elicit similar pharmacodynamical results at a lower administered dose when the barrier opened.

2.4.2 Pharmacodynamical Behavior Modulation

To this date, investigation using FUS BBB opening as a method for delivering neuroactive drugs that can modulate naive brain behavior to external stimuli (visual, auditory, tactile cues) has not been reported. There has been one study opening the BBB in the somatosensory cortex in rats with successful delivery of GABA while monitoring the local neural activity [105]. Results showed a dose dependent suppression of

somatosensory evoked potential amplitudes where the BBB had been successfully opened. This study only investigated the neural activity and did not test how the suppression effected processing of external stimuli since the rats were anesthetized. In this thesis, the potential of the FUS technique be utilized for targeted drug delivery allowing pharmacodynamical behavior modulation was investigated. This was an important facet to explore as many neurological diseases such as Parkinson's and Alzheimer's disease affect the sensory-motor functions of the brain and how the patient reacts to external stimuli [25].

2.5 Targeted Brain Regions

2.5.1 Basal Ganglia

The basal ganglia is a collection of subcortical nuclei situated at the base of the forebrain. It is has been implicated in various functions such as voluntary motor and eye movement control, as well as procedural, cognitive and emotional learning [106, 107, 108]. Motor signals initiating from the motor cortex pass through the basal ganglia and the cerebellum before continuing to the spinal cord. The dorsal parts of the caudate and putamen are associated with sensorimotor while the ventral parts are associated with the limbic processing [108]. It has been proposed the basal ganglia plays a role in the activation of learned motor functions in the cerebral cortex [109]. Thus neurological diseases and disorders that disrupt the basal ganglia, such as Parkinson's disease, typically manifest motor deficits. Parkinson's disease affects the basal ganglia by causing degeneration of the dopamine-producing cells in the substantia nigra pars compacta [25]. This degeneration affects the other subcortical nuclei such as the putamen and caudate which can lead to motor impairment if dopamine levels decrease [110]. This motor impairment can be mimicked by injecting D2 antagonists into the putamen, which block the native dopamine and bind to D2 receptors. This binding

prevents the inhibition the indirect pathway between the striatum and the substantia nigra [111]. The caudate nucleus is also implicated in voluntary motor control as well as other cognitive functions such as goal-directed action, memory and learning [109, 112, 113]. As FUS could potentially be used as a tool for drug delivery treatment of PD, the putamen and caudate regions of the basal ganglia were selected as target regions for the studies in this thesis. The locations of these subcortical nuclei are indicated in Figure 5.

2.5.2 Thalamus

The thalamus is located in the forebrain and facilitates signaling from the sub-cortical structures to the cerebral cortex [114]. Similar to the basal ganglia, the thalamus region of the brain has been implicated with visuomotor activity as well as motivation [115, 116, 117]. Parkinson's disease also affects the thalamus causing neurodegeneration in the region of the thalamus that provides feedback to the putamen [118, 119]. Damage to this region can impair awareness, cognition and perception. The thalamus was also selected as a target region for the FUS technique in this thesis as it also plays a critical role in PD and functions in parallel with the basal ganglia pathways.

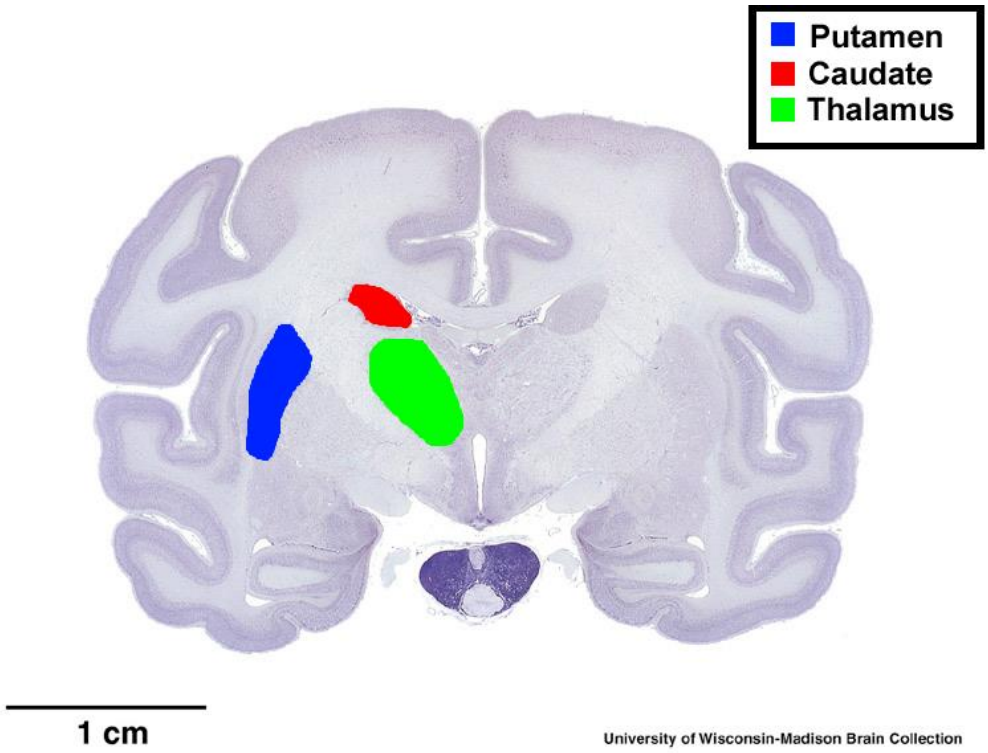

Figure 5: Targeted Brain Regions in the NHP. The color-masked regions indicate the brain targets selected for the experiments conducted in this thesis. (Source: University of Wisconsin-Madison Brain Collection)

2.6 Behavioral Tasks

2.6.1 Reward Magnitude Bias

The well-established reward magnitude bias (RMB) paradigm is suitable for testing motivation and decision-making [120]. The RMB task in its simplest form consists of two discriminable visual cues, one stimulus of which is worth more reward than the other stimulus. If the task requires a saccadic eye movement or manual reach, the reaction times between the two conditions can be compared. Prior studies implementing this paradigm have reported significantly faster reaction time to the high reward [121]. The RMB paradigm has been used to test motivation with a visually guided saccade task in NHP while modulating the response to reward stimuli via

intracranial injections of D1 and D2 antagonist into the caudate [120]. This RMB paradigm was implemented in behavioral tasks throughout all the specific aims of this thesis, testing the visual perception, motivation and motor functions of the NHP.

2.6.2 Random Dot Motion

The random dot motion (RDM) task is effective for evaluating decision-making and accuracy of responding to the correct target indicated by direction of moving dots [122, 123]. The task assesses the subject's visual acuity and decision making by ranging the speed of dots moving in one coherent direction, or varying the amount of dots moving in one coherent direction [123, 124]. After presentation of the dots, the subject must decide between two response targets that correlate either for the speed, or the coherent direction of the dots. For the behavioral tasks employed in this thesis, the coherent motion of the dots was implemented. This means a percentage of the dots presented will move towards the correct target, while the remaining percentage of dots move randomly. Results from the RDM task provides the threshold level for correctly discerning the coherent direction of the dot motion. As both the basal ganglia and thalamus regions are implicated with visuomotor pathways, the RDM task was well suited to test for potential neurological changes after applying the FUS procedure to those regions in NHP.

Chapter Three

Specific Aim 1

Longitudinal Study of the Effects from Focused Ultrasound Through the Microbubble-Mediated Blood-Brain Barrier Opening in the Non-Human Primate Brain

As discussed in chapter 2, prior short-term studies have been conducted investigating this topic, but to date no investigations have explored the potential neurological side effects from chronic applications of the FUS technique to a specific brain region. The first specific aim of this thesis addresses that question by verifying the safety and efficacy of long-term application of the focused ultrasound with microbubble technique to the basal ganglia in non-human primates.

3.1 Abstract

Focused ultrasound (FUS) coupled with intravenous administration of microbubbles (MB) is a non-invasive technique that has been shown to reliably open (increase the permeability of) the blood-brain barrier (BBB) with multiple *in vivo* models including non-human primates (NHP). This procedure has shown promise for clinical and basic science applications, yet the safety and potential neurological effects of long-term application in NHP requires further investigation under parameters shown to be efficacious in that species (500kHz, 200-400 kPa, 4-5μm MB, 2 minute sonication). In this study, the BBB was repeatedly opened in the caudate and putamen regions of the basal ganglia of 4 NHP using the FUS technique over 4 – 20 months. The safety of the FUS technique was assessed using MRI to detect edema or hemorrhaging in the brain. Contrast enhanced T1-weighted MRI sequences showed a 98% success rate for openings

in the targeted regions. T2-weighted and SWI sequences indicated a lack edema in the majority of the cases. The potential of neurological effects from the FUS technique were evaluated through quantitative cognitive testing of visual, cognitive, motivational, and motor function using a random dot motion task with reward magnitude bias presented on a touch panel monitor. Reaction times during the task significantly increased on the day of the FUS procedure. This increase returned to baseline within 4-5 days after the procedure. Visual motion discrimination thresholds were unaffected. The results indicate FUS with MB can be a safe method for repeated opening of the BBB at the basal ganglia in NHP for up to 20 months without any long-term negative physiological or neurological effects with the parameters used.

3.2 Introduction and Study Design

Our group and others have shown focused ultrasound with microbubble is an effective technique to open the BBB for multiple *in vivo* animal models [9, 10, 11, 12]. FUS is a promising technique for targeted drug delivery in the central nervous system, but before clinical application of this technique in humans can occur, the long-term effects of the technique on behavioral and cognitive function must be further investigated.

The introduction of MB coupled with lower-pressure FUS has been shown not to damage tissue or cause neurological deficits in mice [13, 20]. Our group and others have shown that for specific parameters the FUS with MB procedure can be safe for non-human primates [15, 16]. The primary method of evaluating potential damage from FUS BBB opening in NHP is MRI, specifically T2-weighted and Susceptibility-Weighted Imaging (SWI) scans [12]. There has been one study utilizing histological evaluation of the FUS BBB opening procedure in NHP over a period of 2-26 weeks [16]. While MRI and histology are useful for detecting cellular damage from the procedure, neither

method can detect if the FUS with MB procedure has an effect on neurological function. The same study reported the effects of several weeks of FUS with MB application on the thalamus (lateral geniculate nucleus) in the NHP model using a visual acuity task [16]. To date there has not been any study conducted on the neurological effects on motor and cognitive processing of repeated (> 13 months) FUS procedures with BBB opening in NHP.

In this study, the effects of repeatedly applying FUS to the basal ganglia of four NHP over periods ranging from 4 to 20 months was investigated. Acoustic pressures for the FUS procedure were varied through the initial part of the experiment to determine safe ranges of these parameters in the basal ganglia. Within the basal ganglia, the caudate and putamen regions were selected as targets for FUS BBB opening as they are both implicated in voluntary motor control, goal-directed action, memory, learning, and decision-making, and are affected in Parkinson's Disease [24, 25, 125]. The FUS with MB procedure was applied to NHP under general anesthesia using a stereotaxic targeting system. Constant monitoring of vital signs (respiration, blood pressure, heart rate and blood oxygenation levels) before, during, and after the FUS procedure was used to evaluate any potential physiological changes from repeated procedures. Following each FUS procedure, the safety of the procedure (lack of edema or hemorrhage) was evaluated with T2-weighted MRI and SWI sequences. The BBB opening was verified with contrast enhanced 3D T1-weighted MRI sequences. The safety of the FUS with MB procedure was also investigated with behavioral assessment using a reaching task based on a combination of a reward magnitude bias (RMB) paradigm and a random dot motion (RDM) task [120, 131, 122]. This combined task tested visual perception, decision-making, motivation and motor function to determine if the BBB opening affected known neurological pathways of the putamen [26, 108]. The behavioral

evaluation coupled with the MRI results established a multi-faceted approach for verifying safety of long-term FUS BBB opening in NHP.

3.3 Materials and Methods

Subjects and Ethics Statement

All NHP procedures described herein were approved by the Institutional Animal Care and Use Committees of Columbia University and the New York State Psychiatric Institute. Adult male macaques (n=4) were used in all experiments (ages 8-20 years, weights 5-9 kg); one Macaca fascicularis (NHP A) and three Macaca mulatta (NHP O, Ob, N). The NHP were housed (N & O were paired with each other) in a room with a 12 hour light dark cycle. NHP were housed in a 3 ft^3 Erwin-Steffes Enhanced Environmental Housing System (Primate Products Inc., Immokalee, FL, USA) and given access to play cages (total area 3 ft^2 x 7 ft) with various enrichment toys (wooden food logs, plastic chew stars, mirror balls). They were fed constant rations of vitamin enriched dry primate biscuits and given 1L of water on days when they were not tested behaviorally. On testing days, the NHP performed the behavioral task for water reward until they were satiated. NHP were not given additional fluids even if they did not work for a full liter as supplementing the water they received from working with 'free' water would reduce their motivation to perform the behavioral task. Each day, after the behavioral session was completed, they were given a fruit treat.

For each FUS with MB procedure, NHP were initially sedated with ketamine (10-12 mg/kg) and given a dose of atropine (0.04mg/kg). An endotracheal catheter was inserted, after which the NHP were anesthetized with isoflurane (1-2%) mixed with O_2 (2 L/min) for the duration of the procedure. A stereotactic frame (David Kopf Instruments, CA, USA) was used for head fixation to ensure accuracy of the FUS targeting. The scalp was shaved and depilatory cream removed remaining hair to

reduce interference with the acoustic transmission. A catheter was placed in the saphenous vein for IV delivery of 0.9% saline, MB and the MRI contrast agent gadodiamide (Omniscan, 573.66 DA, GE, Healthcare, Princeton, NY, USA). A heated water blanket was used to maintain body temperature during the FUS with MB procedure. Heart rate (EKG), blood oxygenation (SpO_2), end-tidal CO_2 expiration, respiratory rate, and non-invasive blood pressure were recorded during the procedure. Five time-points were used for analysis of the vitals: immediately after the NHP was placed in the stereotax, 30 seconds prior to MB injection, 60 seconds into the sonication, 30s after sonication, and the last point at the end of the procedure when the NHP was taken out of the stereotax.

FUS with MB procedure

All MB used in the procedure were made in-house and centrifuged for size isolation with a mean MB diameter of 4-5μm [126]. A 500-kHz center frequency focused ultrasound transducer was used for all experiments (H-107, Sonic Concepts, WA, USA). The built-in water bladder system on the transducer was filled with de-ionized water and circulated through a degasser (Sonic Concepts, WA, USA) for a minimum of 30 minutes before the FUS with MB procedure. Acoustic pressures ranging from 200-400 kPa were applied with a pulse length of 10ms, pulse repetition frequency of 2 Hz with a total sonication duration of 2 minutes per target location. The caudate and putamen regions of the basal ganglia were selected as the two main targeting regions. A detailed list of acoustic pressures and targeted locations for each NHP are located in Table 1. The transducer was mounted on a 9-degrees-of-freedom stereotactic arm (David Kopf Instruments, CA, USA) that was attached to the stereotactic frame securing the head of the NHP. Stereotactic coordinates were found with an in-house targeting algorithm calibrated for the focal distance of the transducer [15]. An initial six-second sonication without MB was used as a control for real time cavitation monitoring [18]. A bolus

injection of MB with a concentration of 2.5^8 MB/kg was used for each initial sonication. The FUS procedure was initiated at the onset of IV MB injection with an average circulation time of 10s before MB reached the focal area. Real-time monitoring via a hydrophone (Y-107, Sonic Concepts, WA, USA) was used to verify that MB had reached the focal zone and to monitor harmonic, ultraharmonic and inertial cavitation levels [18]. The hydrophone was placed through a center hole in the FUS transducer allowing overlap of their focal regions. A pulse generator (Olympus, PA, USA) drove the initial signal which was passed through a 20-dB amplifier (5800, Olympus NDT, MA, USA) providing the signal to the transducer. Output from the hydrophone was filtered through a pulse-receiver (5072PR, Olympus, PA, USA) before being digitized (Gage Applied Technologies, Inc., Lachine, QC, Canada) and recorded. For some experiments (n = 31), a second sonication was conducted < 1 min after first sonication at an area adjacent (average 1.5 cm shift on anterior-posterior axis) from the initial sonication location, but still within the same targeted subcortical nuclei. For those sonications, real-time monitoring verified that MB remained in circulation and had not yet been filtered out, thus a second injection of MB was not necessary. If the caudate and the putamen were both sonicated on the same day, a 20-min waiting period occurred between sonications allowing the MB to be filtered from the bloodstream. Once the 20 minutes passed, another negative control was acquired to verify the MB had been filtered before the second bolus injection and sonication occurred.

Table 1. Targets and acoustic pressures of FUS with MB procedures for each NHP.

NHP	Brain Target	Acoustic Pressures (kPa)	Duration
A	L. Putamen	300 (n = 12)	10 mo*
N	L. Putamen	200 (n = 1), 275 (n = 8)	11 mo
N	R. Putamen	400 (n = 9)	10 mo*
N	L. Caudate	250 (n = 6), 300 (n = 3)	12mo
O	L. Putamen	250 (n = 4), 275 (n = 6)	12 mo
O	L. Caudate	200 (n = 4), 250 (n = 3), 275 (n = 1)	20 mo
Ob	L. Putamen	400 (n = 4)	4 mo*

The n indicates the number of time FUS was applied to that region at that pressure. The duration was the amount of time over when the FUS with MB procedures occurred. Asterisk durations indicate time while completing RDM + RMB task.

MRI Analysis

MRI scans (3T, Philips Medical Systems, MA, USA) for each NHP were acquired either 30 minutes (n = 36) or 30 hours (n = 25) after the FUS with MB procedure. T2-weighted sequences (TR = 10ms, TE = 27ms, flip angle = 90˚, spatial resolution = 400 x 400 μm^2, slice thickness = 2mm with no interslice gap) and 3D Susceptibility-Weighted Image (SWI) sequences (TR = 19ms, TE = 27ms, flip angle = 15˚, spatial resolution = 400 x 400 μm^2, slice thickness = 1 mm with no interslice gap) were used to verify safety of the procedure. 3D Spoiled Gradient-Echo (SPGR) T1-weighted sequences (TR = 20ms, TE = 1.4ms, flip angle = 30˚, spatial resolution = 500x 500 μm^2, slice thickness = 1 mm with no interslice gap) were acquired after IV administration of gadodiamide at a dose of 0.2 ml/kg to confirm BBB opening. Gadodiamide was selected as the contrast agent as it does not cross the intact BBB. There was a 30-min diffusion period after IV administration of gadodiamide before the post T1-weighted (T1-Post) scan was

acquired. On a separate day when the BBB was not open (no FUS with MB procedure for > 1 week), another contrast enhanced T1-weighted sequence was acquired for post-processing purposes (T1-Gado). Each T1-Post sequence was post-processed to find the opening location and the volume of the induced BBB opening (Figure 6). The T1-Post and T1-Gado sequences were aligned to a high-resolution stereotaxically oriented T1-weighted sequence for each NHP with the FSL toolbox (Figure 6 B) [127]. A grey and white matter segmentation map of each brain was generated and used to find the average voxel intensity of the grey and white matter for image normalization of the T1-Post and T1-Gado sequences (Figure 6 C). Subsequently, the normalized T1-Post was divided by the normalized T1-Gado to locate of voxels where the contrast was increased over baseline (Figure 6 D). The focal area was determined and all voxels that had a contrast increase of 10% within the focal region were counted to determine the volume of the BBB opening (Figure 6 E). The center of the opening was found by weighing each voxel above the threshold with its intensity and then averaging all weighted voxel locations. Contrast enhanced T1-weighted MRI scans were also acquired at least one week after any FUS with MB procedures at the midpoint and after the final FUS with MB procedure for each animal. These scans were processed using the aforementioned pipeline to verify closure of the BBB in the targeted regions.

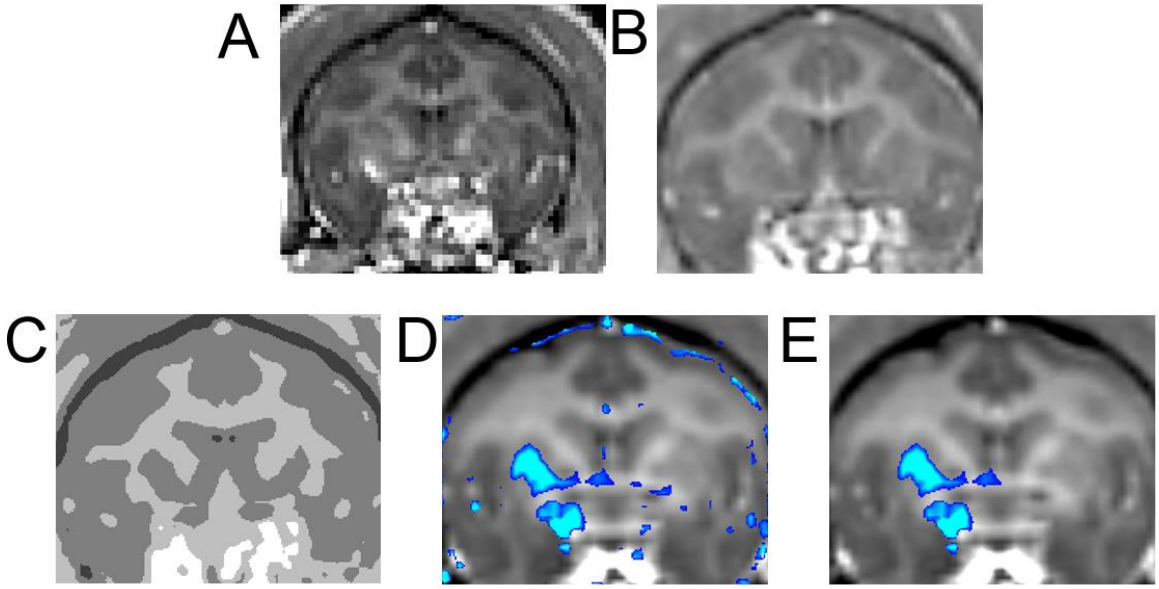

Figure 6: Blood-Brain Barrier Opening Post-Processing Pipeline. A) Initial raw contrast enhanced T1-weighted image (T1-Post). B) Stereotactically aligned and smoothened image constructed from A. C) Grey white segmentation map created from B. D) Contrast enhanced results from dividing normalized T1-Post by normalized T1-Gado. E) Contrast enhanced result after applying focal area thresholding.

Behavioral Testing

Three of the NHP (A, N, Ob) were trained to touch visual stimuli presented on a 20-inch color LCD touch panel monitor (NEC 2010X with 3M SC4 touch controller, Figure 7). Each successful trial was rewarded with 1 or 5 drops of water delivered through a spout positioned in front of the mouth. Daily sessions ranged between 1- 3 hours during which the NHP would typically perform 700-2000 trials of the task and receive 100-400 ml of fluids. At the start of each session, the NHP was placed in an IACUC-approved chair in which their head and both hands were free to move. A vertical divider was placed between the chair and the monitor to prevent the NHP from

reaching across the display. Thus, stimuli presented on the right side of the monitor were only accessible to the right hand, and likewise for the left side.

The reaching task combined the well-established Random Dot Motion detection paradigm (RDM) with a Reward Magnitude Bias (RMB) [121, 122, 123]. The combined task tested reaction time (RT), touch error (TE), motivation and decision-making. For each trial an initial cue, a horizontal or vertical yellow bar was presented randomly on either the left or right side of the screen (the pixel area and intensity was the same for both orientations). A horizontal bar signified a large reward of five drops of water while a vertical bar signified a small reward of one drop of water (5:1 reward bias). Previous studies implementing a RMB paradigm have used smaller reward differentials, but a larger bias was selected to make the difference more salient to the animals and thereby increase the likelihood or magnitude of any effect of the FUS with MB procedure on motivation.

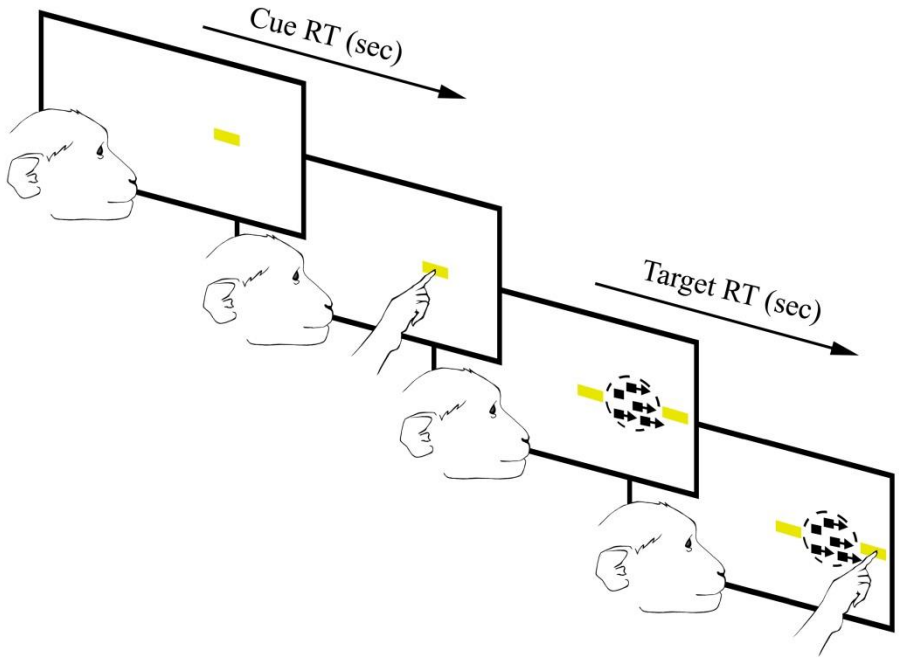

Figure 7. Random Dot Motion and Reward Magnitude Bias Task. Cues appear in the center of the left or right side of the screen randomly. Once the initial cue is touched three new stimuli

appear: A correct target appears on either the inside (towards the middle of the screen) or the outside (towards the edge of the screen) on the same side the intial cue, and a distractor target will appear opposing the correct target as well as moving dots will appear where the initial cue was. Horizontal and vertical bars indicate high and low reward respectively. Reward magnitude is random so subjects cannot predict reward order.

Once the NHP touched the initial cue, the display was updated to show a random dot motion stimulus and two secondary targets of the same shape, color and intensity as the cue. The dots appeared in a circular aperture. A percentage (0-70%, step size of 10%) of the dots moved coherently toward one target while the remaining dots moved randomly [123]. If the NHP touched the target towards which the dots were moving, the response was scored as correct and the NHPs. received the amount of water reward corresponding to the orientation of the targets. If the NHP touched the other target (the "distracter"), the response was scored as incorrect and no reward was given. If the NHP touched any other part of the display or failed to touch the display altogether, the trial was scored as a failure and was not rewarded.

Each trial took a maximum of 4 seconds, and each stage of the trial had a time limit for the NHP to respond or the trial would reset. The initial cue was present on the screen for a maximum of 1.5 seconds, and the dots with the targets were on the screen for a maximum of 2.5 seconds. Trials that were ignored or aborted would be recycled and presented again. Reaction time (RT) to the initial cue was defined as the time from the visual onset of the cue until the first touch registered by the touch panel screen. Reaction time to the correct target or distracter was defined as the time from the onset of the moving dots until the subsequent touch registered by the to

All NHP were full trained on the task (accuracy at discriminating dot direction > 75%) prior to recording. NHP O was excluded from this portion of the study as they did not achieve criterion performance on the RDM task.

Data Analysis

All analysis pipelines were written and implemented in Matlab (Mathworks, MA, USA). The data were examined with two separate pipelines: The first examined the data sequentially over the duration of the experiment. The second divided the data into groups depending on the day of acquisition relative to the day of the FUS with MB procedure (-1, 0, 2, 3, 4 and 5+ days).

For the first pipeline the mean raw reaction time (RT) were sorted by day, and response (to either the initial cue or correct target). A one-way ANOVA was used to detect significant variance within each NHP across the duration of the experiment. Touch error (TE) to the cue and target were also analyzed using this pipeline. TE was defined as the distance between where the NHP touches the screen and the center of the cue or target stimulus

For the second method, days -1 and 5+ were considered to be a baseline since previous work has shown that the BBB openings created with the pressures being applied with this study close within three days [14]. This gives an additional two-day buffer to ensure the BBB has completely closed. A one-way ANOVA with Tukey's HSD criterion ($p < 0.05$) was used for analysis of the RT and TE between groups to the initial cue and correct target. These groups were further divided according to which hand was used to respond and reward level. The average difference and confidence interval between low and high reward as well as ipsilateral and contralateral hand for RT and TE was found for each day. Days were determined to have significantly different means to day 0 if the 95% confidence interval of the mean did not overlap with the 95% confidence interval of day 0.

Random dot motion accuracy was divided into groups using the same conditions as in the second method described above. The performance accuracy (percentage of

correct trials) from each group was sorted by coherence level and fit with a psychometric curve (Naka-Rushton). Psychophysical threshold for detecting direction of motion was determined as the coherence level corresponding to 80% correct responses.

3.4 Results

Vital Signs

Throughout the duration of the FUS procedure, the NHP vital signs were monitored and recorded. There were no significant differences between the recorded values for all the NHP in this study and previously published data for average vitals of macaques under isoflurane for heart rate and mean arterial pressure (student t-test, $p < 0.05$) [128]. Figure 8 shows the average heart rate, blood O^2 levels, respiration rate and blood pressure throughout the FUS procedure. There was no significant difference between vital recordings with the same NHP when either the targeting region or the acoustic pressure changed (one-way ANOVA, $p < 0.05$). Once the NHP regained full consciousness (3 hours after the FUS with MB procedure), no qualitative differences in their behavior within the husbandry room was observed. NHP would return to normal locomotion, eating, drinking and in the case of N and O, normal social behavior (grooming, playing). The weight for all NHP stayed consistent across the study. The only decrease occurred on days after there was no behavioral testing due to a restriction of fruit rewards since testing did not occur. Food and water intake stayed consistent and the fluctuations were not significant when compared to a control NHP not being used in the FUS procedures housed in the same facility (one-way ANOVA, $p < 0.05$).

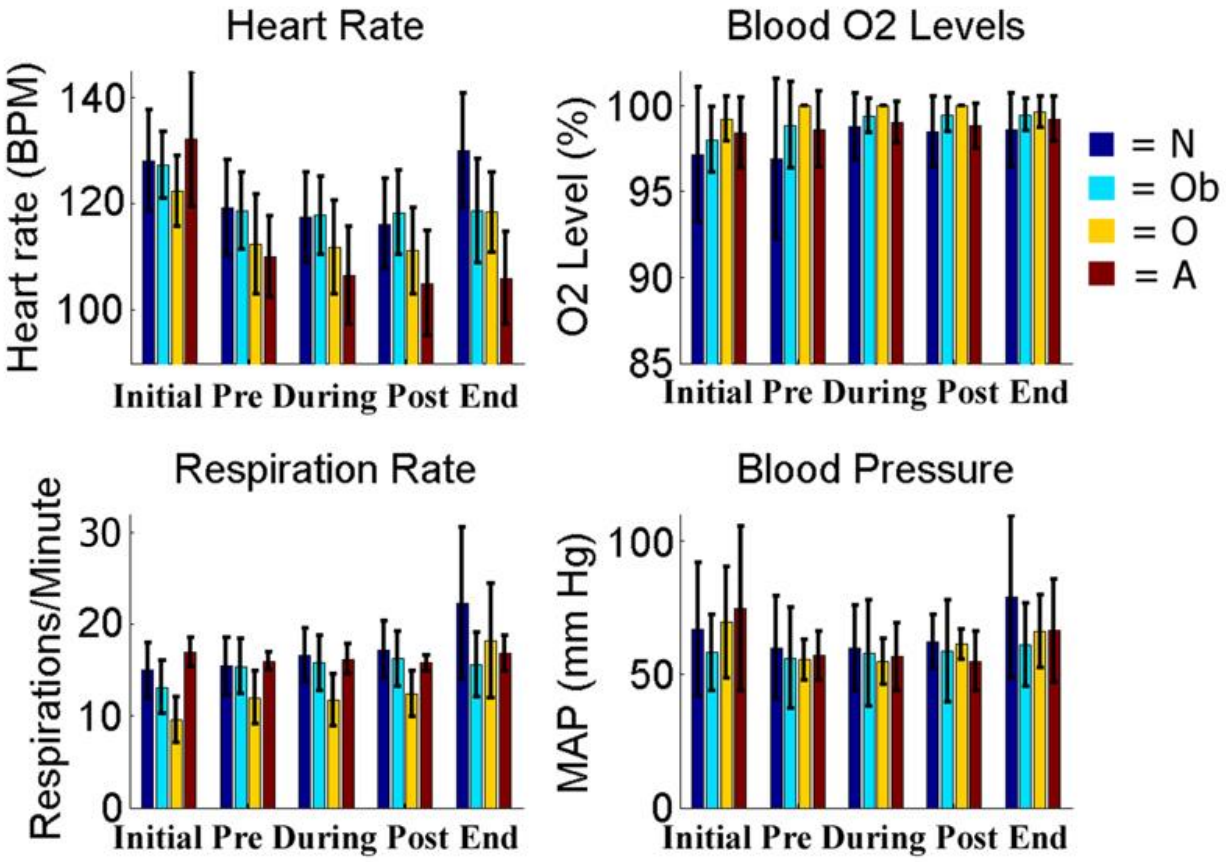

Figure 8. Vital Monitoring. Vitals collected at five points throughout the duration of the FUS with MB procedure. Results in the grey shaded region indicate time-points acquired during the FUS proceure.

MRI Analysis

The BBB opening was verified in 98% of the FUS procedures by comparing each NHP T1-post with the respective T1-Gado. Table 2 shows the number of times opening was achieved per location in each NHP. A typical representation of size and location of openings for the NHP is presented in Figure 9. Average volume of opening was 203 mm^3 with an average focal shift of 3 mm between the center of BBB opening and the planned target region. Table 3 lists the sizes of openings per NHP for each targeted area. No damage (hemorrhage or edema) was observed in the T2-weighted and SWI scans for the majority of the NHP using pressures in the range 200-400 kPa with 4-5µm

MB (n = 57). There were four cases where the T2-weighted scans exhibited hyperintense voxels in the area of targeting indicating possible edema. These occurred with NHP N and A only. These cases appeared on the final FUS procedure for N and the final three procedures for A. Figure 10 shows T2-weighted scans from two of the four cases with hyperintense voxels in the target area as well as T2-weighted scans one week later showing no hyperintense voxels in the target area. No hyper- or hypointense voxels were detected in the target region on the SWI scans for all NHP.

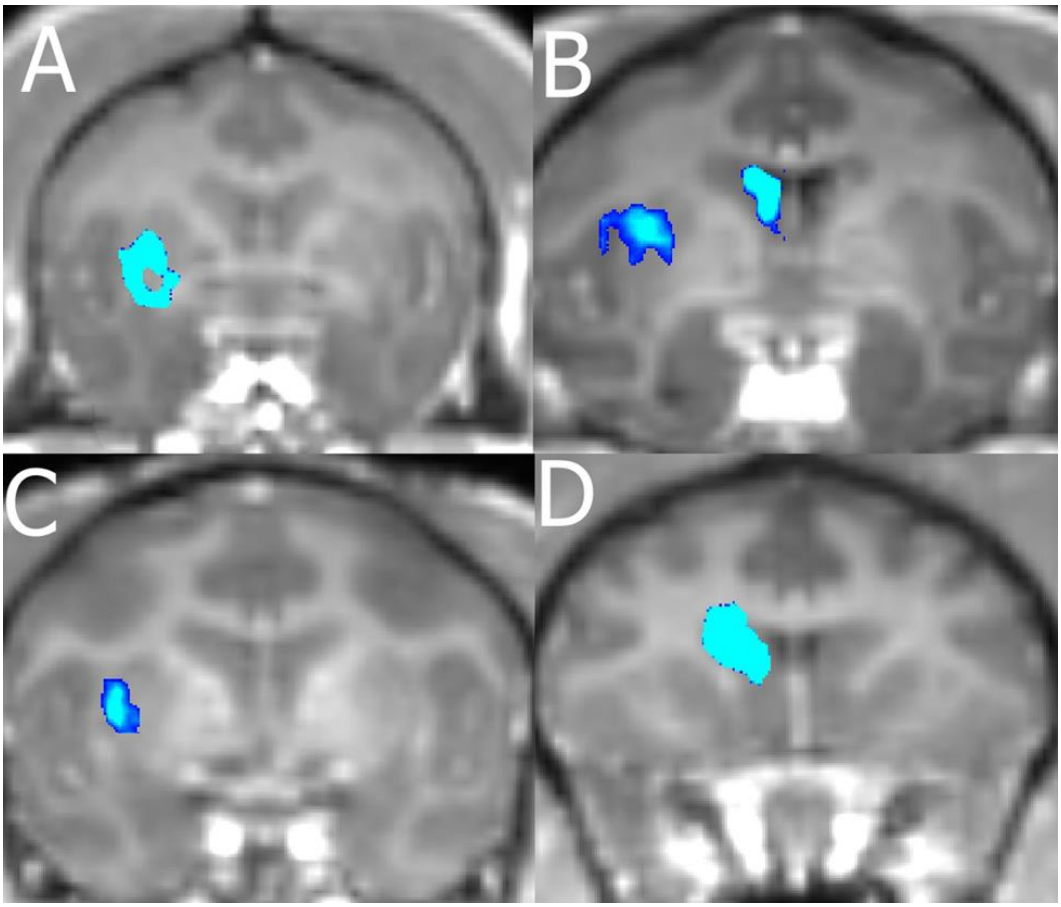

Figure 9. Contrast Enhanced Blood-Brain Barrier Opening. The blue region shows a 10% increase in contrast over the background. A) Opening in the putamen of A. B) Opening in the caudate and putamen of N. C) Opening in the putamen of Ob. D) Opening in the caudate of O.

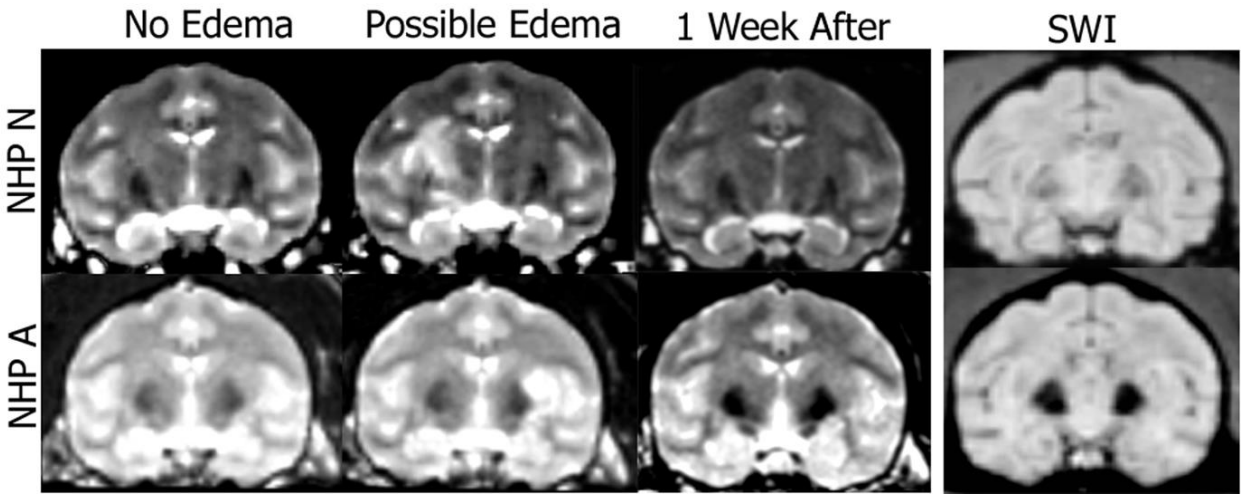

Figure 10. T2-weighted MRI and SWI scans of NHP N and A. T2-weighted sequences can be used to detect potential edema. The first column shows no atypical hyperintense voxels in the target region. The second column shows atypical hyperintense voxels in the target region. The third column verifies the atypical hyperintense voxels from the previous week were no longer present. The fourth column shows the SWI scans from the day when hyperintense voxels were detected on the T2 scan (acquired the same day as column 2).

Table 2. Targets and BBB openings of FUS with MB procedures for each NHP and duration of RDM + RMB task.

NHP	Target	# of FUS	BBB opening	Duration of Task
A	L. Putamen	12	12	13 mo
N	R. Putamen	9	8	15 mo
Ob	L. Putamen	4	4	4 mo

Table shows the times the FUS targeted each location, the success of each procedure and the duration the NHP were conducting the behavioral task.

Table 3. Volume of BBB opening per NHP and location.

NHP	Brain Target	Acoustic Pressures (kPa) and Volume of Opening (mm^3)
A	L. Putamen	300: 494 ±185
N	L. Putamen	200: 704, 275: 118 ±18
N	R. Putamen	400: 29 ±23
N	L. Caudate	250: 177 ± 182 , 300: 326
O	L. Putamen	250: 1792± 1447, 275: 2480±1550
O	L. Caudate	200: 459 ± 61 , 250:1438 ± 823 , 275: 220
Ob	L. Putamen	400: 418 ± 347

Table shows the BBB opening volume per target location, animal and pressure.

Behavioral Task

Three NHP (A, N, Ob) were tested on the RDM + RMB task outlined in the methods section that recorded RT, TE, motivation and decision-making. Throughout the 4-15 month duration of the experiment, the FUS procedures were conducted targeting the putamen as shown in Table 2. RT for the initial reach to the cue is a simple reaction time. RT for the second reach to the target is a choice reaction time, as the NHP must choose between the correct and incorrect targets.

The within session average raw RT and TE for each animal was examined across the duration of the experiment and shown in Figure 11. Only NHP A showed a large fluctuation (> 200 ms) in RT across sessions. These fluctuations were not associated with the FUS with MB procedures. NHP N did show an increase in RT to the cue during days 150-178 but returned to baseline. Similarly, there was a trend of increased RT to the target for NHP N starting on day 77 in which the RT remained elevated for the remainder of the experiment. Average raw TE was more consistent for each NHP, fluctuating less than 5 mm for NHP N and Ob. NHP A showed a sharp decrease in TE

to the correct target over the first 30 days then remained at the lower TE value the remainder of the experiment.

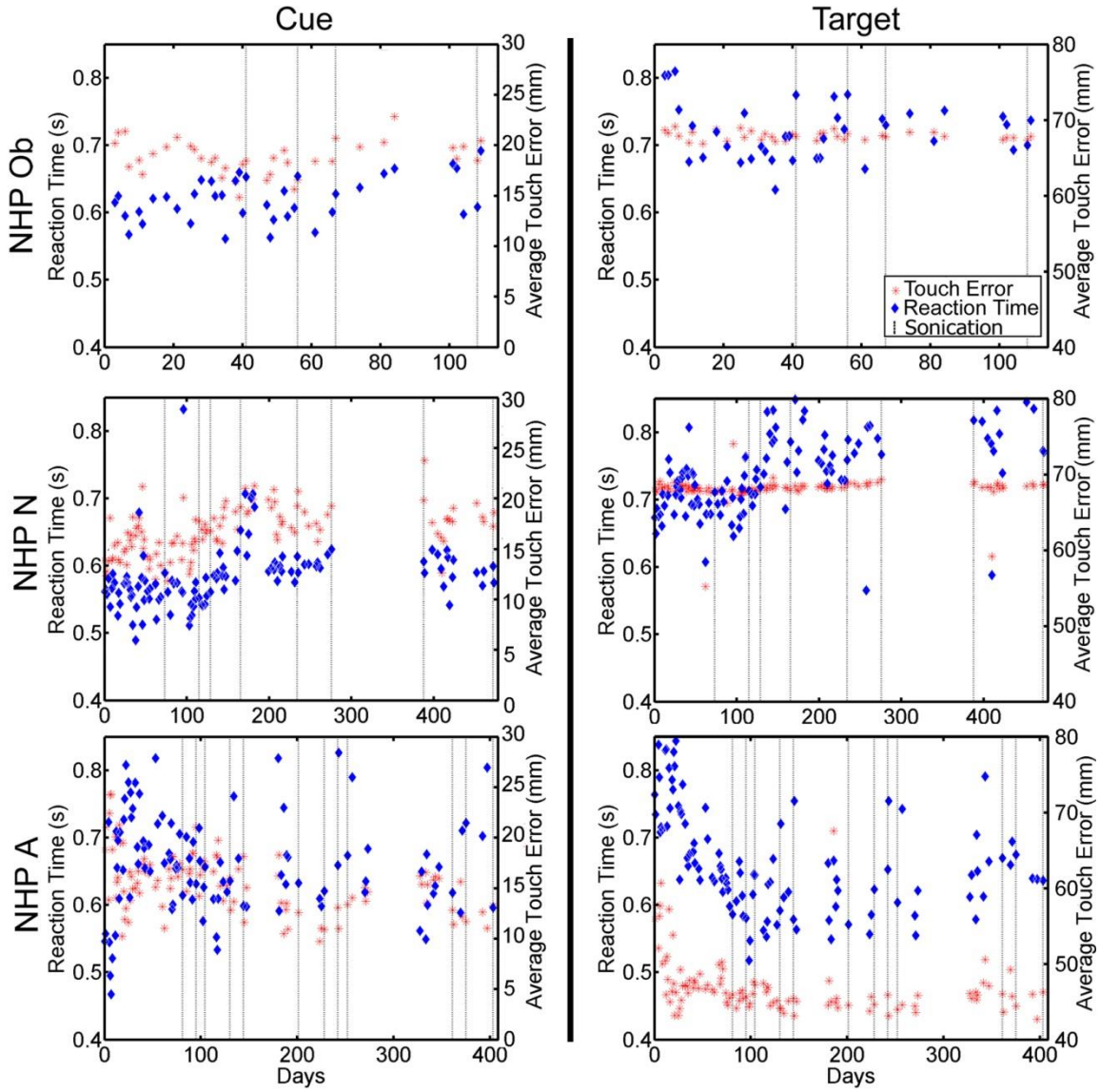

Figure 11. Raw Reaction Time and Touch Error to Initial Cue (left column), and to the Correct Target (right column). Blue diamonds indicate raw reaction time in seconds to either the initial cue or correct target. Red asterisks indicate raw touch error to either the initial cue or correct target. Reaction time is plotted on the left vertical axis while touch error is plotted on the right vertical axis. Dashed vertical lines indicate days when the FUS with MB procedure occurred.

Figure 12 shows data grouped by day relative to the day of sonication. Average RT to the cue and target increased significantly (one-way ANOVA with Tukey's HSD criterion $p < 0.05$) for all NHP on the day of the FUS with MB procedure compared with other days. Figure 12 shows that for NHP N and Ob there was a decrease in RT on days 2 and 3 after the FUS with MB procedure compared to the other days. A similar decrease was only observed on day 4 for NHP A. Within five days RT had returned to baseline for all NHP.

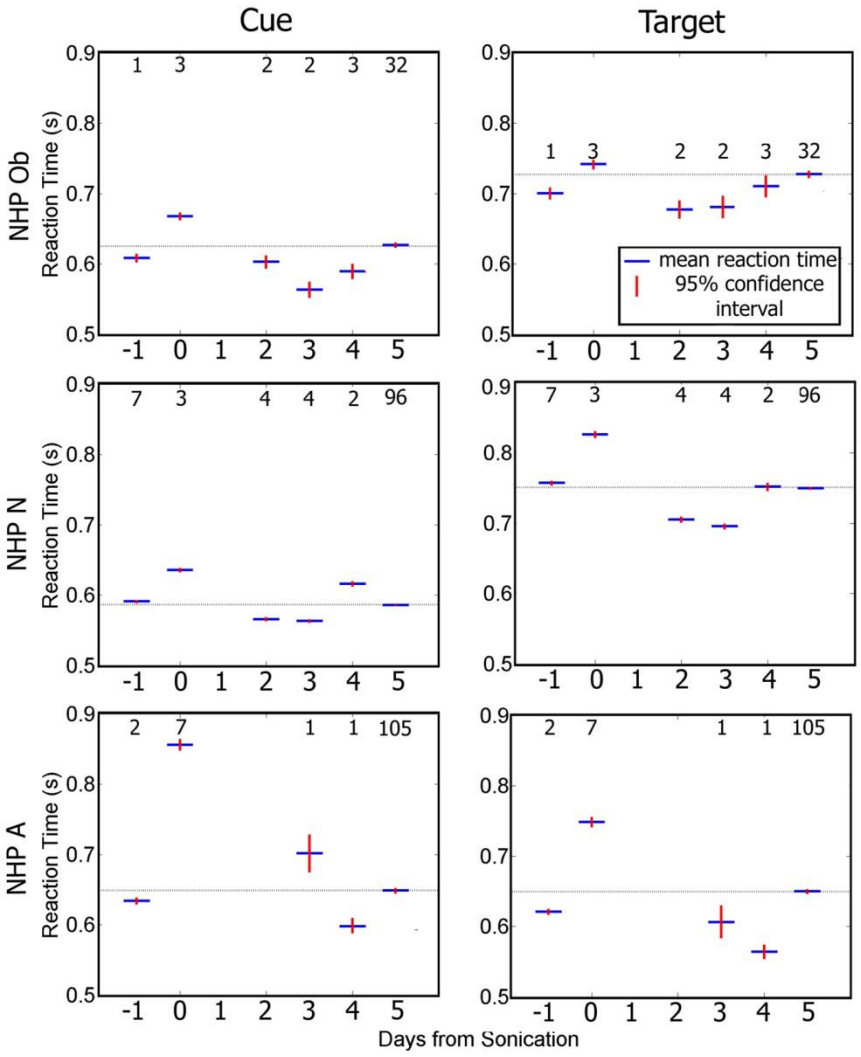

Figure 12. Average Reaction Time to Initial Cue (left column), and to the Correct Target (right column). Blue indicates group average while red is the 95% confidence interval for the mean.

For all NHP there is a significant increase in reaction time on day 0 compared to the rest of the days ($p < 0.05$). The numbers above each average indicate the n value for that group. The horizontal bar indicates baseline reaction time.

Touch error (TE) was assessed as the distance from where the NHP touched the screen to the center of the cue or target stimuli. Reaching errors are shown in Figure 13. The average TE to the cue increased significantly for NHP Ob and N but decreased for NHP A on the day of the FUS with MB procedure compared to the other days (one-way ANOVA with Tukey's HSD criterion $p < 0.05$). As shown in Figure 13, the TE to the correct target had less variance than the TE to the cue for all NHP. There was no significant change in TE to the correct target on day 0 compared with the rest of the days for NHP Ob. NHP N and A showed multiple days with significantly different TE to the correct target from that of day 0.

Each FUS procedure was performed on only one hemisphere at a time. It might be expected that sonication would have stronger effects on reaches made with the hand contralateral to the sonicated hemisphere. This result was quantified by separating responses made with the hand contralateral or ipsilateral to the treated hemisphere. The ipsi-contra difference was used because overall RT and TE can vary from day to day. Figure 14 shows the average ipsi-contra RT difference for each day. When initially reaching for the cue, all NHP showed a significant hand bias on most non-sonicated days (student t-test, $p < 0.05$), but the bias was not consistent across animals; Ob was faster with the contra hand, N was faster with the ipsi hand and A showed different biases on different days. The biases for all NHP were smaller and less likely to be significant when reaching for the target. On sonication days (day 0), none of the NHP showed significant hand biases when reaching for either the cue or target.

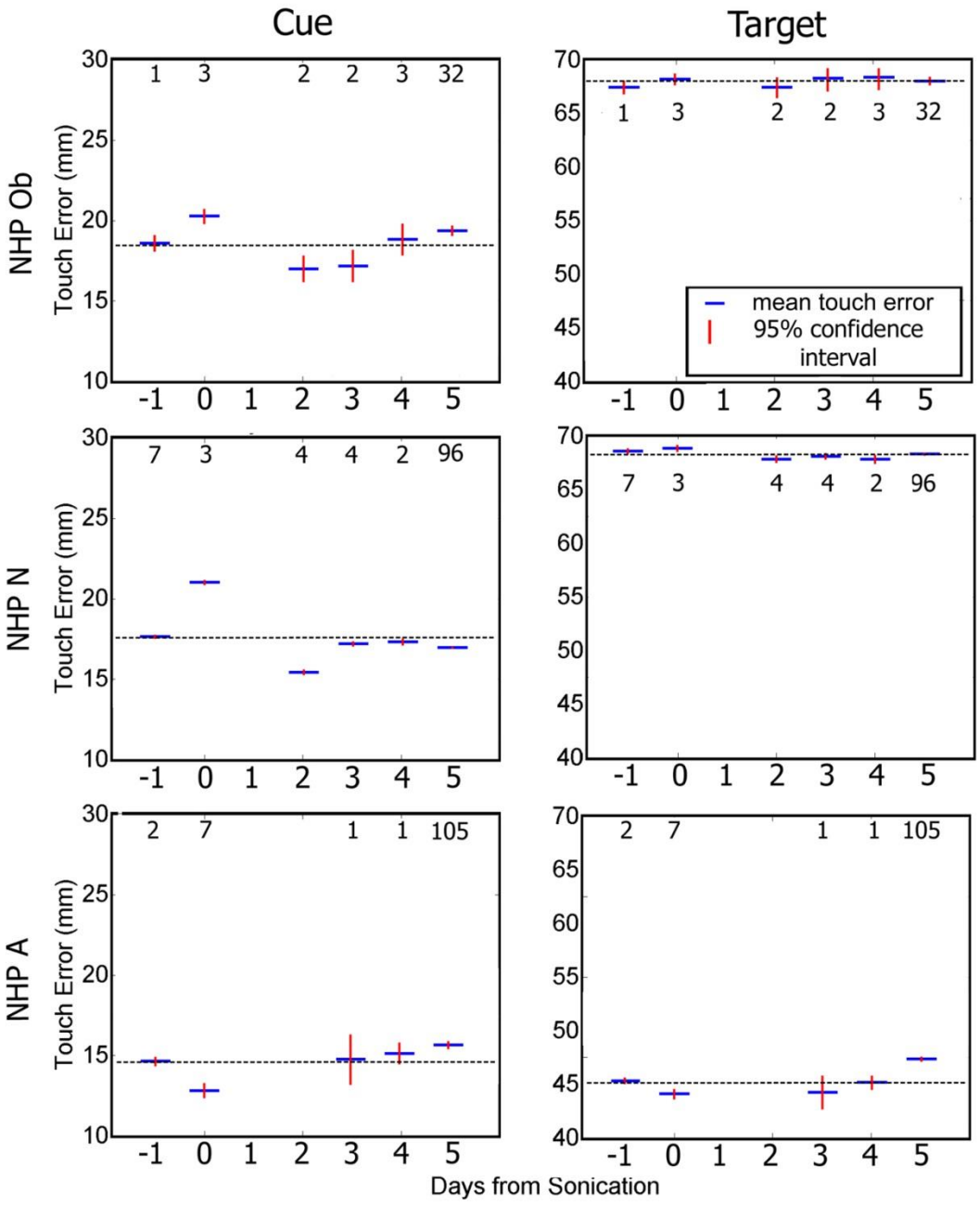

Figure 13: Average touch error to initial cue (left column), and to the correct target (right column). Blue indicates group average while red is the 95% confidence interval for the mean. There was a significant difference touch error to the cue on day 0 and the majority of the rest of the days ($p < 0.05$). There was a significant difference touch error to the correct on day 0 and some of the other days ($p < 0.05$). The numbers above each average indicate the n value for that group. The horizontal bar indicates baseline reaction time.

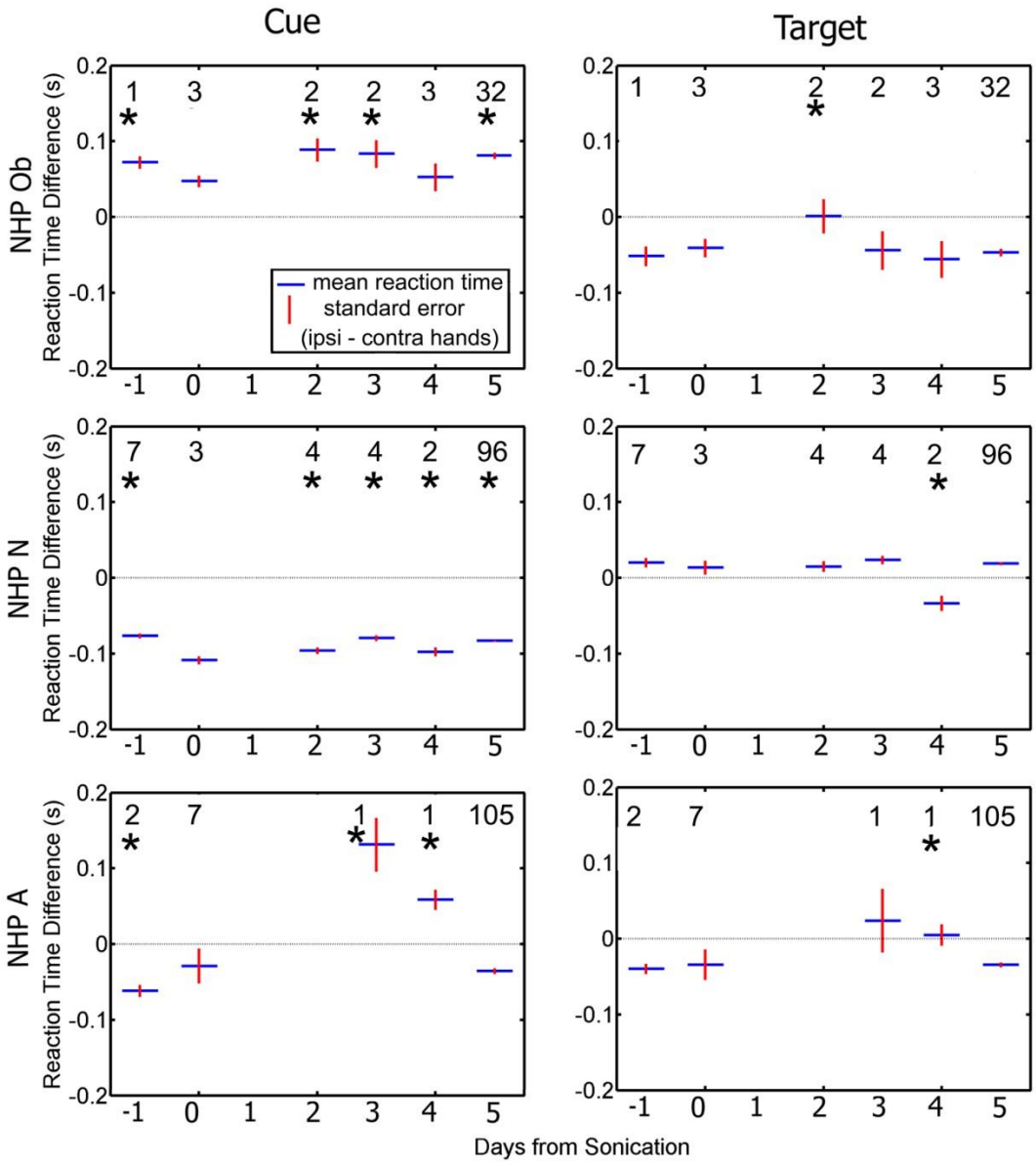

Figure 14. Difference in Average Reaction Time between the Ipsilateral and Contralateral Hands as a Function of day Relative to the Day of the FUS Procedure. Responses to the cue are plotted in the left column. Responses to the target are plotted in the right column. Blue indicates group average (average ipsilateral hand reaction time – average contralateral hand reaction time) while red is the standard error of the mean. The numbers indicate the n value for that group. Asterisks above each average indicate a significant difference between the differences in reaction time on day 0 compared to the rest of the days ($p < 0.05$).

Figure 15 shows hand bias for touch error as the difference in average TE between ipsilateral and contralateral. Similar to the RT results, all NHP show significant hand biases (student t-test, $p < 0.05$) when reaching to the cue on non-sonicated days, but no significant differences on the day of sonication. When reaching for the target, no NHP showed a significant hand bias on the day of sonication. Only NHP A showed significant differences on non-sonicated days. Considering the RT and accuracy data together, sonication tended to reduce the significance of the animal's pre-existing hand bias. However, because these biases were idiosyncratic, sonication did not systematically make reaches with the contralateral hand slower or less accurate.

Differences in RTs to high and low reward stimuli can be an index of motivation. Figure 16 shows the difference in RT between the low and high reward to the initial cue and correct target. On non-sonicated days, NHP Ob and N were faster in reaching for the initial cue and slower in reaching for the target when the reward was high. NHP A showed the opposite pattern. On sonicated days, reward magnitude had no effect on reaction time for either the cue or target.

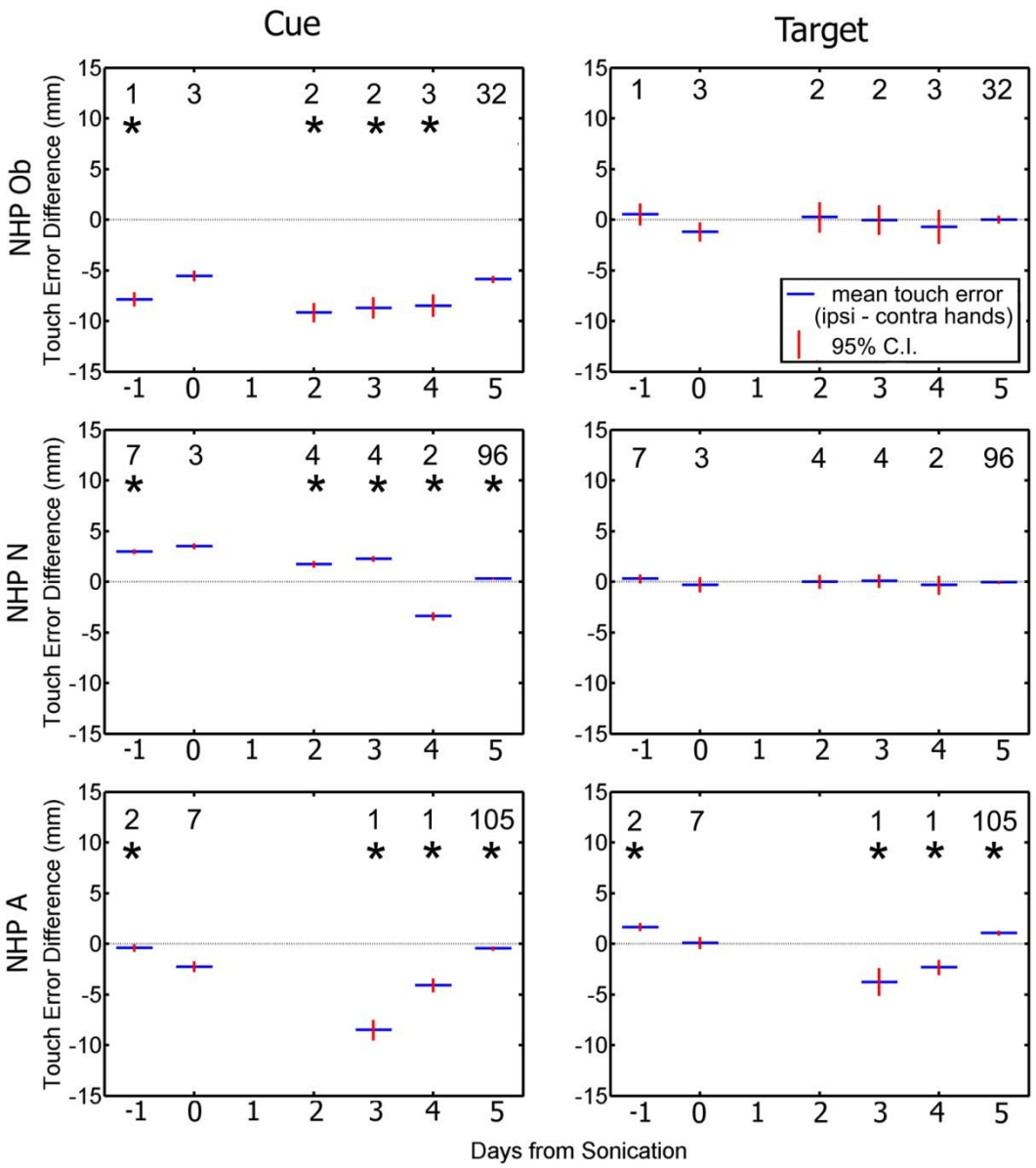

Figure 15. Difference in Average Touch Error Between Ipsilateral and Contralateral Hands as a Function of Day Relative to the Day of the FUS Procedure. Responses to the cue are plotted in the left column. Responses to the target are plotted in the right column. Blue indicates group average (average ipsilateral hand touch error – average contralateral hand touch error) while red is the standard error of the mean. The numbers indicate the n value for that group. Asterisks above each average indicate a significant difference between the differences in reaction time on day 0 compared to the rest of the days ($p < 0.05$).

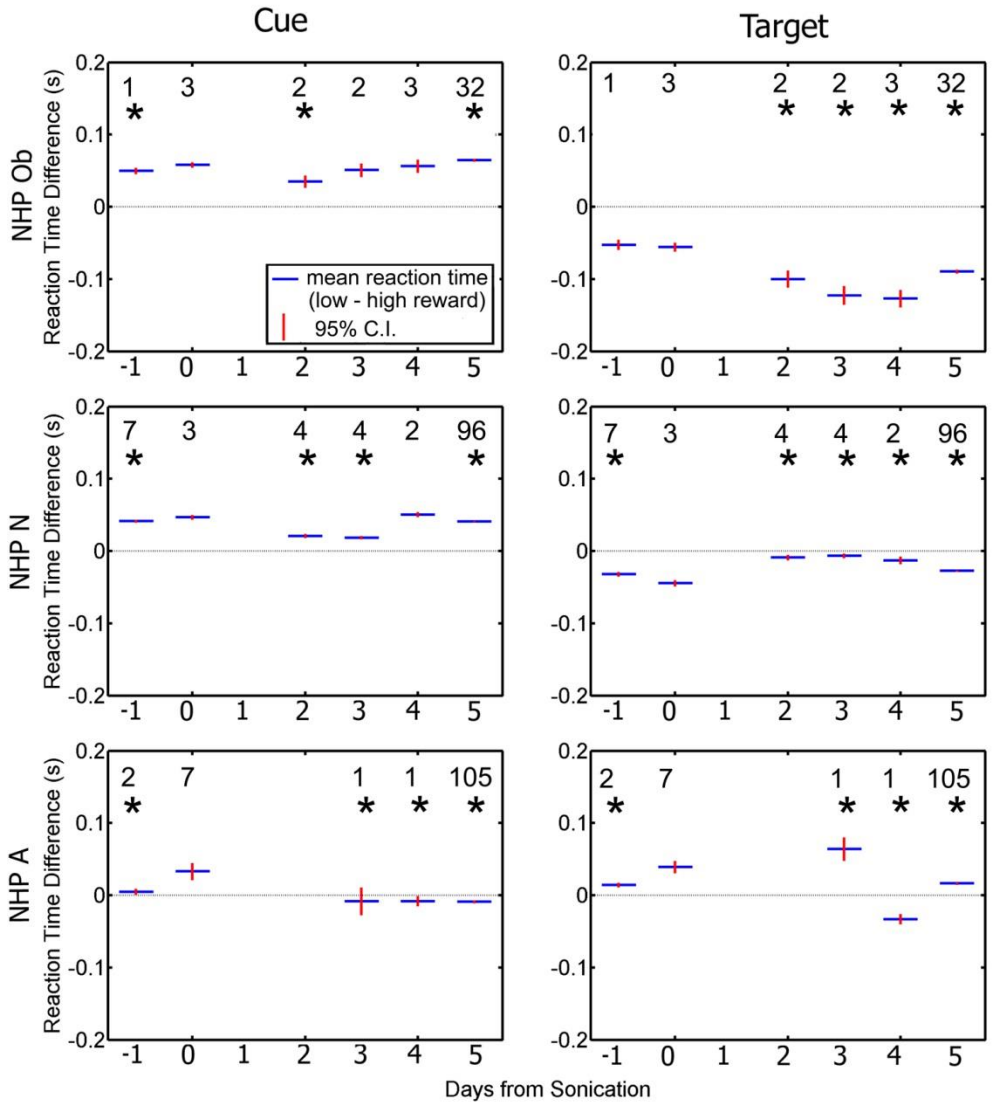

Figure 16. Difference in Average Reaction Time Between Low and High Reward as a Function of Day Relative to the Day of the FUS. Responses to the cue are plotted in the left column. Responses to the target are plotted in the right column. Blue indicates group average (average low reward reaction time – average high reward reaction time) while red is the standard error of the mean. The numbers indicate the n value for that group. Asterisks above each average indicate a significant difference between the differences in reaction time on day 0 compared to the rest of the days ($p < 0.05$).

The difference between the low and high reward on TE was also investigated. Figure 17 shows the average difference in TE between the low and high reward for both the initial cue and the correct target. On non-sonicated days, NHP Ob and N tended to be less accurate in reaching for the cue on low-reward trials (as well as being slower, as shown in Fig 16). When reaching for the target, Ob and N rarely showed any accuracy difference between low and high reward trials. NHP A showed mixed results when reaching for either the cue or target. On sonicated days, none of the NHP showed any difference in accuracy between high and low reward trials.

Considering the RT and accuracy data together, all NHP showed significant differences between high and low rewards on non-sonication days. These differences could be attributed to the motivational significance of reward size, especially NHP Ob and N's tendency to be faster and more accurate on high reward trials when reaching for the cue. The lack of any significant difference in RT or accuracy on sonicated days suggest that sonication may have slightly dampened the NHP's motivation to reach faster and more accurately for large rewards.

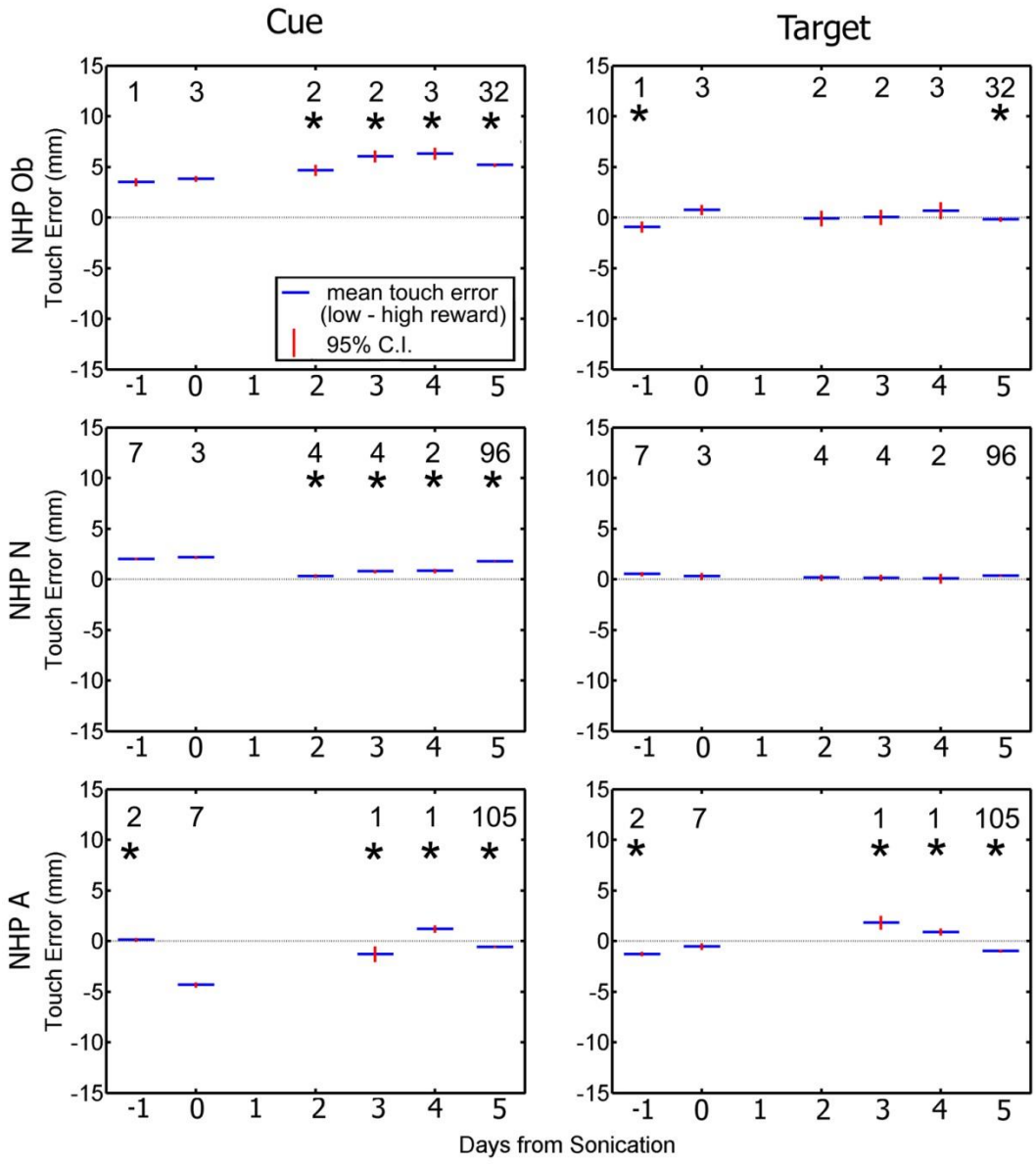

Figure 17. Difference in Average Touch Error Between Low and High Reward as a Function of Day Relative to the Day of the FUS Procedure. Responses to the cue are plotted in the left column. Responses to the target are plotted in the right column. Blue indicates group average (average low reward touch error – average high reward touch error) while red is the standard error of the mean. The numbers indicate the n value for that group. Asterisks above each average indicate a significant difference between the differences in reaction time on day 0 compared to the rest of the days ($p < 0.05$).

The previous results raise the question of whether sonication affects the NHP's cognitive abilities. Decision-making can be assessed by performance accuracy, i.e. frequency of selecting the correct target. Overall, each animal exhibited > 76% accuracy in selecting the target indicated by the dot direction which was significantly over chance. This accuracy did not significantly change on days when the FUS with MB procedure occurred (student t-test, $p > 0.05$).

A more sensitive measure of decision-making is the coherence threshold for identifying direction of motion. Coherence threshold is the percentage of coherently moving dots for which the subject correctly judged motion direction on 80% of the trials. The average coherence thresholds for all NHP were at or below 31%. Figure 18 plots percent correct direction discrimination as a function of motion coherence for NHP N. The solid curves are the Naka-Rushton curve fits to the raw data. Results for NHP Ob and A were similar. NHP N exhibited the lowest average coherence thresholds across groups for both right and leftward moving dots at 15% and 17% respectively. Coherence thresholds for each group are shown in Table 4. Thresholds were not significantly elevated on the day of sonication (day 0), if anything, they were lower, indicating that sonication did not impair (and may have improved) the NHPs motion perception or decision-making.

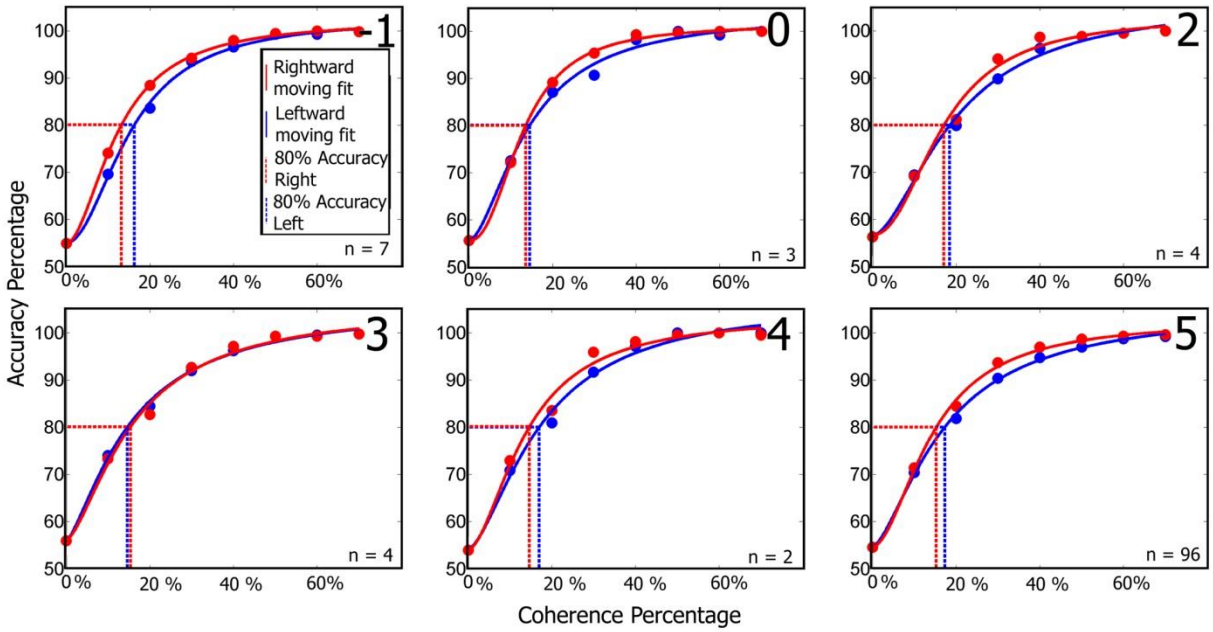

Figure 18. Naka-Rushton Model Fits of Accuracy Against Coherence for the RDM Task Completed by NHP N. The red and blue circles indicate the average percent correct for each coherence level for the right and leftward moving dots respectively. The numbers in the top left corners correspond to days relative to the FUS with MB procedure. Other NHP coherence plots follow similar trends of no large variation in response to the FUS with MB procedure.

Table 4. Dot coherence percentages for 80% accuracy.

Day	-1	0	2	3	4	5
A Right	19%	13%	N/A	24%	15%	22%
A Left	14%	22%	N/A	33%	23%	26%
N Right	13%	14%	17%	15%	15%	15%
N Left	16%	15%	19%	15%	17%	17%
Ob Right	22%	30%	66%	N/A	31%	41%
Ob Left	24%	19%	34%	30%	27%	34%

Table 4 is divided into days relative to the FUS with MB procedure, animal and the direction of the moving dots.

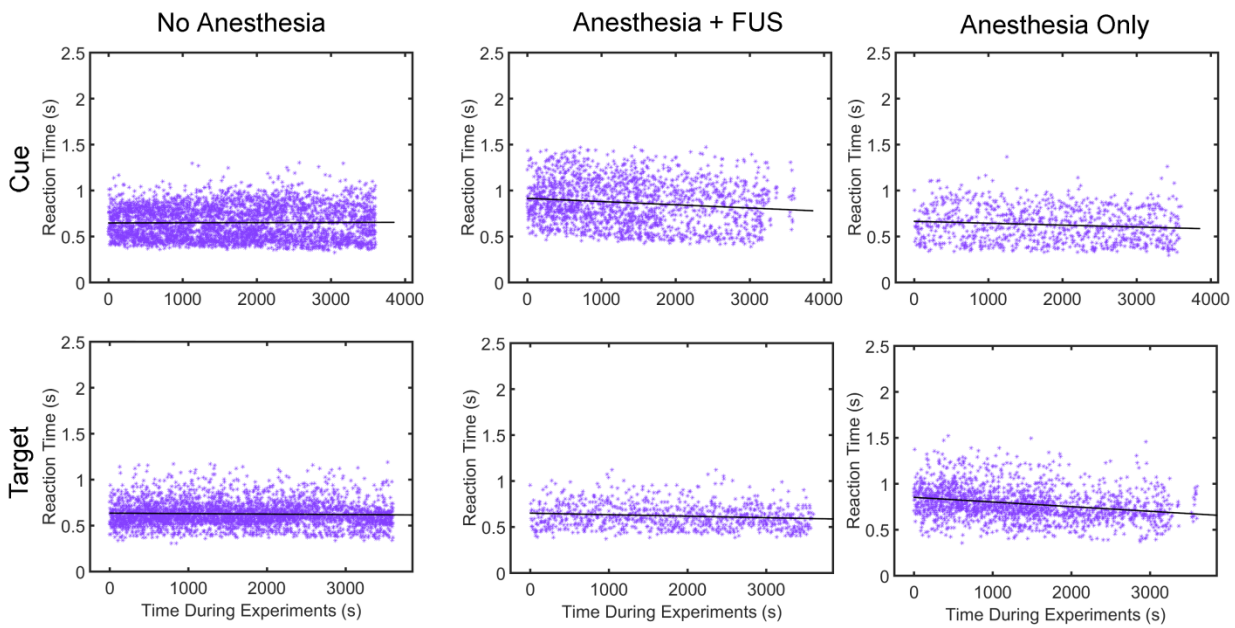

Figure 19: Raw Reaction Time Data for Alert Behavioral Testing for NHP A. Reaction times for individual trials as a function of time during the experiment. A linear regression was performed on all the data sets and is shown as the black line. The slope of the black line is positive for the No Anesthesia group, while the slope of the line is negative for the Anesthesia + FUS and Anesthesia Only groups.

Individual responses to the RMB + RDM task are shown in Figure 19. The data sets in the No Anesthesia and the Anesthesia + FUS columns are plotted in figures 11, 12, 14, and 16. A linear regression was performed on all the data sets and plotted as the black line in Figure 19. The slope of the No Anesthesia linear fit is positive while the slope of the Anesthesia + FUS linear fit is negative. Typically, as the NHP complete the task they become satiated and are less motivated to respond as quickly to the stimuli, and thus have an increase in reaction time over the duration of the experiment. This was observed in the No Anesthesia group, but the opposite was observed for the Anesthesia + FUS group. The negative slope for a linear fit is also observed with the Anesthesia Only group. This suggests that there were lingering effects of the anesthesia even after the three-hour recovery period following experiments. This analysis was

performed after the study had been completed, and thus the effects of the lingering anesthesia were not removed from the prior study figures. This linear regression analysis method was applied to all subsequent studies described in this thesis to ensure that the observed effects were not affected by the anesthesia or the FUS procedure.

The behavioral data recorded on the days when the hyperintense voxels were observed on the T2-weighted MRI scans did not significantly vary from data acquired when there were no hyperintense voxels detected (student's t-test, $p < 0.05$). Average RT and TE were not significantly different from the data acquired on other days when the FUS with MB procedure occurred. The difference in RT between the contralateral and ipsilateral hands also did not significantly vary from the other days when the procedure had occurred.

3.5 Discussion

A major hurdle for developing therapies prior to clinical trials is determining the safety of the procedure. Previous studies have shown that short-term applications of FUS with MB can safely open the BBB in multiple *in vivo* models such as mice and NHP. Here the safety for long-term applications of FUS with MB BBB opening in NHP was verified through vital sign monitoring, MRI analysis and behavioral testing. The combined results show that FUS-mediated BBB opening in the basal ganglia does not have long-term effects on the general physiology of the NHP, the structure of the targeted brain regions nor on decision and motor function.

Safety

As this technique moves closer to clinical testing, the safety of the procedure must be thoroughly investigated. During surgical procedures, heart rate, respiration rate, and blood pressure all increase with stimulation (cutting, drilling) even after the

NHP has been at a deep steady state of anesthesia for prolonged periods [129]. The vital signs monitored during the FUS with MB procedure did not exhibit any significant variations outside of normal cardiovascular or pulmonary function. Figure 8 shows inter-NHP but no intra-NHP variations in heart rate, blood pressure, respiratory rate, CO_2 emissions and SPO_2 levels. An initial drop of the heart rate occurred after induction of anesthesia and can be attributed to the effects of isoflurane (Figure 8).

Agreeing with previous long-term studies on mice, gross physiological changes in weight, food and water consumption, activity levels, mobility or emotional state with the NHP over the course of repeated FUS with MB procedures were not observed [20]. The contrast enhanced T1-weighted MRI scans obtained at least 5 days after the FUS with MB procedure at the middle and end of the experiment did not indicate increased permeability in the targeted regions. These scans show that repeated BBB opening via the FUS with MB applications does not permanently increase the permeability of the targeted area.

T2-weighted MRI and SWI sequences were used to determine possible damage at the BBB opening region. Previous work suggests that the MB size and acoustic pressure are the critical parameters in dictating both the opening size and safety [14, 130]. Only NHP N and A exhibited hyperintense spots in the T2-weighted MRI sequences for one and three applications of FUS with MB, respectively. The hyperintense spots on the T2-weighted scans suggest possible, blood, or edema [92]. There was no hypointense signal in the same area for the SWI scans, which eliminates the possibility of hemorrhage [131]. To rule out permanent lesions T2-weighted and SWI sequences were acquired a week after the initial detection and revealed no hyperintense or hypointense voxels in the region where they were previously observed (Figure 10). Thus, the hyperintense spots could have been caused by edema which was cleared over the course of a week. The acoustic pressures used for these cases were 300kPa for NHP A and 400kPa for

NHP N with 4-5μm MB. Previous pressures of 440-700 kPa with Definity MB were shown to cause hypointense spots in T2*-weighted imaging as well as hemorrhaging in the thalamus region after histological investigation [16]. In the current study, the NHP were not euthanized as they were already selected to be used in future experiments and therefore histology was not available. This was a limitation to the scope of this study as the histology might have revealed blood cell extravasation, neuronal death or an immune response in the areas of repeated BBB opening. From previous studies where histology was conducted after short-term application of the FUS with MB procedure on NHP, one could expect some petechiae and possible damaged capillaries [16]. No significant variations in RT or TE on days when the hyperintense voxels were detected compared to the days without any hyperintense voxels. Thus, the presence of possible edema did not have an effect on the behavioral results for that given day. Over the course of all FUS with MB procedures, there was no change in the NHP ability to perform daily functions or a change in their disposition. With the parameters and targets selected within this study, it was demonstrated that repeated FUS with MB procedures could be safely applied long-term.

As mentioned previously the parameters utilized for the FUS with MB procedures within this study were originally derived from previous studies in the Konofagou lab [12, 15]. Although the NHP are within the same relative size/age group, each NHP has FUS parameters that are optimal for them. NHP A and O were smaller subjects (5-6kg) and substantial BBB opening could be achieved with lower pressures (300 kPa), while NHP N and Ob (8-9kg) were physically larger and required higher pressures (400 kPa) to achieve similar opening sizes. These selected pressures also allowed for safe BBB opening with the majority of the experiments conducted in this study. This supports the notion that while there are general guidelines for parameters ensuring safe BBB opening for a specific species, optimized parameters should be

identified for individual subjects. This will be important in the future when the FUS with MB procedure makes the step into the clinic with patients.

Behavioral task

The regions of the basal ganglia targeted in these experiments are involved in decision-making and motor control. Gold and colleagues have shown that neurons in the caudate nucleus of NHP signal decision variables during a random-dot motion task similar to the one used in this study [132]. Hikosaka and colleagues have documented the involvement of the caudate in reward-based reaction-time differences [109, 120]. Pilot experiments in our lab undertaken in preparation for the current study also provided evidence that targeting the basal ganglia with FUS technique can have profound behavioral effects. In one NHP (M, adult male rhesus), unilateral delivery of FUS with MB to the caudate resulted in hemispatial neglect contralateral to the treated hemisphere that lasted for roughly 24 hours. This was likely due to excessive FUS pressure. For the results reported from the experiments in this study, no NHP responded to the FUS procedures with physical deficits as discussed above.

The RDM + RMB task was well suited for determining if there were any effects of the FUS with MB procedure on either the motor signal pathway or the decision making pathways associated with the basal ganglia [26, 106]. Movement commands initiated in the motor cortex are processed through the basal ganglia and the cerebellum before being sent to the spinal cord [106]. The dorsal parts of the caudate and putamen are associated with sensorimotor function while the ventral parts are associated with limbic functions [107]. Thus, if the FUS with MB procedure disrupted the pathways in the basal ganglia regions, motor and decision making deficits should be observable [107]. It is of interest that there was a significant increase in the RT to both the initial cue and the correct target on the day of the FUS procedure for all NHP, but this returned to baseline

within five days. Similarly, the average TE to the initial cue was elevated for NHP N and Ob and decreased for NHP A, which also returned to baseline within 5 days. Behavioral testing that occurred on the same day as the FUS procedure was done several hours after the procedure, and therefore after a period of about an hour of anesthesia. However, it was unlikely that the isoflurane had an effect on behavioral responses. It has previously been shown that isoflurane has the fastest recovery time of anesthetic drugs for NHP with a recovery time of 20 minutes even for high doses (3-4%) [129]. Lower doses of isoflurane (2% max when placing the NHP into the stereotax) were applied, and the dosage was decreased to 0.5% during the final five minutes of the procedure minimizing their total exposure to anesthesia.

Examining the RT difference between hands was a useful indicator if the FUS with MB procedure had disrupted the motor processing pathways in the basal ganglia as only one hemisphere was targeted during each procedure. Similar to humans, NHP have a preferred hand for most tasks, and thus have faster RT for that hand [134, 135]. This hand preference can be seen on the baseline days (-1, 5+) for the RT to the cue for all NHP in Figure 14. If the FUS procedure had affected the basal ganglia only in the targeted hemisphere, the effects should have been observed in the contralateral hand, thus changing the difference in RT between the two hands. As the average difference RT between the ipsilateral and contralateral hand to the initial cue for NHP N and A was below 0 indicating his ipsilateral hand was dominant for both the baseline days and days where the FUS procedure occurred. Similarly, average difference in RT between hands for NHP Ob was above 0, indicating his contralateral hand was dominant. Interestingly this dominance switches when responding to the correct target for both NHP Ob and N. This inversion in dominance to the correct cue and correct target was not observed in NHP A. Regardless, hand dominance was not affected by the FUS with MB procedure for any of the NHP. The results do not indicate that the FUS

procedures have an effect on handedness nor specifically on the RT of the contralateral hand for two of the three NHP.

As expected with the RMB portion of the task, most of the NHP responded with faster RT to the high reward cue, than the low reward cue for most of the days as the average difference between the low and high reward was above 0 (RT to cue seen in Figure 16). These results agree with previous studies where NHP made saccadic eye movements to complete an RMB task [120]. In that study, NHP had faster saccades to the high reward, while slower saccades to the low reward. The bias in responding faster to the high reward was reversed for RT to the correct target as the average difference in RT between the low and high reward was below 0 indicating a faster response to the low reward. This could be attributed to a speed accuracy tradeoff, as the higher reward was more salient and thus the NHP took additional time to select the correct target [136]. The responses from NHP A were more varied across days and did not show the bias that was observed in both NHP N and Ob. The bias seen with NHP N and Ob was not affected by the FUS with MB procedures. Overall, the FUS with MB procedures did not have an effect on the reward bias for the two NHP that followed the paradigm originally.

Touch error was an important factor for determining if the FUS with MB procedure had an effect on the basal ganglia. If the average distance between the target and the point where the NHP touched the screen increased or became more erratic between separate days to the point of significant variation, it could indicate that the FUS BBB opening procedure had an effect on the voluntary motor control pathway [107]. As with Parkinson's, the disruption of the motor pathway can lead to undershooting when reaching for a target [137]. As seen in Figure 13 most NHP showed a significant difference between day 0 and the other days for the initial cue. There were fewer days with a significant difference in TE to the correct target between day 0 and the other

days. This could have been caused from the prior position of the NHP hand before selecting the correct target, as it would be in the relative same position for each trial having just selected the initial cue. There would be more variation in TE to the initial cue as the NHP could have its hand resting in various positions before reaching to the initial cue, increasing the variability of the TE. NHP N did not exhibit any significant variation of the TE to the target between day 0 and the other days over the duration of the behavioral recordings independent of hand or reward magnitude. NHP Ob only showed two days where there was a significant difference in TE to the correct target between day 0 and the rest of the days with respect to reward magnitude, but similar to NHP N did not show any significant variation with respect to the difference between hands. This indicates the FUS with MB procedure did not have an effect on touch error to the target.

The RDM component of the task tested whether the FUS with MB procedure was having an effect on the decision-making pathways associated with the basal ganglia [138, 139]. The coherence threshold in Figure 18 does not vary more than 4% across each group. The variance of the detection threshold between days and the individual daily threshold for detection was low and consistent with previous investigations using the RDM task for the majority of the days [140, 141]. NHP Ob exhibited the largest variation between baseline coherence threshold and the day of the FUS with MB procedure with a 10% variation, while NHP A and N exhibited less than 8% variation. This percentage was comparable to variation between non-FUS with MB procedure days and does not indicate the FUS with MB procedure had an effect on the decision-making pathways in the basal ganglia of the NHP subjects.

3.6 Conclusion

As FUS mediated BBB opening moves closer towards clinical feasibility, the safety of repeated FUS BBB opening procedures must be characterized in the NHP model. Here the results demonstrate that repeated BBB opening at the caudate and putamen regions in NHP can be achieved safely without hemorrhage or permanent edema, and to not cause a permanent effect on RT and decision making responses with the applied FUS parameters. The findings support that FUS is a promising technique for clinical applications as it is the only non-invasive procedure that can be used to chronically and accurately open the BBB safely in both cortical and subcortical regions of the brain without causing damage to the structure or neurological pathways within it.

3.7 Contributions

In this chapter, the safety and efficacy of chronic FUS BBB openings in the basal ganglia of NHP was investigated. While there was one prior study that repeatedly applied this technique to NHP, their study was short-term and lasting a maximum of six weeks. For the first time the results demonstrate that the FUS technique can be applied to the same brain structure over a period of 4-20 months without any long-term side effects. This is critical as the technique progresses towards clinical testing in humans. As current drug therapies treating neurological diseases such as PD require repeated drug administration, this technique may need to be applied for long periods, facilitating the delivery of therapeutic drugs. Results from this study determining the behavioral effects was also important to explore before starting the FUS mediated drug delivery in specific aim 2. It was shown on the day of the FUS procedure, there was an effect on behavior, but this effect was not long lasting and behavioral results returned to baseline within five days. This chapter also introduced the BBB opening analysis

pipeline, along with the base pipeline for behavioral testing which was utilized in the following chapters. The results discussed here have all been published in peer reviewed scientific journal [19].

Regarding the research contributions, Tobias Teichert, PhD (Neuroscience, Columbia University) and Fabrice Marquet PhD (Biomedical Engineering, Columbia University) originally mentored and assisted with the initial FUS experiment. Shih-Ying Wu MS (Biomedical Engineering, Columbia University) assisted with the initial FUS experiments. Carlos Sierra Sanchez, PhD (Biomedical Engineering, Columbia University) and Marilena Karakatsani, MS (Biomedical Engineering, Columbia University), assisted with the FUS experiments and the microbubble fabrication for experiments. Amanda Buch, BS (Biomedical Engineering, Columbia University) assisted with the FUS experiments, the microbubble fabrication for experiments and with the behavioral testing. Shangshang Chen, BS (Computer Science, Columbia University) assisted with the behavioral testing and microbubble fabrication for experiments.

Chapter Four

Specific Aim 2

Drug Delivery to the Basal Ganglia via Focused Ultrasound with Microbubbles Blood-Brain Barrier Opening in Non-Human Primates and Mice

Prior studies verified the delivery of various neuroactive molecules to the brain parenchyma via FUS to treat brain tumors or promote neurogenesis, yet none of those investigations delivered molecules causing a pharmacodynamical effect on the response of the subjects to behavioral testing. The second aim of this thesis addresses this issue and explores the potential of using the FUS technique to deliver large molecules, as well as low doses of D2-antagonists, to the basal ganglia in mice and NHP to elicit pharmacodynamical modulation of their behavior. The study here builds on the findings in chapter 3 and takes into account the effects of the FUS technique on the behavioral testing on day 0. Thus, the effects of successful drug delivery can be determined without the confounding effects of the FUS technique.

4.1 Abstract

The native blood-blood brain barrier (BBB) promotes brain homeostasis, but also greatly impedes the treatment of neurological disorders such as Parkinson's or Alzheimer's disease by preventing 99% of currently available drugs from crossing into the brain parenchyma. Focused-ultrasound with intravenously administered microbubbles (FUS) has been shown as a technique to non-invasively open the BBB in specific brain regions. Here the FUS technique was used to open the BBB in anesthetized non-human primates (500 kHz, 200-400 kPa, 4-5μm MB, 2-minute sonication) and in anesthetized mice (1.5 MHz, 300 kPa, 4-5μm MB, 60-second

sonication) to deliver a low dose of D2-antagonists (haloperidol or domperidone) to the basal ganglia. After administration of the D2-antagonist, behavioral testing was conducted with each species. The open field and rotarod test were employed to test the motor effects of low dose haloperidol on mice after opening the BBB in the striatum. There was a significant decrease in motor activity of mice during the open field test for the group when low dose haloperidol had been administered after the BBB was opened. The NHP performed a random dot motion with reward magnitude bias behavioral task to quantify the effect of the low dose haloperidol on their cognitive, motivational and motor function. Behavioral results show successful delivery of haloperidol after the BBB was opened with a significant increase in the reaction time to the target stimuli. There was also a significant increase in touch error to the initial cue with the hand contralateral to the application of the FUS technique for all NHP. There was no significant effect on the threshold level of dot motion coherence, but there was an increase in overall accuracy to the task for 2/3 NHP. After administration of domperidone following BBB opening targeting the caudate, two of the NHP exhibited hemilateral neglect on the side of their body contralateral to the FUS application. Overall, the results show that the FUS technique can be effecting in facilitating delivery of low dose drugs for pharmacodynamical behavior modulation.

4.2 Introduction and Study Design

As mentioned previously, the blood-brain barrier (BBB) is ubiquitous in all vertebrate physiological systems and regulates the flux of molecules into the brain parenchyma [35]. The protective benefits of the BBB is also a major hindrance when attempting to treat neurological diseases or disorders as it blocks 99% of all small molecule, and almost all large molecule drugs from crossing into the brain [4]. The tight junctions between the endothelial cells act as a physical and metabolic barrier excluding non-lipid soluble molecules as well as molecules larger than 400-600 Da [142] Current

techniques to circumvent the BBB for drug delivery either provide target specificity through invasive procedures, or have nonspecific delivery and are non-invasive [81, 82, 83]. Focused ultrasound coupled with microbubbles (FUS) has been proven to non-invasively open target specific locations in the BBB with multiple *in vivo* models [9, 10, 11, 12]. This technique also allows the BBB to close within hours to days, providing a complete non-invasive procedure to circumvent the BBB [14].

The development of the FUS technique as a non-invasive method to facilitate drug delivery has two specific applications; the first to facilitate the treatment of neurological diseases and disorders in the clinic, the second as a simple technique allowing non-invasive drug delivery for neuromodulation during behavioral experiments within the laboratory. Multiple groups have utilized the FUS technique to delivery various neuroactive drugs across the BBB [21, 22, 23, 93, 94, 95, 96, 97, 98, 99, 100, 101, 102, 103, 104]. These experiments usually involve the treatment of preexisting neurodegenerative disorders, or deliver agents to provide neuroprotection or neuroregeneration. Doxorubicin, a drug utilized in cancer chemotherapy, has been successfully delivered to the rat brain for treatment of tumors after applying the FUS technique to the diseased region of the brain [22]. Neuoprotective and growth factors such as neurturin and GDNF have also been delivered in mice brains after the FUS procedure [21, 103]. The successes of the aforementioned studies were validated by the reduction of the targeted tumor, or the prevention of neurological tissue damage in Parkinson's disease (PD) model mice. Recently, McDannold *et. al.* showed a dose dependent suppression of somatosensory evoked potentials when GABA was delivered to the somatosensory cortex in rats [105]. To date, FUS facilitated drug delivery for neuromodulation to external stimuli has not be investigated in NHP.

Another challenging issue with treating neurological diseases using current drug therapies is the potential negative side effects from the drugs [143, 144, 145, 146]. A

common treatment for Parkinson's disease involves daily doses of levodopa [147]. Since dopamine cannot cross the BBB, levodopa, which can cross the BBB, is administered orally and is converted into dopamine once it reaches the brain parenchyma [148]. Although this technique can be effective in the treatment of PD, levodopa is not brain region specific and increases the dopamine levels throughout the brain. Chronic applications of levodopa can also cause negative debilitating side effects such as dyskinesia [149]. The FUS technique could enhance current or pipeline drug therapies by allowing targeted delivery of the drug to brain regions intended for interaction with the drug. This would allow for a lower administered dose, reducing the overall chances for adverse side effects.

In this study, the results demonstrate that the FUS technique is an effective tool for delivering low dose D2-antagonists to the basal ganglia region in both mice and NHP. Haloperidol and domperidone were selected as the D2-antagonists as domperidone does not readily cross the native BBB, while haloperidol can [150, 151]. A threshold dosage of haloperidol was determined as a dose that did not significantly affect behavioral testing after administration when the BBB was intact. This threshold dosage was used to explore if a low dose of a drug could achieve the same therapeutic effects when the BBB was opened at the target region as a full dose of the drug while the BBB was intact. The basal ganglia region was selected as it has been associated with voluntary motor control, motivation and decision-making [120, 121, 122]. After opening the BBB with the FUS technique and administering the D2-antagonist, each species completed behavioral tasks to determine the effect of the drug. The NHP performed either a random dot motion with reward magnitude bias task testing cognitive, motivational and motor function (haloperidol experiments), or were observed in an open field (domperidone experiments). Mice performed an open field and rotarod test to determine any motor effects. MRI verification of the safety of the FUS technique as

well as verification of the BBB opening was conducted with both species. Behavioral results with both species indicate successful delivery of both haloperidol and domperidone to the basal ganglia.

4.3 Materials and Methods

Subjects and Ethics Statement

The procedures with NHP described in this study were approved by the Institutional Animal Care and Use Committees (IACUC) of Columbia University and the New York State Psychiatric Institute (NYSPI). Two adult male Macaca mulatta (NHP: N, Ob) and one adult Macaca fascicularis (NHP: A) were used in all experiments (9-20 years old, 5.5-9.5 kg). Husbandry practices employed during these experiments were described in chapter 3.3.

For the mice experiments, all procedures were approved by the Columbia University IACUC and Columbia University's Research and Compliance Administration System. Fifteen wild-type adult male mice (strain: C57BL/6, Harlan Sprague Dawley, IN, USA), weighing 20-25g were used for the mice experiments. There were three study groups of n = 5: Haloperidol/FUS+, Haloperidol/FUS- and Saline/FUS+. All mice were housed in husbandry rooms with a 12-hour light dark cycle with an average temperature of 22°C. The mice were provided standard rodent chow (3 kcal/g; Harlan Laboratories, IN, USA) and bi-distilled water *ad libitum*.

FUS Procedure

The MB used in the both the mice and NHP procedures were fabricated in-lab a day before the FUS procedure and size isolated for an average diameter of 4-5μm [126].

The FUS technique applied to all anesthetized NHP was previously described in chapter 2.3. The FUS technique was applied to NHP A 10 times, (n = 5 per behavioral group, Haloperidol/FUS+, Saline/FUS+) and the technique was applied a total of 8 times to NHP Ob and N (n = 4 per behavioral group, Haloperidol/FUS+, Saline/FUS+).

The FUS technique for the mice was conducted with a single-element spherical-segment 1.5 MHz FUS transducer. The center of the transducer was bored out allowing placement of a 10 MHz pulse-echo transducer for target alignment. The focal regions from both transducers were aligned. The FUS transducer was driven by a function generator (Agilent, CA, USA) with a 50-dB amplifier (E&I, NY, USA). A cone of degassed water was coupled with the transducer submersing the bottom membrane of the cone into a water bath above the head of the mouse. Anesthesia of the mice was maintained using 1.25-2% isoflurane mixed with oxygen. Mice were placed into stereotax positioning with incisor and ear bars. Targeting was achieved by positioning the transducer over the caudate/putamen region relative to the sagittal suture. The same MB used in the NHP experiments (chapter 3.3) were administered via tail vein injection as a bolus of 1ml/g with a concentration of 8×10^8/mL. An acoustic pressure of 300kPa with a PRF of 5 Hz at 100 cycles and a 60-second sonication duration were used for all mice FUS applications.

Drugs

Haloperidol, a D2 antagonist (R&D Systems, Inc., Minneapolis, MN), was selected as the drug for neuromodulation. Haloperidol powder was dissolved in saline and titrated to the concentration of 0.01mg/kg. D2 receptors in the putamen have been implicated with the indirect pathway between the striatum and the substantia nigra [152]. Before the task began, NHP were administered either saline or haloperidol (0.01mg/kg) intramuscularly. The threshold dose of haloperidol was determined as the

maximum dose to not elicit a significant difference on the behavioral results compared to saline injections when the BBB was intact. On days when the FUS technique was applied, a five-hour wait period occurred before behavioral testing began allowing the NHP to fully recover from the anesthetics.

Domperidone, another D2-Antagonist, was also selected for behavioral drug trials (Sigma Aldrich, MO, USA) [150]. Domperidone was initially dissolved in a low pH solution (0.5M lactic acid and saline) and titrated back to blood pH levels (between 7.35-7.45). Domperidone was either administered five days after the most recent FUS application (to ensure BBB was closed) or three hours following FUS applications targeting the caudate.

Behavioral Testing

All NHP were fully trained for three months to respond via touch to visual stimuli presented on a 20-inch color LCD touch panel display (NEC 2010X with 3M SC4 touch controller). The behavioral task was a random dot motion (RDM) decision-making task with a reward magnitude bias (RMB) paradigm [120, 121, 122] The full description of the behavioral task employed can be found in chapter 3.3. As before, reaction time to the cue was defined as the onset of the cue stimulus appearing on the touchscreen monitor to the first contact recorded by the touchscreen. Reaction time to the target was defined as the onset of the target stimuli appearing on the touchscreen monitor until the first contact recorded by the touch panel. Touch error was defined as the distance between the point of first contact to the touchscreen monitor and the center of the stimuli.

The pharmacodynamical effects of domperidone after opening the BBB at the caudate in NHP were observed in a controlled open field test. Following application of

the FUS technique the NHP were allowed to regain muscle posture (ability to sit up unassisted) and placed in a primate work chair. This allowed monitoring of the NHP and prevention of the NHP removing the IV catheter. Three hours after the application of the FUS procedure targeting the caudate region, domperidone was administered IV (2.5 mg/kg). Following injection NHP were allowed to move around the surgery suite while attached to a guidance pole. During this time qualitative observations from graduate student, professors as well as veterinary staff at NYSPI were recorded. Following this observation session NHP were returned to their husbandry rooms.

All mice were tested with the open field and rotarod behavioral test on day -1 (one day prior to the FUS application). This was to establish a baseline for each individual animal. The open field test had a duration of ten minutes and recorded the total distance traveled, amount of rotations, and direction of rotations. The rotarod test lasted for a maximum of 200 seconds with a linearly increasing speed to 40 RPM. Mice were always tested with the open field before the rotarod test and given a ten-minute break between tests.

MRI Analysis

All MRI scans (3T, Philips Medical Systems, MA, USA) for verification of safety and BBB opening in NHP were acquired 36 hours after the FUS procedure. Due to initial sedation for the FUS procedure, the NHP were not allowed to be anesthetized a second time in the same day, thus the MRIs were acquired on day 1. The MRI parameters used to acquire the images, as well as the image post processing were discussed in chapter 3.3.

To validate the BBB opening in mice, the mice were anesthetized and placed into a 9.4 T vertical bore (DRX400, Bruker Medical, Germany) to acquire FLASH T1-

weighted 2D scans (TR: 230 ms, TE: 3.3 ms, NEX: 18, resolution: 86 μm x 86μm, 500 μm slice thickness, FOV: 22 mm x 16.5mm). These scans were acquired pre and post administration of contrast agent (gadodiamide). For safety verification T2-RARE sequences were acquired (TR: 330 ms TE: 10.9 ms, FOV: 22mm x 16.5mm, resolution: 86 μm x 86μm, 500 μm).

Data Analysis

The data acquired for each NHP conducting the RDM + RMB task were divided into four groups determined by the drug administered (saline or haloperidol) and if the FUS technique had been applied on that day, or had not been applied for a minimum of 5 days. The four main data groups were Haloperidol/FUS+, Haloperidol/FUS-, Saline/FUS+ and Saline/FUS- (the + and – here indicate days when the FUS procedure occurred and did not occur respectively). Prior studies had shown the BBB in NHP closes within three days of opening, thus selecting five days for the FUS- groups gave an additional two days to ensure the BBB was closed [15]. As discussed in chapter 3.4, the longitudinal safety study found applying the FUS technique to anesthetized NHP had an effect on their behavioral testing results on the same day (day 0) [19]. Thus, a linear regression was performed on the Saline/FUS+ data set and used to remove effects of the sonication from the Haloperidol/FUS+ data set. Linear regression was also performed on the Saline/FUS- to normalize the Haloperidol/FUS- group. This normalization was done with independently for the cue and target stimuli for both reaction time, and the touch error data.

Average reaction times (RT) were calculated for both normalized Haloperidol/FUS+ and Haloperidol/FUS- groups. Significance between groups was determined with the student t-test ($p < 0.05$). These main two data groups were then divided by hand, and reward magnitude. Comparisons of the average RT and TE

between the subgroups were done with student t-tests ($p < 0.05$). The difference in touch error between the Haloperidol/FUS+ and Haloperidol/FUS- groups for individual parameters (high, low reward; ipsilateral, contralateral hand) was found for each NHP. The change in RT and TE between those two main groups was determined to be significant if the 95% confidence interval for each mean did not overlap.

The accuracy in discerning the coherent direction of dot motion was divided similarly into the initial four main groups: Haloperidol/FUS+, Haloperidol/FUS-, Saline/FUS+ and Saline/FUS-. The performance accuracy for each hand with the main groups was sorted by coherence level and fit with a Naka-Rushton psychometric curve. The psychophysical threshold for detecting the direction of motion was determined as the coherence level corresponding to an 80% correct response to the task. These coherence thresholds were then compared across groups using student t-test ($p < 0.05$). Overall accuracy at selecting the correct target was determined for each group, and the significant difference in accuracy between groups was determined with a student t-test ($p < 0.05$).

Distance traveled, total rotations per direction and duration spent on the rotarod were analyzed from the mice behavioral experiments. Analysis was carried out with a 1-way ANOVA ($p < 0.05$) to detect variation between the groups (Haloperidol/FUS+, Haloperidol/FUS-, Saline/FUS+). Student t-test ($p < 0.05$) was used to determine significance between individual groups.

4.4 Results

4.4.1 Low Dose Haloperidol in NHP

MRI Analysis

Contrast enhanced T1-weighted MRI scans verified the BBB remained open 36 hours (day 1) after the FUS procedure for 75% of the cases. NHP A and Ob still exhibited BBB opening at day 1 while NHP N only expressed a 42% detection of BBB opening on day 1. The red transparent overlays in Figure 20 show typical cases of detected BBB opening on day 1. For both NHP A and Ob the opening still covers most of the putamen, while NHP N only shows coverage along the edges. NHP A also had the largest volume of BBB opening on average (508 mm^3) followed by NHP Ob (192 mm^3) and NHP N (87 mm^3).

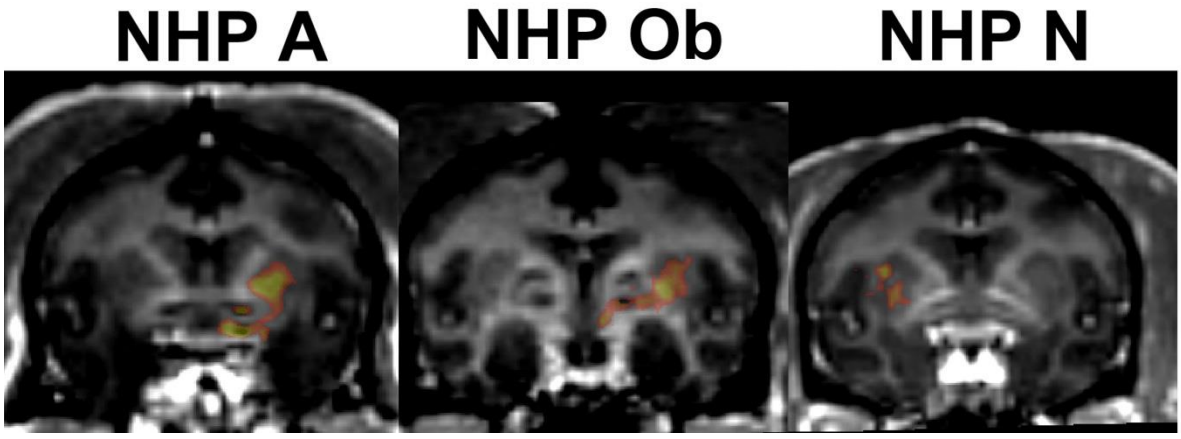

Figure 20: Contrast Enhanced Blood Brain Barrier Opening for Drug Study. The red/yellow transparent color map indicates areas where BBB opening was detected 36 hours after application of the FUS technique.

The T2-weighted and susceptibility weighted image (SWI) scans for the majority of the FUS procedures did not show any abnormal hyper- or hypointense voxels in the target regions. Figure 21 shows typical T2-weighted and SWI scans for all three NHP.

There were three cases when NHP A exhibited abnormal hyperintense voxels in the target region on the T2-weighted scans during day 1. These hyperintense voxels were not present on day 7. The experiments with hyperintense voxels were not correlated with the haloperidol administered during behavioral testing on day 0 as two cases were after haloperidol administration and the third case was after saline administration. NHP N also exhibited one case with abnormal hyperintense voxels on the T2-weighted scan during day 1 that were not present on day 7 (Figure 22). For NHP N saline had been administered on day 0 for behavioral testing. For both NHP A and N, no hyper- or hypointense voxels were detected with the SWI scans. This suggests a transient edema without microhemorrhaging occurred, and was not present within seven days. The behavioral data recorded on the day prior to detection of the abnormal hyperintense voxels were not significantly different from the other data collected within the same group (Haloperidol/FUS+, and Saline/FUS+), thus the edema was determined to not have an effect on the behavioral results (1-way ANOVA, $p > 0.05$).

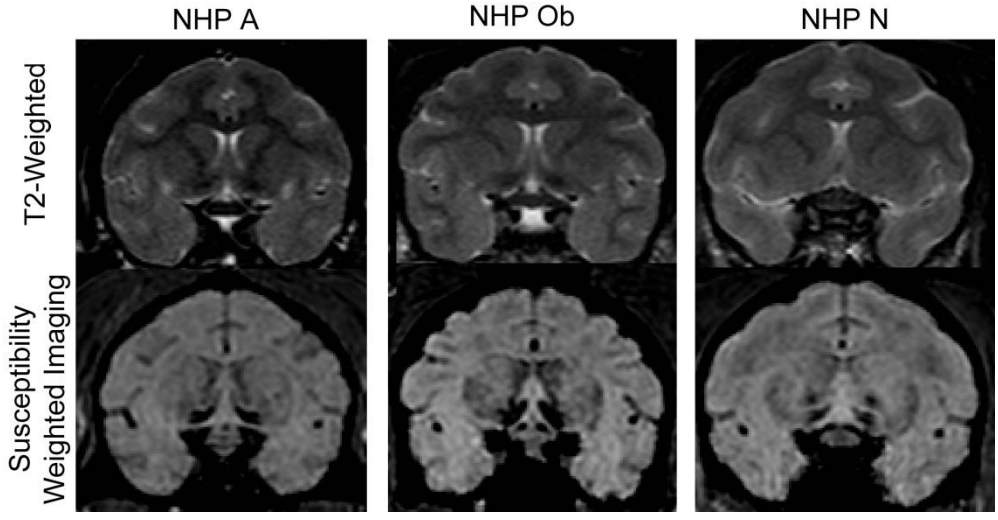

Figure 21: T2-Weighted and SWI Scans for the Haloperidol Non-Human Primate Study. The scans here represent the majority of the FUS procedures, without hyper- or hypointense voxels for both the T2-weighted and SWI scans.

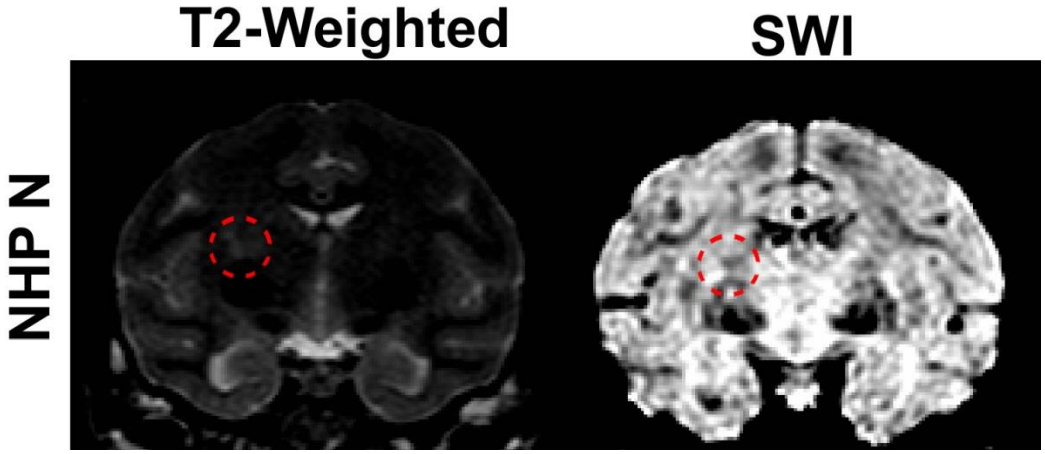

Figure 22: Case of Hyperintense Voxels for the Haloperidol Non-Human Primate Study. The Figure shows the T2-weighted and SWI scans for NHP N during the one case where hyperintense voxels were detected. The detection of the hyperintense voxels on the T2-weighted image suggests potential edema. No hyper- or hypointense voxels were detected in the region of interest on the SWI scan. Detection of hyperintense voxels on a T2-weighted scan only occurred once for NHP N and three times for NHP A.

Behavioral Analysis

All three NHP completed the random dot motion with reward magnitude bias behavioral task after IM administration of either a low dose of haloperidol (0.01mg/kg) or saline. Behavioral testing occurred either on the day of the FUS application (day 0), or at minimum five days after the FUS application to ensure the BBB was closed (day 5+). Average reaction times to the cue and the target stimulus for both the normalized Haloperidol/FUS+ and Haloperidol/FUS- group for each NHP can be seen in Figure 23. Only NHP A exhibited a significant decrease in reaction time to the initial cue between the Haloperidol/FUS+ and Haloperidol/FUS- groups (student t-test, $p < 0.001$). NHP Ob and N did not show any significant difference in RT to the cue between those two groups. There was a significant increase in RT to the target stimuli between Haloperidol/FUS+ and Haloperidol/FUS- groups for both NHP N and Ob (student t-test, $p < 0.001$). Although both NHP N and Ob showed a significant increase, NHP A

showed a significant decrease between those groups to the target stimuli (student t-test, $p < 0.001$).

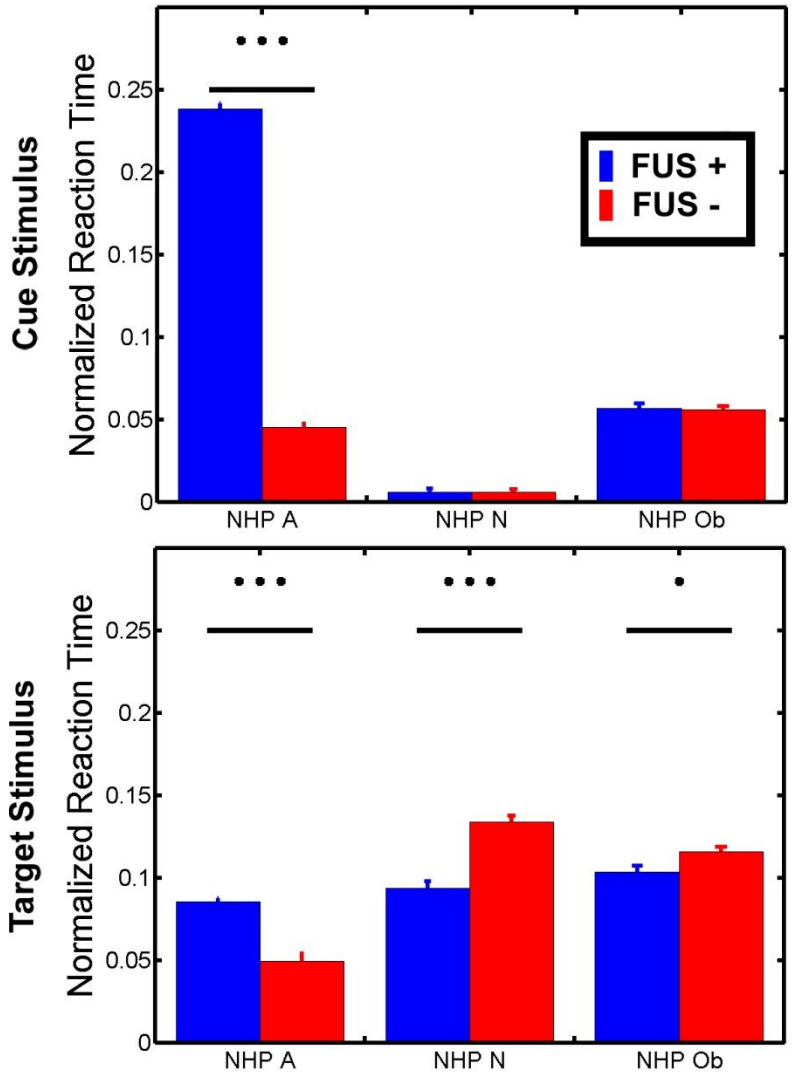

Figure 23: Normalized Reaction Times to Cue and Target Stimuli Following Threshold Haloperidol Administration. Average normalized reaction time is plotted with the 95% confidence interval. Dots indicate significance as follows: • for $p < 0.05$, ••• for $p < 0.001$.

The main data groups of normalized Haloperidol/FUS+ and Haloperidol/FUS- data were divided into subgroups by reward value and response hand. Examining the difference between the Haloperidol/FUS+ and Haloperidol/FUS- in these subgroups

revealed two interesting trends. Table 5 shows the p-values for comparing Haloperidol/FUS+ and Haloperidol/FUS- data within each subgroup per each NHP (student t-test). The results in Table 5 illustrates that NHP A had a consistent significant decrease in reaction time between the Haloperidol/FUS+ and Haloperidol/FUS- groups regardless of the subgroup (hand, reward level or stimuli; student t-test, $p < 0.001$). The other trend was both NHP N and Ob showed a significant increase in RT between the Haloperidol/FUS+ and Haloperidol/FUS- groups to the target stimuli for the majority of the parameters (student t-test, $p < 0.001$).

Table 5: p-Values for Significance Between the Haloperidol/FUS+ and Haloperidol/FUS- normalized groups per parameter.

	NHP A	NHP N	NHP Ob
Cue-High	$p < 0.001$	N/A	N/A
Cue-Low	$p < 0.001$	N/A	N/A
Target-High	$p < 0.001$	$p < 0.001$	N/A
Target-Low	$p < 0.001$	$p < 0.001$	$p < 0.001$
Cue-Contra	$p < 0.001$	$p < 0.001$	$p < 0.001$
Cue-Ipsi	$p < 0.001$	$p < 0.001$	$p < 0.001$
Target-Contra	$p < 0.001$	$p < 0.001$	$p < 0.001$
Target-Ipsi	N/A	N/A	$p < 0.01$

Green indicates a significant increase while yellow indicates a significant decrease. N/A indicates $p > 0.05$.

Since haloperidol could have an effect on the motor accuracy, and not just reaction time, touch error to the stimuli was also recorded during the behavioral testing. Touch error was defined as the distance between the first location the NHP contacted the touch monitor and the center of the displayed stimuli. The difference between the Haloperidol/FUS+ and Haloperidol/FUS- groups were found for each individual parameter in the subgroups (high or low reward, ipsilateral or contralateral hand relative to the brain hemisphere where the FUS procedure was applied). This was

compared to the other parameter within that subgroup (i.e. the difference in TE between Haloperidol/FUS+ and Haloperidol/FUS- groups for the high reward compared to the difference in TE between Haloperidol/FUS+ and Haloperidol/FUS- groups for the low reward). There was a significant increase in the difference of TE between the Haloperidol/FUS+ and Haloperidol/FUS- groups to the cue stimulus for the contralateral hand compared to the ipsilateral hand for all NHP (table 6, student t-test, $p > 0.05$). This significant increase was also observed between the high and low reward cue stimulus for NHP N only.

Table 6: p-Values for Significance Between the Touch Error for Haloperidol/FUS+ and Haloperidol/FUS- normalized groups per parameter.

	NHP A	NHP N	NHP Ob
Cue: High - Low	N/A	$p > 0.05$	N/A
Target: High - Low	N/A	N/A	N/A
Cue: Contra - Ipsi	$p > 0.05$	$p > 0.05$	$p > 0.05$
Target: Contra- Ipsi	N/A	N/A	N/A

Yellow indicates a significant increase of the contralateral hand / high reward to the ipsilateral hand / low reward.

While RT and TE are useful for detecting changes with the motor activity of the NHP, they are not sufficient indicators of changes with the cognitive ability of the NHP. The decision-making performance of the NHP was determined by the accuracy of the NHP selecting the correct direction the dots were coherently moving in. Both NHP N and Ob showed an increase in overall accuracy in the Haloperidol/FUS+ over the Haloperidol/FUS- group, while NHP A showed a decrease in overall accuracy (Table 7). Each NHP exhibited at least 70% accuracy in selecting the correct target per each group. NHP A was also the only NHP to have a decrease in accuracy to the low reward for the Haloperidol/FUS+ compared to the Haloperidol/FUS- group (table 8). There was a

larger increase in accuracy to the low reward compared to the high reward for both NHP N and Ob.

Table 7: Overall Accuracy Percentage for Discriminating Dot Direction per Drug/Sonication Parameter

	NHP N	NHP Ob	NHP A
Halo/FUS+	83.43	77.80	76.39
Saline/FUS+	83.93	81.16	70.25
Halo/FUS-	81.48	72.73	77.88
Saline/FUS-	84.71	72.24	76.26

Numbers displayed in the Table are in percentages.

Table 8: Accuracy Percentage for Discriminating Dot Direction per Reward Level and Drug/Sonication Parameter

	NHP N		NHP Ob		NHP A	
	High	Low	High	Low	High	Low
Halo/FUS+	84.62	82.60	78.60	74.87	82.14	80.58
Saline/FUS-	85.07	82.87	81.34	81.36	81.34	83.25
Halo/FUS+	83.72	79.56	77.99	69.75	81.01	82.13
Saline/FUS-	85.28	84.47	77.16	70.21	81.43	80.68

Numbers displayed in the Table are in percentages.

Determining the coherence threshold for detecting discrete motion is a sensitive parameter for quantifying decision-making performance. The coherence threshold is determined as the percentage of coherently moving dots to the correct target that can be discerned by the subject with an 80% success rate. The percent correct of dot direction discrimination as a function of motion coherence is shown in Figure 24 B for both NHP N and Ob. Both NHP responded more accurately accuracy for the FUS+ group compared to the FUS- group (Figure 24 A, student t-test, $p > 0.05$).

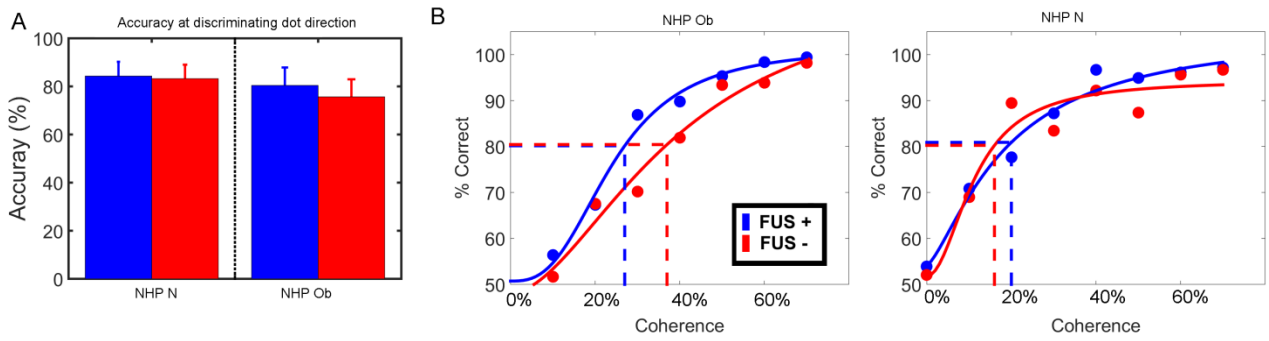

Figure 24: Naka-Rushton Model fits of Accuracy to Coherence for the Random Dot Motion Task. A) The red and blue bars here indicate the responses to the accuracy of the FUS + and FUS- respectively. The whiskers indicate the 95% confidence interval. There was no significant difference across groups. B) The red and blue lines here indicate the Naka-Rushton fit to the accuracy per coherence level for the FUS + and FUS- data sets. The red and blue circles indicate the percent correct for each coherence level. The vertical and horizontal dashed lines indicate the coherence threshold for detecting the direction of the dots with an accuracy of 80%.

4.4.2 Low Dose Haloperidol in Mice

Blood-brain barrier opening was observed in all mice. Figure 25 shows a contrast enhanced T1-weighted MRI representative of the average BBB opening achieved in the caudate-putamen region of the mice. Hyperintense voxels were only detected in the T2 RARE sequences for 3/15 of the procedures. Those mice were excluded from the behavioral analysis as prior studies have shown the presence of edema in the mice can induce behavioral deficits [153]. There was no significant difference observed between the groups for the duration the mice could remain on the rotarod without falling off (1-way ANOVA, $p > 0.05$), with the majority of the mice remaining on the rotarod for the full 200 seconds. There was a significant decrease in the distance traveled in the Haloperidol/FUS+ compared to the Haloperidol/FUS- group (Figure 26, student t-test). This agrees with previously published reports of intracerebroventricular (ICV) injection of D2 antagonists eliciting motor retardation in rats [154].

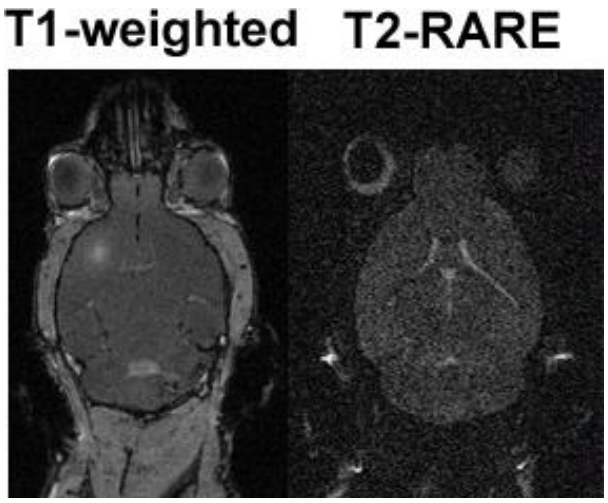

Figure 25: MRI Blood-Brain Barrier Opening and Safety Validation for the Mice Study. Contrast enhanced regions for the T1-weighted scan indicate BBB opening. The T2-RARE image shows no abnormal hyperintense voxels, indicating lack of edema. Potential edema was only detected for 3/15 cases.

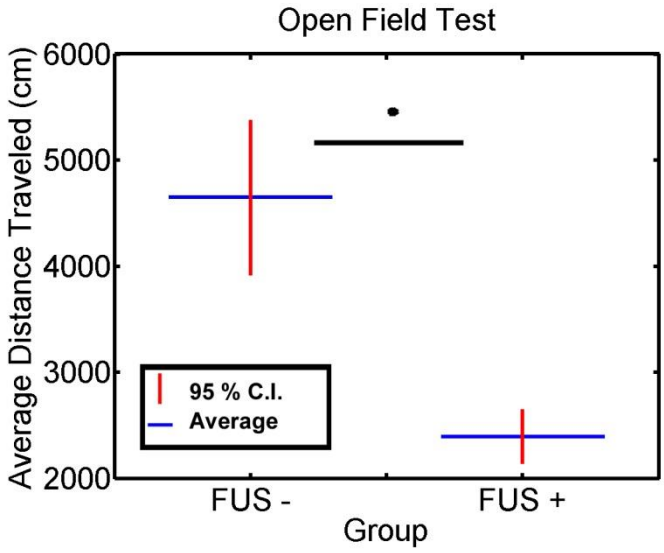

Figure 26: Distance Traveled During an Open Field Test. The average and 95% confidence interval for both cases where low dose haloperidol had been administered IP with and without BBB opening. There was a significant decrease in the distance traveled between the two groups (student's t-test, $p < 0.05$)

4.4.3 Domperidone in NHP

MRI Analysis

T2-weighted MRI scans acquired following the domperidone behavioral experiments indicated abnormal hyperintense voxels in the caudate region for NHP N, O and Ob. Abnormal hypointense voxels were also detected on T1-weighted scans in the caudate region of NHP N and O. No abnormal voxels were detected on T2-weighted or SWI scans for NHP B. This initially suggests the presence of edema in NHP N, O and Ob (Figure 27). The hyperintense voxels were not detected on day 7 with T2-weighted scans for any of the NHP. On day 7 there were hypointense voxels detected on the SWI scans for NHP N and O. This suggests the potential presence of a hematoma in the targeted region of the caudate for both NHP. The volume of area covered by the hypointense voxels did not decrease in size over the duration of two years and appears to be permanent.

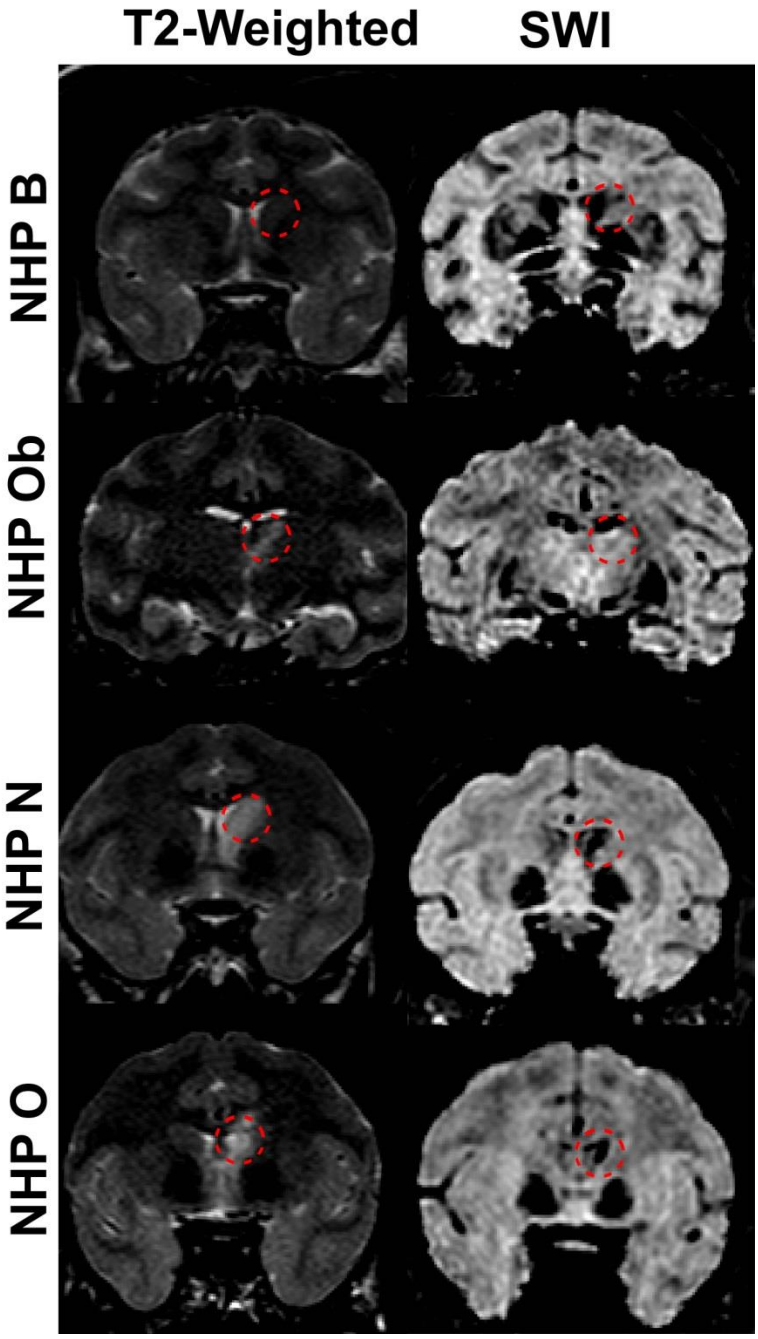

Figure 27: T2-Weighted and SWI Scans after Domperidone Administration with Blood-Brain Barrier Opening. Abnormal hyperintense voxels on the T2-weighted MRI (day 0) indicate edema in the caudate region. Hypointense voxels on the SWI scans (day 7) suggest microhemorrhage and possible hematoma. The red dotted circles indicate region of interest.

Behavioral Analysis

Qualitative observations of NHP B, O, Ob and N moving around in a contained room after domperidone administration revealed two drastically different outcomes. During observation sessions when the BBB was not open (the FUS procedure had not occurred for at minimum five days), all NHP moved around the room with normal locomotion without any signs of neglect. All NHP exhibited normal posture while sitting on the floor and had full muscle strength and control while climbing out of and into the primate work chair. When domperidone was administered following the FUS procedure both NHP N and Ob exhibited signs of hemilateral neglect. These symptoms manifested specifically on the side contralateral to the FUS procedure. Neglect symptoms included weak muscle tone in both the arm and leg, inability to sit with correct posture, and they were only able to rotate their body towards the ipsilateral side of the FUS application. The animals would only respond to touch stimuli (stroking of the cheek, ear and arm) on the ipsilateral side of the body as the BBB opening. Eyes would only track treats towards the ipsilateral side and neck motion was strongly biased towards the ipsilateral side as well. Animals were not able to complete hand-reaching tasks for treats with the contralateral arm, though their ipsilateral arm was unaffected. Symptoms subsided 40 minutes after onset. Neither NHP O nor B exhibited any neglect symptoms to the IV administration of domperidone following the FUS procedures.

4.5 Discussion

While the FUS technique has been shown effective for delivering various drugs across the brain for treatment of tumors or to facilitate neuroprotection, the transport of neuromodulatory drugs has not been fully explored. Prior longitudinal studies investigating the safety of the FUS technique in NHP utilized behavioral testing and

reported no long-term changes in behavioral responses to a visuomotor task [143]. Results from chapter 3.4 showed the short-term increase in reaction time on day 0 due to the FUS technique, which was why the Haloperidol/FUS+ group was normalized by the Saline/FUS+ group to remove these effects of the FUS technique [19]. This allowed for the detection of changes in the behavioral responses due to the low dose haloperidol reaching the putamen region of the basal ganglia and not the effect of the FUS technique.

Contrast enhanced T1-weighted MRI scans were acquired 36 hours (day 1) after the FUS technique was applied to the putamen region of the NHP. Prior studies reported a closing timeline up to three days in NHP depending on the parameters used [14]. While both NHP A and Ob still had considerable average volume of BBB openings on day 1 (508 mm^3 & 192mm^3 respectively), NHP N exhibited only small openings (87 mm^3). An acoustic pressure of 400 kPa was utilized with the FUS technique for both NHP N and Ob, current work within the Konofagou lab suggests the incident angle of the transducer beam with the skull has an effect on the resulting BBB opening volume [155]. Here NHP N exhibited smaller incident angles between the transducer beam and the skull, which is associated with smaller BBB opening volumes. This could account for the discrepancy in the volume of BBB opening between NHP N and Ob as the same FUS parameters were utilized, and they are of similar physical stature. As it has been shown the BBB volume can close at a rate up to 50 mm^3 per day, NHP N may have had a smaller volume of opening on day 0 with the majority of it closing by day 1.

Although both NHP Ob and N exhibited smaller openings than NHP A, all three NHP displayed a significant increase of the difference in the touch error for their contralateral hand between the Haloperidol/FUS+ and Haloperidol/FUS- groups. As haloperidol is a D2 antagonist, it should bind with the D2 receptors in the putamen [156]. The D2 receptors in the putamen are associated with the indirect pathway

between the substantia nigra and the striatum [26, 152, 157]. When haloperidol binds with these receptors, dopamine is blocked from binding and the indirect pathway is not inhibited. This creates a unique scenario where the dopamine continues to bind with the direct pathway, promoting motor activity, while the indirect pathway is not inhibited, which will impede motor activity. This could account for the increased variability in the touch error for the contralateral hand compared to the ipsilateral hand as the signals for motor activation could be in conflict, generating more erratic hand responses.

Both NHP N and Ob showed a significant increase in reaction time to the target stimuli. This also agrees with the haloperidol binding to the D2 receptors and inhibiting motion. Multiple studies have reported a decrease in locomotion in animal models after administering D2 antagonists [158, 159, 160, 161]. This significant increase in reaction time for NHP N and Ob also corresponded with an increase with their overall accuracy at determining the direction of the dot motion. These results agree with the speed-accuracy tradeoff paradigm where an increase in reaction time typically correlates with responses that are more accurate [136, 142, 163]. The RDM task forces the NHP to determine a speed-accuracy trade-off when responding to the stimuli. Results from NHP A also agree with this paradigm as NHP A exhibited a significant decrease in reaction time between the Haloperidol/FUS+ and Haloperidol/FUS- groups (faster responses to the stimuli), corresponding with a decrease in the accuracy of determining the coherent direction of the dots.

While both NHP N and Ob exhibited significant increases in reaction time, NHP A showed significant decreases in reaction time to both stimuli regardless of parameters (hand, reward value). As NHP A had the largest detected BBB opening, the haloperidol may have had effects on the surrounding subcortical nuclei and these additional interactions could have generated the increase in motor activity. The location of haloperidol delivery and binding could have been visualized through PET imaging, but

that was outside of the scope of this study [156]. Regardless of the effect, the administration of haloperidol after opening the BBB resulted in significant behavioral changes in NHP A, signifying successful delivery of the drug. With future experiments, the opening area of the BBB should be more precise, allowing better control of where the drug is being delivered to in the brain.

In the murine experiments, a threshold dose of haloperidol administered IP after opening the BBB in the caudate-putamen region significantly reduced the motor behavioral during the open field test. This agrees with prior studies showing a decrease in locomotor activity during open field-testing after administering a dose of haloperidol (0.1mg/kg) while the BBB was intact [164]. These results are in agreement with those from the behavioral testing for 2 / 3 of the NHP as a significant increase in reaction time to the target stimuli was observed.

The behavioral results from the domperidone experiments are the strongest indicators the FUS technique can facilitate drug delivery to targeted regions of the brain. Prior studies had shown domperidone as a potent and specific dopamine antagonist with *in vitro* binding studies, but did not affect the striatum due to the inability to cross the BBB [145]. This was reflected in the control experiments with domperidone where the BBB was intact as no abnormal behavioral effects were observed. For both NHP N and Ob, there were distinct behavioral changes after domperidone was administered with the BBB opened in their caudate region. The results indicate that domperidone was able to cross the open BBB at the caudate region and bound strongly with the D2 receptors in the caudate eliciting motor impairment through the direct-indirect pathways as discussed prior. The potential hematomas that developed in NHP N and O were not related to the delivery of domperidone as NHP O did not show signs of the drug being delivered, while NHP OB, which did not display a

potential hematoma, did show strong signs domperidone had been successfully delivered.

4.6 Conclusion

Current drug delivery methods do not provide region specificity with a non-invasive procedure, which can lead to unwanted side effects. Other invasive methods can incur adverse complications during the procedures. The overall results from the behavioral task experiments in chapter 4 illustrate a major benefit for using the FUS technique to facilitate targeted drug delivery. Haloperidol is a drug that is currently used in clinics for sedation of manic patients and thus it can pass through the BBB freely [166]. Here, a threshold dose of haloperidol (0.01mg/kg) that does not have behavioral effects when the BBB was intact, elicited changes in the behavioral results after the BBB was opened with the FUS technique in both mice and NHP. As many drugs including levodopa have the potential for negative side effects, the ability to achieve the same effective dose, with a lower administered dose, would greatly lower the chance and occurrence of adverse side effects. Domperidone is a large molecule drug that cannot cross the BBB, and only after successfully opening the BBB in the caudate region in NHP was hemilateral neglect observed due to successful drug delivery. Overall, the FUS technique can be safe and effective to non-invasively deliver drugs that have a pharmacodynamical effect on the responses of NHP to external stimuli.

4.7 Contributions

In this chapter, the ability of the FUS technique to facilitate targeted drug delivery for pharmacodynamical behavioral modulation was investigated. Prior studies had shown the technique effective to deliver various neuroactive drugs to the brain for the treatment of brain tumors or to promote neurogenesis [21, 22]. Here, the results demonstrated that the FUS technique could be effective in delivering D2-antagonists to

the basal ganglia in both mice and NHP eliciting behavioral effects. Successful delivery of domperidone to the caudate in NHP resulted in distinct hemilateral neglect contralateral to the brain hemisphere where the FUS procedure was applied. This is important as it demonstrates the potential for neuroactive drugs that cannot cross the intact BBB due to size to be effective for pharmacodynamical behavioral modulation at targeted regions when the BBB is open. Results from the haloperidol studies in mice and NHP demonstrated a low dose, here a threshold dosage of haloperidol, can elicit similar behavioral effects with an open BBB at the targeted region as a full dose with a native BBB. As many current drug therapies incur undesirable side effects, this technique can allow for the same effective dose at the target site, with a lower initial dosage. The initial lower dosage could potentially reduce adverse side effects. As current techniques for drug delivery to the brain are either non-invasive with non-specific targeting, or region specific and invasive, results in chapter 4 have demonstrated the FUS technique can be non-invasive and target specific allowing the delivery of both large molecules, and a low dose of neuroactive drugs through the BBB. The results discussed here are currently being collected for submission in a peer-reviewed journal.

Regarding the research contributions, Carlos Sierra Sanchez, PhD (Biomedical Engineering, Columbia University) and Marilena Karakatsani, MS (Biomedical Engineering, Columbia University), assisted with the FUS experiments and the microbubble fabrication for experiments. Amanda Buch, BS (Biomedical Engineering, Columbia University) assisted with the FUS experiment and with the behavioral testing. Shangshang Chen, BS (Computer Science, Columbia University) assisted with the behavioral testing and microbubble fabrication for experiments.

Chapter Five

Specific Aim 3

Safety and Efficacy of Blood-Brain Barrier Opening via Focused Ultrasound with Microbubbles in Alert Non-Human Primates

Results from specific aims 1 & 2 have demonstrated that the FUS technique is effective for opening the BBB in anesthetized NHP. Here in specific aim 3, the potential for the FUS technique to open the BBB in fully alert NHP was investigated. Utilizing the FUS technique with alert as opposed to anesthetized subjects is ideal for application in both the clinic and the laboratory as it removes the possibility of adverse side effects from the anesthesia. The behavioral analysis developed in chapters 3 and 4 is once again employed to measure the potential side effects of applying the FUS technique while the NHP conducted a behavioral task.

5.1 Abstract

Focused ultrasound coupled with intravenous microbubbles (FUS) has been proven an effective, non-invasive technique to open the blood-brain barrier (BBB) *in vivo*. This study demonstrates that the FUS technique can safely and effectively open the BBB at the basal ganglia and thalamus in alert non-human primates (NHP) while they perform a behavioral task. The BBB was successfully opened in 86% of cases at the targeted brain regions of alert NHP with an average volume of opening 19% larger than prior anesthetized FUS procedures. Safety (lack of edema or hemorrhage) of the FUS technique was also improved during alert than anesthetized procedures. No physiological effects (change in heart rate, motor evoked potentials) were observed during any of the procedures. Furthermore, the application of FUS did not disrupt

reaching behavior, but in fact improved performance by decreasing reaction times by 23 ms, and significantly decreasing touch error by 0.76 mm on average.

5.2 Introduction and Study Design

Focused Ultrasound (FUS) combined with systemically administered microbubbles (MB) has been shown as an effective, non-invasive technique to open the BBB in multiple *in vivo* models including non-human primates (NHP) [9, 10, 11, 12]. The application of the FUS procedure is multifaceted and can be utilized both in the clinical and laboratory settings. In the clinic, it can be used to facilitate drug delivery for the treatment of neurological diseases or disorders, which currently do not have targeted, or non-invasive treatment options [5, 6, 7]. Within the laboratory, the procedure can be used for targeted drug delivery eliciting pharmacodynamical modulation during behavioral experiments, or evaluation of novel drugs that cannot cross an intact BBB. Currently, FUS has only been shown to be safe and effective in anesthetized animal models [13, 16, 19]. The anesthesia requirement may not be ideal in a future clinical setting. In addition, even in a laboratory setting anesthesia may affect behavioral experiment [167, 168]. For the full potential of this technique to be utilized in both the clinical and laboratory settings, safe and effective performance in alert subjects needs to be shown.

One major difference in physiologic conditions when performing the procedure on an anesthetized rather than an alert subject lies in the effects of the anesthetic on the vascular system. Isoflurane, a common anesthetic used for surgical procedures and anesthetized experiments in animals, causes vasodilation and a decrease of vascular resistance in cerebral vasculature [169, 170]. Average cerebral capillary diameters of NHP are normally around 5 μm, but under isoflurane anesthesia vasodilation occurs which can lead to an increase in cerebral blood flow [171, 172, 173, 174]. One prominent

theory on how FUS causes BBB openings postulates that MB oscillate due to the FUS exposure of the vessels. These MB oscillations physically disrupt the endothelial cells that comprise the BBB [13, 14, 17, 175]. The two main types of bubble activity reported are stable and inertial cavitation [87]. Stable cavitation consists of both harmonic and ultraharmonic oscillations of the MB and is the dominant mechanism for BBB opening when the MB diameters are similar to the vessel diameter [13]. Inertial cavitation is caused when the MB collapse emitting high energy jets, which can damage the vasculature and is the dominant mechanism when the MB diameter are smaller than the vessel diameter [13, 17, 176]. As the experiments utilizes an average 4-5 μm diameter MB, the smaller vessel size during the alert FUS procedures due to the lack of isoflurane could change the occurrence of stable and inertial cavitation compared with anesthetized procedures. This change in cavitation could translate to a difference in BBB opening volume as stable cavitation has been correlated with smaller, safe opening volumes while inertial cavitation has been correlated with larger BBB opening volumes that have the potential to cause damage (edema, erythrocyte extravasation) [15, 87, 177]. The smaller diameter of the vasculature would also increase the overall force the MB apply on the endothelial cells from stable oscillations, potentially causing an increase in damage to the vasculature [85, 177]. Aside from vessel diameter, cerebral blood flow and persistence time of MB in the vasculatures are also affected by the use of isoflurane mixed with pure oxygen as an anesthetic [172, 173, 178]. Changes to those parameters would affect the dosage of the MB reaching the area targeted by the FUS. Overall, isoflurane anesthesia generates unfavorable conditions, the removal of which could have an effect on the safety of the tissue in the targeted region and efficacy of the BBB opening procedures.

In this study, the results demonstrate that the FUS technique can be a safe and effective procedure to open the BBB in alert NHP. The NHP were trained to perform a

visually guided reaching task to receive fluid rewards. The NHP were head-fixated in a primate chair allowing for targeted FUS application while they simultaneously completed the behavioral task for fluid reward. The caudate and putamen regions of the basal ganglia as well as the thalamus were targeted by the FUS as these regions are greatly affected by Parkinson's disease, which currently does not have a reliable long-term treatment solution [24, 124]. These regions are also implicated in memory, voluntary motor control, goal-directed action and decision making [105, 106, 107]. The behavioral task utilized the well-established reward magnitude bias paradigm and measured visual perception, motivation and motor function to test the function of the targeted regions during application of the FUS technique [119, 120]. A contrast enhanced 3D T1-weighted MRI scan was used to verify BBB opening while T2-weighted MRI and susceptibility weighted images were used to investigate the safety of the technique. The results from the behavioral testing paired with the MRI results demonstrate that the FUS procedure for BBB opening can be safe and effective in alert, behaving subjects.

5.3 Methods

All NHP procedures described herein were approved by both the Institutional Animal Care and Use Committees (IACUC) of Columbia University and the New York State Psychiatric Institute. Two adult male Macaca Fascicularis (NHP: Z, A) were used for the majority of the experiments (Ages: 14, 18 years old; weights: 5.3, 5.6 kg) and one Macaca Mulatta (NHP B, 22 years old, 10.1kg). All husbandry room procedures have been previously described in chapter 3.3. Both NHP A & Z underwent IACUC approved sterile surgical procedures for a head post implantation allowing head fixation during the behavioral testing and FUS procedure.

FUS Procedure

The full specifics on parameters utilized with the FUS technique in this chapter are described in chapter 3.3.

Multiple anesthetized FUS procedures were performed on NHP A and Z before conducting the alert procedures (n = 12, n = 4 respectively). An acoustic pressure of 300 kPa with 4-5μm MB and a 2-minute sonication was utilized for all anesthetized FUS procedures. After the FUS procedure, NHP were immediately transported to acquire MRI scans (3T, Philips Medical Systems, MA, USA) for verification of BBB opening and safety.

The lightly sedated FUS procedures were only conducted on NHP B. NHP B was given a low dose of ketamine (5 mg/kg) and placed into partial stereotactical positioning. The top canines were positioned to fit into a custom-made bite bar that kept the NHP head steady and in a position similar to that as if it was in full stereotax positioning. Once the NHP was positioned the FUS transducer was attached to the stereotactic manipulator for targeting of the putamen region. An acoustic pressure of 300 kPa with 4-5μm MB and a 2-minute sonication was utilized for the lightly sedated procedures. MB were administered through a catheter placed in the saphenous vein. Heart rate and blood pressure were monitored throughout the procedure. During the FUS procedure, the veterinary staff at NYSPI were present to observe if the procedure was having any gross negative effects on the body posture of the NHP or on the vitals. 6 hours after the procedure had finished, MRI scans were acquired to verify BBB opening and the safety of the procedure.

The setup of the alert experiment can be seen in Figure 28. Initially the NHP were lightly sedated with ketamine (0.3 ml) for the placement of a catheter in the saphenous vein for IV delivery of the MB. NHP were then placed into the primate chair and head fixated. A pulse oximeter clip was placed on the ear ipsilateral to the placement of the transducer. The two positive EMG leads were placed on the temporalis muscle contralateral to the transducer with the ground placement ipsilateral to the transducer (MP150 Data Acquisition system, BIOPAC Systems Inc., CA, USA). The transducer was then attached to the stereotactic manipulator for targeting of the focal region and the NHP was allowed to begin the behavioral task within a light and soundproof testing booth. Animals were allowed to work for an hour before beginning the FUS procedure. The FUS was applied at the onset of MB injection, which was through surgical tubing attached to the catheter that came out from the work booth. This allowed the NHP to continue to work uninterrupted throughout the application of the FUS procedure. An acoustic pressure of 300 kPa with 4-5μm MB and a 2-minute sonication was utilized for all alert FUS procedures. After the FUS procedure finished NHP were allowed to work until satiated. MRI scans were acquired for each NHP 5 hours after the animal completed the behavioral tasks.

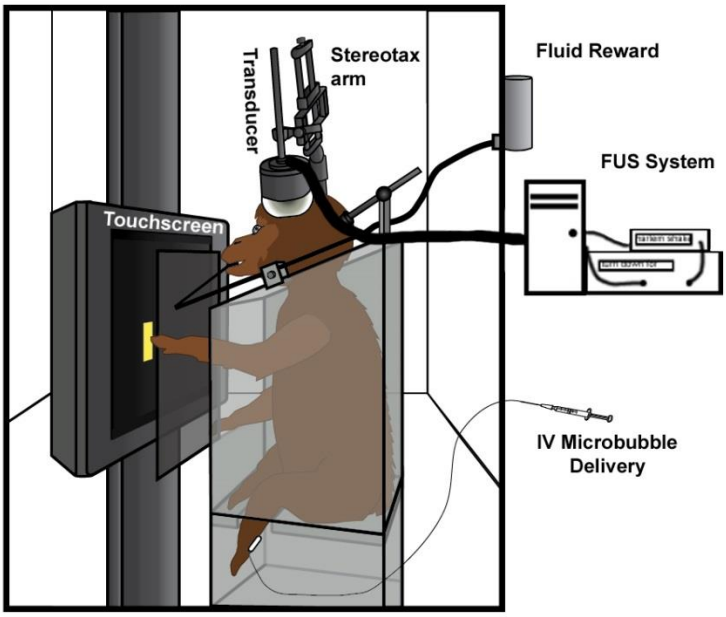

Figure 28: Alert Focused Ultrasound Behavioral Setup. The NHP was placed into a primate work chair and was head fixated. This position allows free movement of their arms to respond with the ipsilateral arm as the stimuli from the behavioral task displayed on the touch monitor. The transducer, EMG leads and pulse oximeter were positioned on the scalp of the NHP. The experiment was run external to the booth allowing the NHP to complete the behavioral task unaware when the FUS technique was applied.

MRI Analysis

MRI scans for the aforementioned FUS procedures were as follows: T2-weighted and Susceptibility Weighted (SWI) scans were acquired to verify the safety of the FUS procedure. Gadodiamide (Omniscan®, 573.66 DA, GE, Healthcare, Princeton, NY, USA) was injected before acquiring contrast enhanced 3D T1-weighted images to verify BBB opening. Gadodiamide was selected as a contrast agent as it cannot cross the intact BBB. Full specifications on the MRI acquisition have been previously discussed in chapter 3.3.

Behavioral Testing

Behavioral control data were acquired with and without ketamine on separate days. For days when ketamine was administered, a dose of 0.3 ml ketamine was injected IM before testing to stay consistent with days when an IV catheter needed to be inserted for the FUS procedure. Non-ketamine control days were used to verify the small dose of ketamine administered during the FUS procedure days did have an effect on the behavioral results. Thus, the ketamine control days were utilized to find a regression curve over time to reduce the effects of ketamine in the experimental days (Figure 29 B). As mentioned previously NHP were placed in a primate chair for head fixation and positioning of the transducer. The transducer was not utilized on days when the FUS procedure did not occur, but was still positioned on control days to create consistent testing conditions for the NHP. Both NHP were trained to respond to visual stimuli presented on a 20-inch color LCD touch panel display (NEC 2010X with 3M SC4 touch controller). The task was designed to employ the well-established reward magnitude bias (RMB) paradigm [77, 120]. This task tested reaction time (RT), touch error (TE), and motivation. Stimuli were presented randomly as either horizontal or vertical yellow bars of equal pixel area and intensity indicating high and low reward respectively (5:1 reward bias). An initial cue was presented randomly on either the left or right side of the screen. Once the NHP touched the cue, a secondary target of same shape, pixel area and intensity appeared. After the NHP touched the target, the water reward was given based on the magnitude indicated by the cue and the target. RT to the cue and target was determined as the onset of the stimuli to the first touch registered by the touch panel. TE to the cue and target was determined by the distance between the center of the stimulus and the location where the NHP first touches the screen.

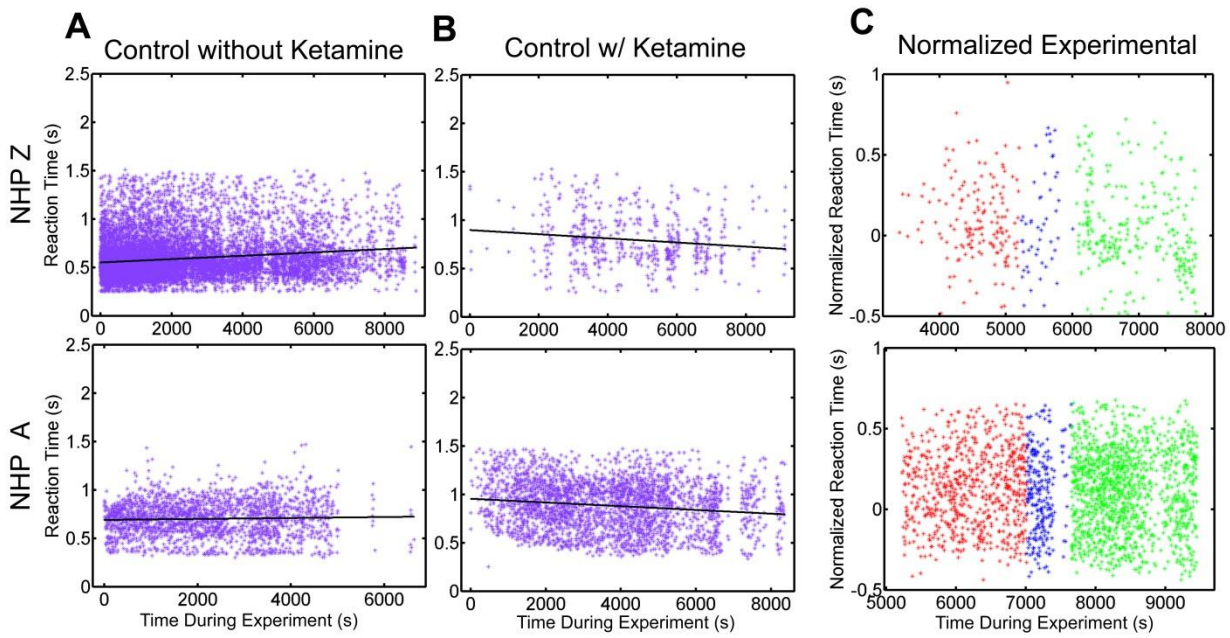

Figure 29: Raw Reaction Time Data for Alert Behavioral Testing. Reaction times for individual trials as a function of time during the experiment. For (A) and (B) magenta dots indicate individual data points and the black line is the linear regression fit. A) shows the control data collected on days when ketamine was not administered. B) shows the control data collected on days when ketamine was administered to mimic the parameters used on experimental days. The regression fit for the ketamine control data was used to normalize the experimental data to remove the effects of ketamine on the behavioral results during experimental days. C) shows the normalized experimental data. Red dots indicate trials completed before applying the FUS technique, blue indicates trials completed during the FUS technique and green indicates trials completed after applying the FUS technique.

Data Analysis

T2-weighted and SWI scans were stereotactically aligned using fsl to determine if there was any hyper- or hypointense voxels in the targeted regions [126]. Post contrast T1-weighted scans were also stereotactically aligned and post processed to determine volume of BBB opening. The full pipeline of MRI processing has been discussed prior in

chapter 3.3. Significance between the volume of opening data from the alert and anesthetized FUS procedures was determined with a Wilcoxon rank-sum test ($p < 0.05$).

Passive cavitation detection (PCD) signals were acquired during all FUS procedures. The full cavitation signal was processed by frequency as harmonic, ultraharmonic and broadband emissions of the MB. Stable cavitation dose was quantified as the energy output from harmonic and ultraharmonic emissions, while inertial cavitation was quantified from the energy of the broadband emissions. Significance between the PCD data from the alert and anesthetized FUS procedures was determined with a student t-test ($p < 0.05$).

Both the raw EMG and heart rate data were initially processed using the same pipeline. Data was recorded during experiments at 2000 Hz. Signals were normalized by the mean to remove machine bias before being passed through a band-pass filter (100-300 Hz) to remove electrical noise and heartrate artifacts [179]. Finally, the absolute value of the signal was taken for full wave rectification. A sliding window step detection algorithm was applied to locate muscle activity. Amplitudes of the detected muscle activity during application of the FUS technique were compared to control signals of the NHP drinking water and moving its jaw. Amplitudes within a maximum threshold recorded during the control were counted to be voluntary movement by the NHP. A peak finding function was used with the heart rate data to determine beats per minute (BPM). BPM was determined for three groups, pre, during and after the FUS procedure. A 1-way ANOVA was used to determine if there was significant variation in heart rate during the FUS procedure ($p < 0.05$).

Behavioral data was divided by ketamine control days (days when no FUS procedure had occurred for at a minimum 5 days) and experimental days (days when the FUS procedure had occurred during behavioral testing). The control days were used

to find normalization curves for both reaction time (RT) and touch error (TE) data to reduce the effects of the ketamine from the experimental days (Figure 29 B). Data from the experimental days were divided into three groups, pre sonication, during sonication and post sonication. For analysis of the experimental data, trials only occurring 30 minutes before and after the sonication were selected. These trials were then normalized with the curve found with the ketamine control data. Variation between each group was evaluated with 1-way ANOVAs ($p < 0.05$). Averages were compared across group for significant differences using a student t-test ($p < 0.05$). Data was also subdivided by reward magnitude (high and low). The average differences (high – low) for these subgroups were compared for significant differences with a student t-test ($p < 0.05$)

5.4 Results

Safety

Initial trials of the FUS procedure on a lightly sedated (single 5mg/kg dose of ketamine) NHP (subject B) did not elicit any autonomic changes. Heart rate and blood pressure remained consistent throughout the procedure (136 beats per minute, 68 mean arterial pressure). These vital recordings agree with the results from the monitoring of the vitals during the longitudinal study in chapter 3. No sudden limb, jaw or eye movement, nor pupil dilations were observed by researchers or the observing NYSPI veterinary staff. After the procedure, NHP B recovered normally from light anesthesia and returned to routine activities (playing, eating, and drinking). T2-weighted MRI and susceptibility weighted image (SWI) scans did not show any abnormal hyper- or hypointense voxels in the targeted regions signifying no edema or hemorrhage had been caused by the procedure.

Having verified the preliminary safety of the procedure in a lightly sedated NHP, the FUS technique was applied to alert NHP. The full setup for the alert FUS technique along with behavioral testing can be seen in Figure 28. As with the lightly sedated experiment, application of the FUS technique did not cause any macroscopic motor effects (sudden limb, body or eye movement) nor did it elicit a pain grimace for either NHP, regardless of the targeted brain region. Heart rate remained consistent throughout the FUS technique and within the normal range for fascicularis macaques (NHP A: 152.4 ±1.2 BPM, NHP Z: 179 ±8.9 BPM). The larger variation in the heartrate for NHP Z arose from motion artifacts in the SpO_2 signal as he was generally more active while he worked. Neither of the NHP exhibited an abrupt change in heartrate with the onset or during the application of the FUS technique. EMG recordings on the temporalis muscle only detected normal jaw and mouth movements (licking reward tube, smacking lips) during the procedures (Figure 30). There were no abnormal or large EMG signals detected either during or after the FUS procedure that surpassed the recorded activity during the control.

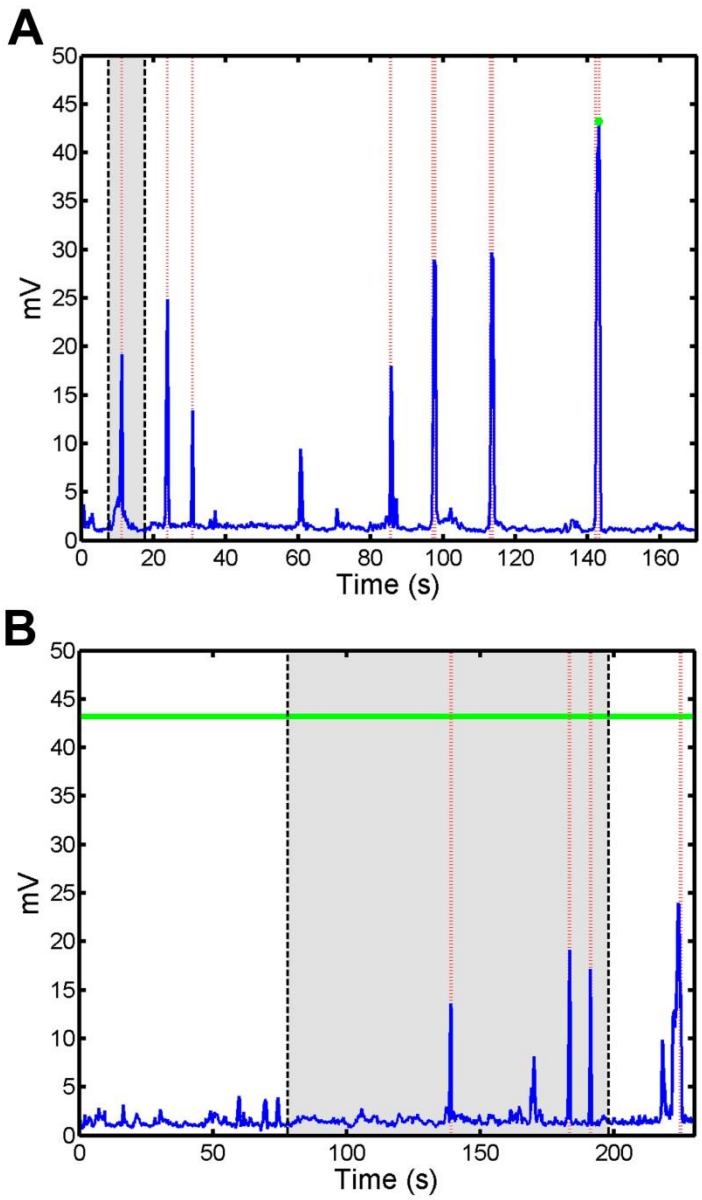

Figure 30: EMG Recordings. EMG signals were recorded from the temporal muscle contralateral to the FUS application. The grey region denotes when either the control (A) or the full sonication (B) with the transducer was being applied. Red dashed vertical lines indicate detected muscle activation. The horizontal green bar indicates the maximum signal recorded during the control period (indicated by the green dot) and subsequently used as the threshold to detect abnormal or large signals that occurred during the application of the FUS technique. Only recordings from NHP Z are shown, but NHP A showed similar responses. There was no abnormal or large muscle activity triggered by the alert FUS procedure.

The majority of the T2-weighted and SWI scans did not show abnormal hyper- or hypointense voxels for both NHP Z and A (Figure 31 A). NHP A exhibited one case of unusual hyperintense voxels on a T2-weighted MRI scan after an alert FUS procedure on day 0 (i.e. the day of the procedure, Figure 31 B). The hyperintense voxels were not present on day 7, which suggests the potential for transient edema in NHP A when targeting the caudate. No hyper- or hypointense voxels were detected in the region of possible edema on SWI scans on either day 0 or day 7. These results show that the FUS technique has some probability to cause a reversible edema without microhemorrhaging in alert NHP. By comparison, during 12 anesthetized procedures, NHP A had 3 cases of hyperintense voxels on the T2-weighted scans on day 0. Similar to the alert experiments, the hyperintense voxels were not present on day 7. Histological evaluation was not conducted on NHP A as he was required for further experiments.

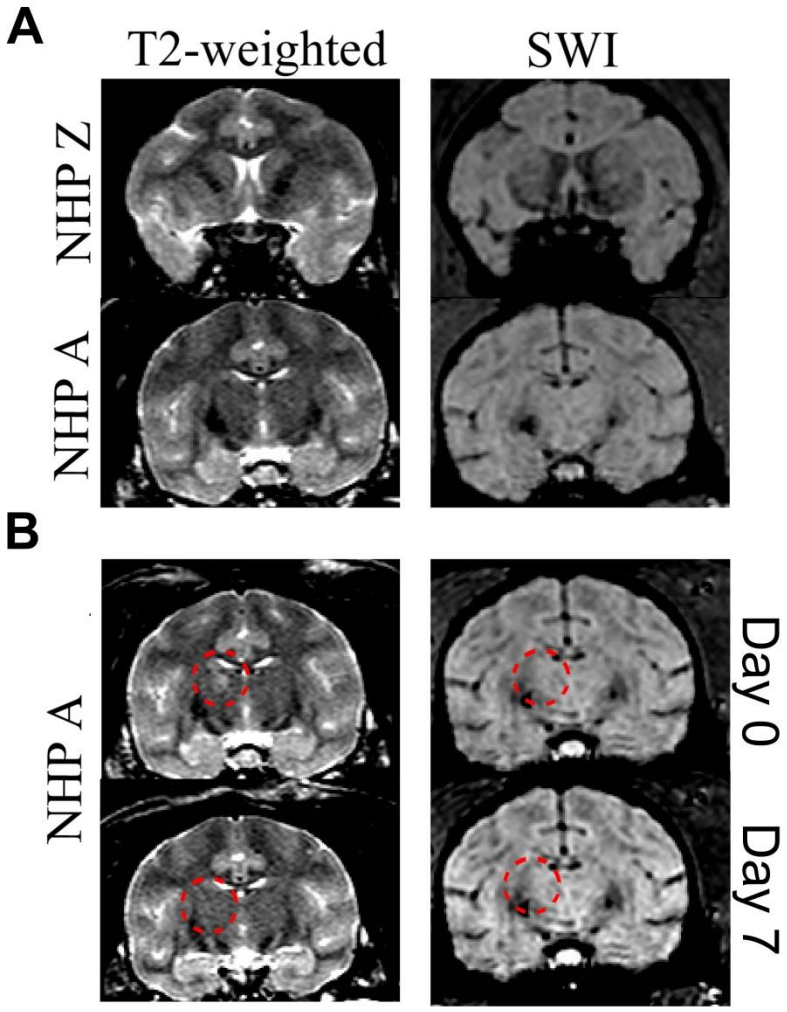

Figure 31: MRI Safety Verification in Alert Non-Human Primates. T2-weighted and SWI sequences were acquired to verify the safety of the alert FUS procedures. A) shows typical cases of both T2-weighted and SWI scans of the targeted regions. There were no abnormal hyper or hypointense voxels present in any of the targeted regions (caudate, putamen or thalamus). B) shows the one case for NHP A when there were hyperintense voxels in the targeted region in the T2-weighted scan, denoted by the red dashed circle. This area of hyperintense voxels could indicate the presence of edema. By day 7 the hyperintense voxels were absent. Neither on day 0 or 7 were any hyper or hypointense voxels detected in the target regions of the SWI scans.

BBB Opening

Post contrast T1-weighted MRI sequences verified BBB opening for the majority of the alert FUS procedures on NHP A & Z. Typical cases of BBB opening are indicated by a transparent red color map overlaid on the T1-weighted MRI scans shown in Figure 32. The contrast enhanced areas cover the targeted putamen region for NHP A and NHP Z. Successful BBB openings were obtained in 6/7 (NHP A) and 7/8 (NHP Z) alert FUS procedures. Figure 33 shows NHP A exhibiting larger BBB openings on average (526 ± 220 mm^3) than NHP Z (450 ± 97 mm^3) after alert FUS procedures. Success rate of BBB opening and the average of the BBB opening volumes per location and NHP are listed in Table 9. Both NHP showed on average 19% larger BBB opening volumes for the alert compared to anesthetized FUS procedures. Only NHP Z exhibited a significant increase in BBB opening volume for the alert compared to anesthetized procedures (WRS test, $p < 0.05$). Figure 34 shows a non-significant increase in the detected stable cavitation dose from the passive cavitation detection (PCD) for the alert procedures over the anesthetized procedures for both NHP (WRS test, $p > 0.05$). There was also a non-significant decrease in inertial cavitation dose between the alert and anesthetized procedures (t-test, $p > 0.05$).

Table 9: BBB opening per location for each NHP.

Target	NHP Z (Alert)	NHP A (Alert)	NHP Z (Anesthetized)	NHP A (Anesthetized)
Caudate	N/A	369 ± 225 mm^3 (n = 2/3)	N/A	N/A
Putamen	335 ± 150 mm^3 (n = 3/3)	657 ± 203 mm^3 (n = 3/3)	270 ± 75 mm^3 (n = 4/4)	500 ± 197 mm^3 (n = 9/12)
Thalamus	462 ± 110 mm^3 (n = 4/5)	442 mm^3 (n = 1/1)	N/A	

Averages volumes and standard deviations here reflect only when BBB opening was successful. The n values signify successful BBB opening/ Total FUS procedures at that location.

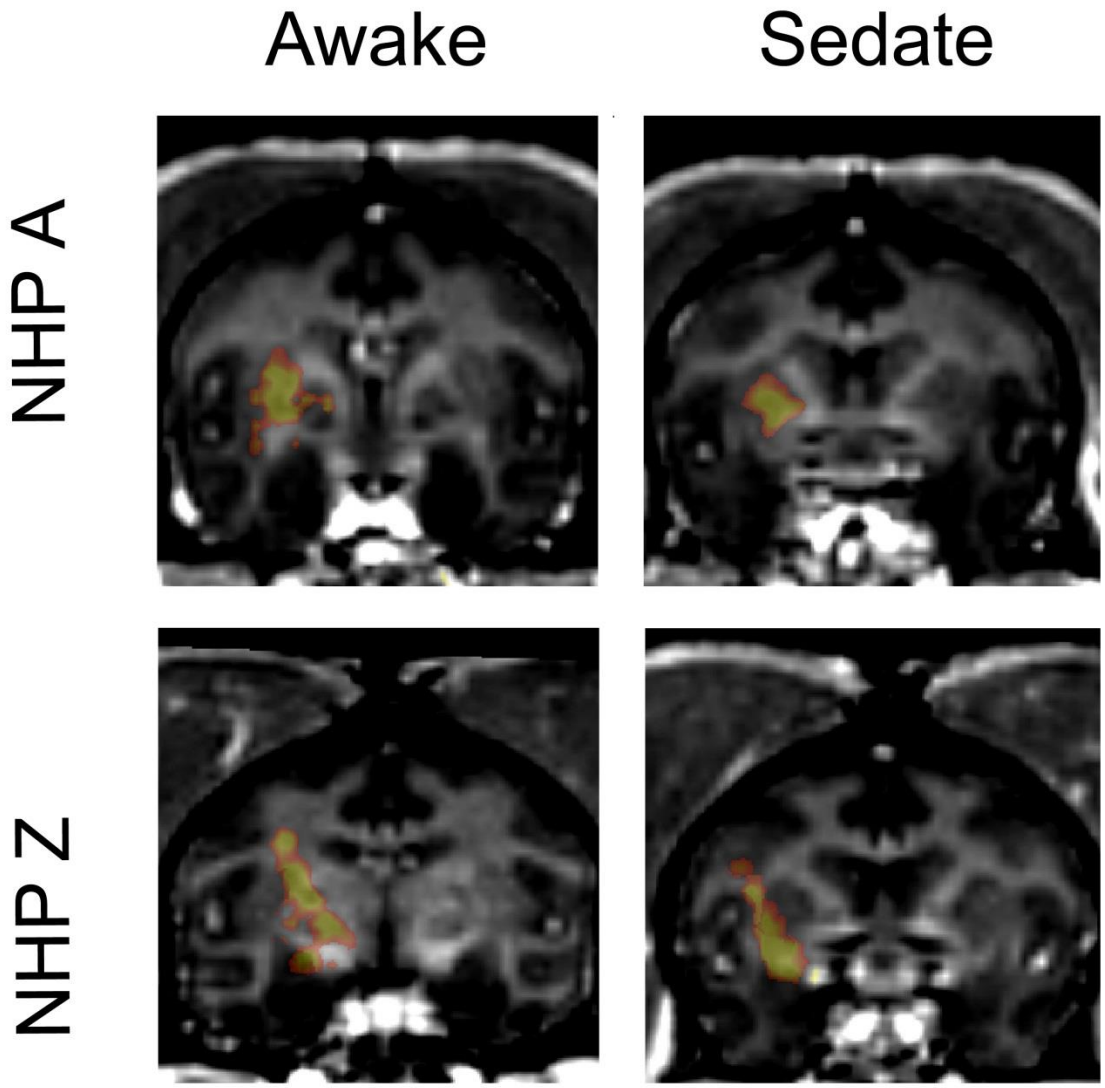

Figure 32: Blood-Brain Barrier Opening Verification in Alert Non-Human Primates. Contrast enhanced T1- weighted sequences were acquired to verify the opening of the BBB. The transparent red regions indicate the BBB opening volume. Typical cases of BBB opening for the alert FUS procedures are in the left column, while typical results from anesthetized FUS procedures are seen on the right column.

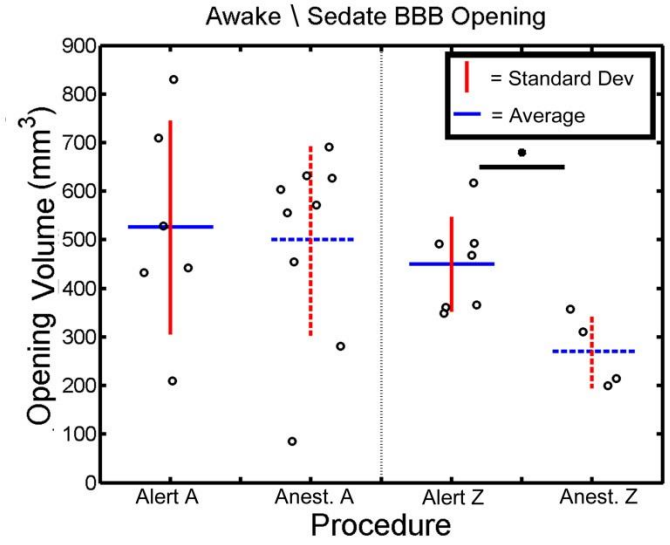

Figure 33: Alert vs Anesthetized Blood-Brain Barrier Volume. The average volume of BBB opening from the alert and anesthetized FUS technique are compared per animal. The mean is indicated with a blue horizontal bar while the standard deviation is indicated by a red vertical bar. The black circles are individual BBB opening cases. The dashed bars indicate anesthetized experiments. Both NHP had a non-significant increase in the volume of BBB opening for alert FUS procedures over anesthetized (2-sided WRS test, p = 0.012).

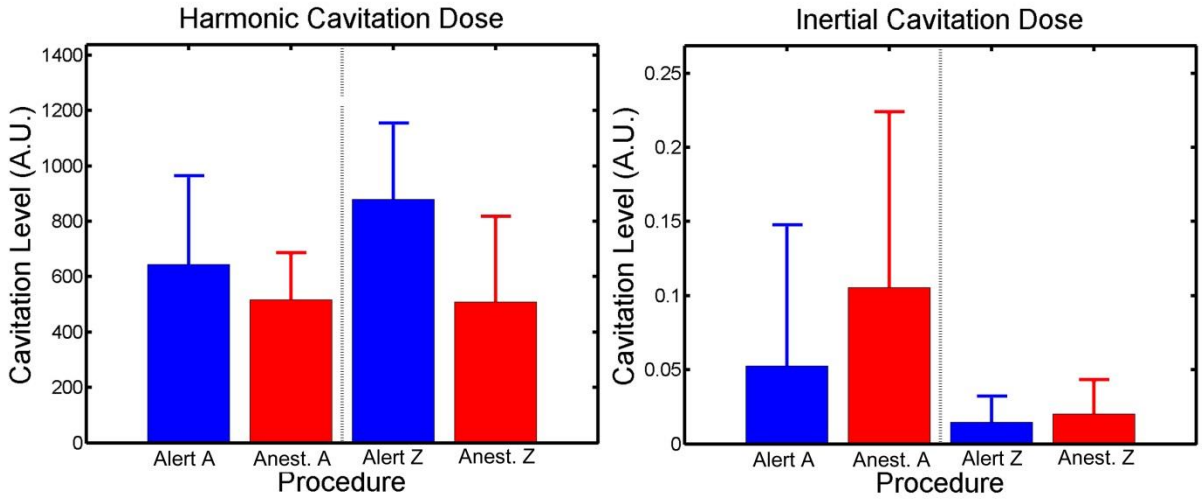

Figure 34: Cavitation Doses for Alert and Anesthetized Non-Human Primates. During both the alert and anesthetized FUS procedures the passive cavitation detection recorded the signals emitted from the MB in the focal area of the transducer. Blue bars indicate average cavitation

dosage and 95% confidence interval of the mean for alert FUS procedures while red indicates average cavitation dosage 95% confidence interval of the mean for anesthetized FUS procedures. A) shows the average harmonic cavitation doses while (B) shows the average inertial cavitation dosages. For both NHP there was a non-significant increase in harmonic cavitation doses between the alert and the anesthetized FUS procedures. The inverse occurred with the inertial cavitation dose with smaller doses detected during the alert compared to the anesthetized FUS procedures.

Behavioral Results:

To determine if the FUS procedure affected visuomotor behavior or motivation, the NHP were trained to perform a visually guided reaching task with differential reward. The RMB task completed by the NHP during the FUS technique was utilized as a more sensitive evaluation of the potential side effects of the technique on the central nervous system of the NHP. The behavioral variables recorded were reaction time (RT) and touch error (TE). Individual responses to the task for the control and experimental days are shown in Figure 29. On days when the FUS technique was administered, the NHP were given a low dose of ketamine for placement of the IV catheter prior to behavioral testing. This resulted in a slight anesthetic effect, which was observed in the behavioral results. The control data after ketamine shows elevated RTs at the beginning of each day's behavioral testing that decrease over the duration of the session (Figure 29 B). This decrease was not observed on days when the animal performed the task without any prior ketamine (Figure 29 A). Thus, this decrease along the entire duration of the behavioral task can be attributed to the lingering effects of the ketamine. As a control, on some days, the same low dose of ketamine used when placing the IV catheter was administered prior to behavioral testing, but the FUS technique was applied. Linear regression was performed on the ketamine control data and used to subtract out the effects of ketamine from the experimental data (days when the FUS

technique was applied, Figure 29 C). This normalization was performed with for RT and TE.

On each trial of the behavioral task, the NHP first touched a cue stimulus and then touched a target presented four cm away from the cue. One benchmark to determine if the FUS procedure had an effect on the NHP while they conducted the behavioral task was to evaluate their reaction times (RT) to the cue and target stimuli. The average RT to the cue and target are shown in Figure 35 A. NHP A did not show significant variation in the means between groups, nor significant difference between the pre- and during or post- and during groups (1-way ANOVA, student's t-test, $p > 0.05$). NHP Z did not show any significant difference across groups for the cue stimulus, but did show a significant increase between the pre-and during groups to the target (1-way ANOVA, student's t-test, $p < 0.01$). This increase persisted into the post-sonication period, which was not significantly different from the during group (student's t-test, $p > 0.05$). Overall, in three out of the four cases there was a slight decrease in reaction time after the application of the FUS procedure.

While variations in RT assess the speed of the visuomotor response, touch error (TE) can be used to detect variations in spatial accuracy of the reaching movement [180]. Touch error was determined as the distance between the center of the stimulus (cue or target) and the first point where the NHP contacted the touchscreen monitor. Figure 35 B shows that for NHP A there was a significant decrease in TE to the cue between the pre- and during groups, as well as between pre- and post groups (student's t-test, $p < 0.001$). This significant decrease in TE was also observed with the response of NHP A to the target stimuli. Similarly, there was a significant decrease in TE for NHP Z responding to the cue stimuli (student's t-test, $p < 0.01$).

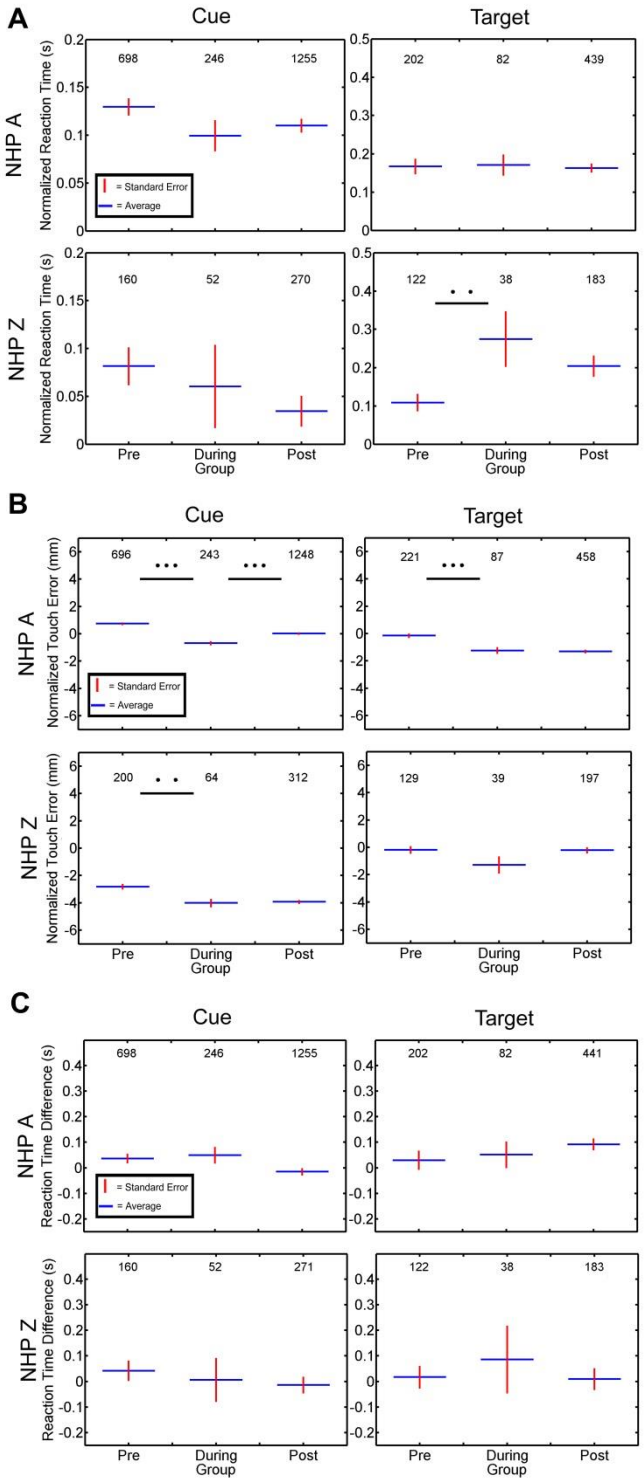

Figure 35: Behavioral Results after Focused Ultrasound Procedures in Alert Non-Human Primates. The responses to the behavioral task were measured in reaction time and touch error. A) Shows the average reaction time to the cue and target for each group (pre, during and post

FUS procedure). The horizontal blue bar indicates the average reaction time for each group while the red vertical bar indicates the standard error. There was a small non-significant decrease across the groups for both NHP reacting to the cue (2-sided student's t-test, $p > 0.05$). NHP A exhibits this decrease in reaction time across groups when responding to the target, but NHP Z shows a significant increase in reaction time to the target (2-sided student's t-test, $p = 0.013$). B) Shows the average touch error for each group. Blue horizontal bars indicate the average touch error while red vertical bars indicate the standard error. For both NHP there was a significant decrease in touch error between the pre- and the during group in response to the cue (2-sided student's t-test, $p < 0.01$). Only NHP A also exhibited a significant difference in touch error between the pre- and during groups to the target. C) Shows the difference in reaction time between the high and the low reward. Horizontal blue bars indicate the average difference in reaction time (high-low) while the red vertical bars indicate standard error.

Our behavioral task included a reward bias; on some trials, the NHP received 5 drops of water as a reward for correct performance. On other trials, the reward was 1 drop. A visual cue (the orientation of the cue and target stimuli) signaled the reward size. The reward value for each trial was random so the NHP could not predict which stimuli would appear next. Once the cue appeared, it informed the NHP as to the reward size. NHP will often respond faster and more accurately on trials with larger rewards [136, 142]. Hence, the reward bias can help to determine if motivation was affected by the FUS procedure. For both NHP there was no significant variation across all groups nor a significant change in RT difference between individual groups (1-way ANOVA, student's t-test, $p > 0.05$, Figure 35 C). This behavioral task has been previously employed in our lab and successfully elicited specific motivational responses to the high/low reward, but these results indicate that this did not occur during these experiments [19]. This lack of reward bias was also absent for the control data sets, and thus was not caused by the FUS technique.

5.5 Discussion

In this study, it was demonstrated that the FUS technique is a safe and effective procedure on alert NHP using MRI verification, physiological recordings and behavioral assessment. An 86% success rate for opening the BBB at the targeted regions was achieved and the volume of the BBB openings in alert NHP were 19% larger than openings achieved with anesthetized FUS procedures in the same NHP. The increase in BBB opening volume could be due to several factors. For example, the dosage of MB that reached the target area could have been larger during alert than anesthetized experiments. As oxygen mixed with 1.1-1.5% isoflurane was used for anesthesia during the anesthetized experiments, the MB would have a shorter circulation time as prior studies have shown that oxygen increases the decay rate of MB in the bloodstream by approximately a factor of three [178]. This would decrease the dosage of MB reaching the target site, and also decrease the overall PCD signal detected during the anesthetized procedures. An increase in stable cavitation dosage in alert subjects was not detected, which could be attributed to the higher MB dose. However, a decrease in the inertial cavitation dosage was observed. This finding agrees with prior studies where the diameter of the vessel has an effect on the behavior of the MB inside the focal area of the transducer. When the vessel diameter is larger than the MB size, inertial cavitation is the dominant mechanism for BBB opening, and conversely when the diameter of the vessel and the MB size are comparable, stable cavitation becomes the dominant mechanism [84]. As no isoflurane was used during the alert FUS procedures, the vessels would not have been dilated, retaining their average size of 5 μm, which is comparable to the 4-5 μm diameter MB used for the experiments [169]. This would support the results showing an increased stable cavitation dosage and a decreased inertial cavitation dosage during the alert compared to the anesthetized FUS procedures. Another factor that could have potentially altered the MB dosage was the

cerebral blood flow (CBF). High doses of isoflurane have been correlated with higher CBF, which would produce larger PCD signals as more MB would be passing through the focal region for each ultrasound pulse. This increase in CBF was previously observed at isoflurane doses > 1.6% [173]. For the anesthetized experiments, NHP were only initially dosed with 2% isoflurane for placement into the stereotax before being reduced to 1.1-1.5% for the duration of the experiment. Thus in the previous anesthetized FUS procedures, the level of isoflurane needed to increase the CBF may not have been reached. The increase in stable cavitation dosage during FUS procedures with alert NHP could be attributed to a larger dose of MB, as circulation time was not reduced, as well as smaller vessel diameters that were comparable to MB diameter.

BBB opening was achieved safely (as assessed by T2-weighted MRI and SWI scans) for the majority (13/15) of the alert experiments with only one case of potential edema (out of 7 procedures) in NHP A, which resolved within a week. This was a decrease in the occurrence of hyperintense voxels appearing in the targeted region for NHP A compared to anesthetized experiments when it occurred 3 times in 12 procedures. These findings are concordant with the decrease in inertial cavitation dosage recorded during the alert FUS procedures. Prior studies have shown a correlation between inertial cavitation with edema and red blood cell extravasation [16, 13]. The inertial cavitation dosage was lower in the alert FUS procedures, which explains the less frequent occurrence of edema. Overall, the results show that the alert FUS procedure elicited fewer cases of potential edema on average than prior anesthetized studies.

Importantly, the procedure did not elicit any gross negative physiological reactions (ballistic motor activity, pain grimace) while the NHP were completing the behavioral task. Their heart rate remained consistent before, during and after the application of the FUS technique. EMG data also revealed no abnormal muscle activity

in the local area of the transducer during the procedure. This lack of abnormal EMG signals shows that the FUS technique does not elicit muscle activity in the local area of application.

The FUS procedure was administered during ongoing performance of a self-paced visuomotor reacting task. There was no disruption in the NHP's behavior once the task had begun. The NHP continued to initiate trials at the same rate before, during and after FUS administration. A small, non-significant decrease in reaction time to the cue stimuli was observed after the application of the FUS technique. The procedure also significantly decreased touch error by reducing the average touch error between the pre- and during group for both the cue and target stimuli for NHP A. Another FUS-based technique, transcranial-FUS (tFUS), is currently being investigated as an alternative to transcranial magnetic stimulation and has been shown to successfully elicit neuromodulation in partially sedate and alert NHP and humans [31, 32]. Although tFUS utilizes different transducer parameters (pressure, pulse repetition frequency, duration of sonication) than the FUS BBB opening technique, the results show the FUS technique targeting the basal ganglia and thalamus has the potential for small beneficial effects improving the accuracy of the NHP selecting the targets present on the screen.

5.6 Conclusions

This initial feasibility and safety study verifies the FUS technique was slightly safer and more effective than prior anesthetized experiments with a potential beneficial decrease in reaction time and an increase in tactile accuracy. Results obtained agree with the literature on how modifying the parameters of the FUS technique affect the safety and success of the procedure. This technique will be continued to be investigated as a powerful tool in the lab as it transitions as a therapeutic technique in the clinic.

5.7 Contributions

Results presented here in chapter 5 continue to demonstrate the FUS technique could be a powerful tool in both the clinic and the laboratory. Traditionally the technique had only been conducted in anesthetized *in vivo* models, but here for the first time the results demonstrate the technique can be safe and effective in fully alert NHP. Moreover, the results show that the occurrence of BBB opening was safer and the average volume of BBB opening larger than in anesthetized models. During the application of the FUS technique NHP were not only able to continually respond to a visuomotor task presented to them, their responses improved. Average reaction time decreased while their touch error significantly decreased. The behavioral results combined with the MRI data validate the FUS technique is safe and effective in alert NHP.

Regarding the research contributions, Carlos Sierra Sanchez, PhD (Biomedical Engineering, Columbia University) assisted with the microbubble fabrication for experiments, Marilena Karakatsani, MS (Biomedical Engineering, Columbia University), assisted with the FUS experiments and the microbubble fabrication for experiments and Amanda Buch, BS (Biomedical Engineering, Columbia University) assisted with the FUS experiments.

Chapter Six

Impact

6.1 Conclusions

The current clinical techniques for drug delivery through the blood-brain barrier (BBB) can be effective for treating specific neurological diseases. Unfortunately, none of those approved techniques facilitates drug delivery with a method that is both non-invasive and brain target specific. Focused ultrasound with intravenous microbubbles (FUS) fills this vacancy as it transiently and non-invasively opens the BBB accurately at specific targets in the brain. While this technique has been investigated for fifteen years, it is now reaching the pre-clinical transition period before human testing begins.

The work presented in this thesis focused on validating the safety and efficacy of the FUS technique for both opening the BBB in NHP, and delivering drugs generating pharmacodynamical behavior effects. The majority of the experiments conducted here were with NHP, an ideal subject for pre-clinical testing. Results from the initial longitudinal study verified the FUS technique was both a safe and effective method to open the BBB at specific brain regions in the NHP without adverse long-term effects. The technique was then demonstrated to be effective in facilitating drug delivery, both large molecule or a low dose, to modulate behavior of the NHP. Finally, for the first time, the results illustrated that the FUS technique can be applied to alert NHP inducing safe BBB opening without macroscopic physiological changes.

The first section of this thesis explored the safety of the FUS technique through a longitudinal study spanning 4-20 months in four NHP. Results indicated there were no long-term degenerative effects of repeated application of the FUS technique targeting the putamen and caudate regions of the basal ganglia through MRI verification. Any

cases of potential edema were only transient and not persistent a week after occurrence. Behavioral testing indicated the FUS technique may have caused an increase in the reaction time on day 0 (the day when the FUS technique was performed), but this shift of behavioral responses returned to baseline within five days. Results in this section were important for validating the application of the FUS technique as a long-term therapeutic procedure. This technique may be used as an outpatient procedure for regular (i.e. biannually) drug delivery to specific brain regions to treat chronic neurological diseases such as Parkinson's or Alzheimer's. Here the results indicated that repeated targeting of a specific brain region does not elicit permanent structural or neurological changes, which is the first step in validating this technique for long-term clinical applications.

The second part of the thesis investigated utilizing the FUS technique for drug delivery to the basal ganglia. Domperidone was successfully delivered to the caudate in two NHP while haloperidol was successfully delivered to the putamen in NHP and the caudate-putamen in mice. As both drugs selected were D2 receptor antagonists, their effects were recorded during visuomotor (NHP) and simple motor (mice) behavioral tasks. Domperidone was shown to cause severe hemilateral neglect in 2/4 NHP on the side contralateral to the FUS procedure. This neglect persisted on average 40 minutes after onset and was not correlated with any permanent abnormal safety results. The successful delivery of domperidone demonstrates the FUS technique can deliver large molecule drugs through the BBB allowing for pharmacodynamical behavioral modulation. Haloperidol was also successfully delivered to the putamen region in NHP where it caused significant changes in the reaction time to the visually presented stimuli. Results from the NHP-haloperidol study illustrate the administration of a drug at a low dose while the BBB is opened at the intended region of drug-brain interaction can be as effective as a full dose of the drug nonspecifically crossing the native BBB.

Successful treatment with lower drug doses could alleviate adverse side effects with current drug therapies.

The final section of this thesis focused on a major hurdle of the pre-clinical transition period for the FUS technique of validating the procedure as a safe and effective procedure in alert subjects. The technique was applied to the basal ganglia and thalamus region of two alert NHP while they completed a visuomotor behavioral task. As the FUS procedures were conducted without isoflurane, there were no vasodilatory effects as seen with prior anesthetized procedures. This resulted in larger BBB opening sizes, as well as an increase in stable cavitation dose, while decreasing the inertial cavitation dose. This change in cavitation dose produced less cases of potential edema for the alert FUS procedures compared to the anesthetized procedures using the same FUS parameters. The FUS technique did not elicit any macroscopic abnormal behavioral effects. Conversely, it slightly improved reaction time and significantly reduced touch error during the FUS procedure. Results demonstrate that the FUS technique can be safely applied to alert subjects without the potential of negative side effects.

In conclusion, the work presented here continues to validate the FUS technique as a safe and effective technique for transient BBB opening in NHP. Safety and efficacy were demonstrated for long-term application in anesthetized subjects. The technique was also shown as an effective method for facilitating both large molecule, or low dose drug delivery allowing pharmacodynamical modulation of responses to behavioral tasks in both NHP and mice. Finally, both the safety and efficacy of the FUS technique were verified in alert subjects. Continued research utilizing the FUS technique will prove the technique to be a powerful tool assisting in the treatment of neurological diseases in the clinic.

6.2 Future work

Building from the findings presented here, the FUS technique can be used for drug delivery in alert NHP. This allows for targeted, non-invasive drug delivery during behavioral testing. Specifically, this technique could be coupled with electrophysiology studies investigating the neural activity of selected regions in response to the behavioral task.

Other potential investigations within the laboratory include utilizing the FUS technique to deliver drugs to a 6-hydroxdopamine (6-OHDA) NHP PD model. Targeted delivery of dopamine to affected areas of the 6-OHDA NHP while completing a behavioral task should demonstrate recovery of neurobehavioral deficits induced by the 6-OHDA. This would be a pivotal study demonstrating the FUS technique is well suited to facilitate treatment of diseases such as Parkinson's disease.

Building on the aforementioned project, the technique could be applied to open the BBB at the basal ganglia and substantia nigra in Parkinson's patients to deliver dopamine or other currently available drugs. Results from chapter 4 in this thesis demonstrate the successful delivery of large molecule drugs, thus the delivery of dopamine should be achievable in patients. Treatment of PD using dopamine instead of levodopa would reduce the potential for the development of adverse side effects such as dyskinesia.

References

1. Abbott, N. J. & Romero, I. A. Transporting therapeutics across the blood-brain barrier. *Molecular Medicine Today* **2,** 106–113 (1996).

2. Habgood, M. D., Begley, D. J. & Abbott, N. J. Determinants of passive drug entry into the central nervous system. *Cell. Mol. Neurobiol.* **20,** 231–253 (2000).

3. Pardridge, W. M. The blood-brain barrier: bottleneck in brain drug development. *NeuroRx* **2,** 3–14 (2005).

4. Pardridge, W. M. Drug targeting to the brain. *Pharm. Res.* **24,** 1733–1744 (2007).

5. Drago, F. *et al.* Dopamine neurotransmission in the nucleus accumbens may be involved in oxytocin-enhanced grooming behavior of the rat. *Pharmacol. Biochem. Behav.* **24,** 1185–1188 (1986).

6. Maurer, T. S., DeBartolo, D. B., Tess, D. A. & Scott, D. O. Relationship between exposure and nonspecific binding of thirty-three central nervous system drugs in mice. *Drug Metab. Dispos.* **33,** 175–181 (2005).

7. Alam, M. I. *et al.* Strategy for effective brain drug delivery. *European Journal of Pharmaceutical Sciences* **40,** 385–403 (2010).

8. World Health Organization, (2006). Neurological disorders public health challenges. Chapter 2, p32. ISBN 978 92 4 156336 9

9. Hynynen, K., McDannold, N., Vykhodtseva, N. & Jolesz, F. A. Noninvasive MR imaging-guided focal opening of the blood-brain barrier in rabbits. *Radiology* **220,** 640–646 (2001).

10. Choi, J. J., Pernot, M., Small, S. A. & Konofagou, E. E. Noninvasive, transcranial and localized opening of the blood-brain barrier using focused ultrasound in mice. *Ultrasound Med. Biol.* **33,** 95–104 (2007).

11. Xie, F. *et al.* Effects of Transcranial Ultrasound and Intravenous Microbubbles on Blood Brain Barrier Permeability in a Large Animal Model. *Ultrasound Med. Biol.* **34,** 2028–2034 (2008).

12. Tung, Y.-S., Marquet, F., Teichert, T., Ferrera, V. & Konofagou, E. E. Feasibility of noninvasive cavitation-guided blood-brain barrier opening using focused ultrasound and microbubbles in nonhuman primates. *Appl. Phys. Lett.* **98,** 163704 (2011).

13. Tung, Y.-S., Vlachos, F., Feshitan, J. A., Borden, M. A. & Konofagou, E. E. The mechanism of interaction between focused ultrasound and microbubbles in blood-brain barrier opening in mice. *The Journal of the Acoustical Society of America* **130,** 3059 (2011).

14. Samiotaki, G., Vlachos, F., Tung, Y.-S. & Konofagou, E. E. A quantitative pressure and microbubble-size dependence study of focused ultrasound-induced blood-brain barrier opening reversibility in vivo using MRI. *Magn. Reson. Med.* **67,** 769–77 (2012).

15. Marquet, F. *et al.* Real-time, transcranial monitoring of safe blood-brain barrier opening in non-human primates. *PLoS One* **9,** e84310 (2014).

16. McDannold, N., Arvanitis, C. D., Vykhodtseva, N. & Livingstone, M. S. Temporary Disruption of the Blood-Brain Barrier by Use of Ultrasound and Microbubbles: Safety and Efficacy Evaluation in Rhesus Macaques. *Cancer Research* **72,** 3652–3663 (2012).

17. Tung, Y.-S. *et al.* In vivo transcranial cavitation threshold detection during ultrasound-induced blood-brain barrier opening in mice. *Phys. Med. Biol.* **55,** 6141–6155 (2010).

18. Wu, S. Y. *et al.* Transcranial cavitation detection in primates during blood-brain barrier opening-a performance assessment study. *IEEE Trans. Ultrason. Ferroelectr. Freq. Control* **61,** 966–978 (2014).

19. Downs, M. E. *et al.* Long-Term Safety of Repeated Blood-Brain Barrier Opening via Focused Ultrasound with Microbubbles in Non-Human Primates Performing a Cognitive Task. *PLoS One* **10,** e0125911 (2015).

20. Olumolade O, Samiotaki G, Konofagou EE. Longitudinal Behavioral and Motor Control Studies of Repeated Focused Ultrasound Induced Blood-Brain Barrier Openings in Mice. 3rd International symposium on Focused Ultrasound, Bethesda, MD, USA. (2012)

21. Samiotaki, G., Acosta, C., Wang, S. & Konofagou, E. E. Enhanced delivery and bioactivity of the neurturin neurotrophic factor through focused ultrasound—mediated blood–brain barrier opening in vivo. *J. Cereb. Blood Flow Metab.* **35,** 611–622 (2015).

22. Aryal, M., Vykhodtseva, N., Zhang, Y. Z., Park, J. & McDannold, N. Multiple treatments with liposomal doxorubicin and ultrasound-induced disruption of

blood-tumor and blood-brain barriers improve outcomes in a rat glioma model. *J. Control. Release* **169,** 103–111 (2013).

23. Alonso, A. *et al.* Focal Delivery of AAV2/1-transgenes Into the Rat Brain by Localized Ultrasound-induced BBB Opening. *Mol. Ther. Nucleic Acids* **2,** e73 (2013).

24. Jankovic, J. Parkinson's disease: clinical features and diagnosis. *J. Neurol. Neurosurg. Psychiatry* **79,** 368–376 (2008).

25. Obeso, J. A. *et al.* The evolution and origin of motor complications in Parkinson's disease. *Neurology* **55,** S13–S20; discussion S21–S23 (2000).

26. Middleton, F. A. & Strick, P. L. Basal ganglia and cerebellar loops: Motor and cognitive circuits. in *Brain Research Reviews* **31,** 236–250 (2000).

27. Pardridge, W. M. Blood-brain barrier delivery. *Drug Discovery Today* **12,** 54–61 (2007).

28. Mas, S. *et al.* Secondary nonmotor negative symptoms in healthy volunteers after single doses of haloperidol and risperidone: A double-blind, crossover, placebo-controlled trial. *Hum. Psychopharmacol.* **28,** 586–593 (2013).

29. Repantis, D., Laisney, O. & Heuser, I. Acetylcholinesterase inhibitors and memantine for neuroenhancement in healthy individuals: A systematic review. *Pharmacological Research* **61,** 473–481 (2010).

30. Jankovic, J. Management of motor side effects of chronic levodopa therapy. *Clin. Neuropharmacol.* **5 Suppl 1,** S19–S28 (1982).

31. Deffieux, T. *et al.* Low-Intensity Focused Ultrasound Modulates Monkey Visuomotor Behavior. *Current Biology* (2013). doi:10.1016/j.cub.2013.10.029

32. Legon, W. *et al.* Transcranial focused ultrasound modulates the activity of primary somatosensory cortex in humans. *Nat. Neurosci.* **17,** 322–9 (2014).

33. Abbott, N. J., Patabendige, A. A. K., Dolman, D. E. M., Yusof, S. R. & Begley, D. J. Structure and function of the blood-brain barrier. *Neurobiology of Disease* **37,** 13–25 (2010).

34. Golden, P. L. & Pollack, G. M. Blood-brain barrier efflux transport. *Journal of Pharmaceutical Sciences* **92,** 1739–1753 (2003).

35. Ballabh, P., Braun, A. & Nedergaard, M. The blood-brain barrier: An overview: Structure, regulation, and clinical implications. *Neurobiology of Disease* **16,** 1–13 (2004).

36. Abbott, N. J. Blood-brain barrier structure and function and the challenges for CNS drug delivery. *Journal of Inherited Metabolic Disease* **36,** 437–449 (2013).

37. Knowland, D. *et al.* Stepwise Recruitment of Transcellular and Paracellular Pathways Underlies Blood-Brain Barrier Breakdown in Stroke. *Neuron* **82,** 603–617 (2014).

38. Pardridge, W. M. Drug transport across the blood-brain barrier. *J. Cereb. Blood Flow Metab.* **32,** 1959–72 (2012).

39. Cloughesy, T. F. & Black, K. L. Pharmacological blood-brain barrier modification for selective drug delivery. *J. Neurooncol.* **26,** 125–132 (1995).

40. Pavan, B. *et al.* Progress in drug delivery to the central nervous system by the prodrug approach. *Molecules* **13,** 1035–1065 (2008).

41. Anand, B. S., Dey, S. & Mitra, A. K. Current prodrug strategies via membrane transporters/receptors. *Expert Opin. Biol. Ther.* **2,** 607–620 (2002).

42. Slattery, D. A. & Neumann, I. D. Chronic icv oxytocin attenuates the pathological high anxiety state of selectively bred Wistar rats. *Neuropharmacology* **58,** 56–61 (2010).

43. Broadwell, R. D., Salcman, M. & Kaplan, R. S. Morphologic effect of dimethyl sulfoxide on the blood-brain barrier. *Science* **217,** 164–166 (1982).

44. Saija, A., Princi, P., Trombetta, D., Lanza, M. & De Pasquale, A. Changes in the permeability of the blood-brain barrier following sodium dodecyl sulphate administration in the rat. *Exp. Brain Res.* **115,** 546–551 (1997).

45. Azmin, M. N., Stuart, J. F. & Florence, A. T. The distribution and elimination of methotrexate in mouse blood and brain after concurrent administration of polysorbate 80. *Cancer Chemother. Pharmacol.* **14,** 238–242 (1985).

46. Kaplitt, M. G. *et al.* Safety and tolerability of gene therapy with an adeno-associated virus (AAV) borne GAD gene for Parkinson's disease: an open label, phase I trial. *Lancet* **369,** 2097–2105 (2007).

47. Cosolo, W. C., Martinello, P., Louis, W. J. & Christophidis, N. Blood-brain barrier disruption using mannitol: time course and electron microscopy studies. *Am. J. Physiol.* **256,** R443–R447 (1989).

48. Simon, M. J., Kang, W. H., Gao, S., Banta, S. & Iii, B. M. TAT is not capable of transcellular delivery across an intact endothelial monolayer in vitro. *Ann. Biomed. Eng.* **39,** 394–401 (2011).

49. Dou, H. *et al.* Macrophage delivery of nanoformulated antiretroviral drug to the brain in a murine model of neuroAIDS. *J. Immunol.* **183,** 661–669 (2009).

50. Bartus, R. T. *et al.* Intravenous cereport (RMP-7) modifies topographic uptake profile of carboplatin within rat glioma and brain surrounding tumor, elevates platinum levels, and enhances survival. *J. Pharmacol. Exp. Ther.* **293,** 903–911 (2000).

51. Moriyama, E., Salcman, M. & Broadwell, R. D. Blood-brain barrier alteration after microwave-induced hyperthermia is purely a thermal effect: I. Temperature and power measurements. *Surg. Neurol.* **35,** 177–182 (1991).

52. Qiu, L.-B. *et al.* The role of protein kinase C in the opening of blood-brain barrier induced by electromagnetic pulse. *Toxicology* **273,** 29–34 (2010).

53. Yang, F. Y., Horng, S. C., Lin, Y. S. & Kao, Y. H. Association between contrast-enhanced MR images and blood-brain barrier disruption following transcranial focused ultrasound. *J. Magn. Reson. Imaging* **32,** 593–599 (2010).

54. Gynther, M. *et al.* Large neutral amino acid transporter enables brain drug delivery via prodrugs. *J. Med. Chem.* **51,** 932–936 (2008).

55. Gynther, M. *et al.* Glucose promoiety enables glucose transporter mediated brain uptake of ketoprofen and indomethacin prodrugs in rats. *J. Med. Chem.* **52,** 3348–3353 (2009).

56. Craft, S. *et al.* Intranasal insulin therapy for Alzheimer disease and amnestic mild cognitive impairment: a pilot clinical trial. *Arch. Neurol.* **69,** 29–38 (2012).

57. Wise, R. A. & Hoffman, D. C. Localization of drug reward mechanisms by intracranial injections. *Synapse* **10,** 247–263 (1992).

58. Ferguson, S. D., Foster, K. & Yamini, B. Convection-enhanced delivery for treatment of brain tumors. *Expert Rev. Anticancer Ther.* **7,** S79–S85 (2007).

59. Fleegal, M. A., Hom, S., Borg, L. K. & Davis, T. P. Activation of PKC modulates blood-brain barrier endothelial cell permeability changes induced by hypoxia and posthypoxic reoxygenation. *Am. J. Physiol. Heart Circ. Physiol.* **289,** H2012–H2019 (2005).

60. Kielian, T., Barry, B. & Hickey, W. F. CXC chemokine receptor-2 ligands are required for neutrophil-mediated host defense in experimental brain abscesses. *J. Immunol.* **166,** 4634–4643 (2001).

61. Sanovich, E. *et al.* Pathway across blood-brain barrier opened by the bradykinin agonist, RMP-7. *Brain Res.* **705,** 125–135 (1995).

62. Elliott, P. J. *et al.* Unlocking the blood-brain barrier: a role for RMP-7 in brain tumor therapy. *Exp. Neurol.* **141,** 214–224 (1996).

63. Nasrollahi, S. a, Taghibiglou, C., Azizi, E. & Farboud, E. S. Cell-penetrating peptides as a novel transdermal drug delivery system. *Chem. Biol. Drug Des.* **80,** 639–46 (2012).

64. Suhorutsenko, J. *et al.* Cell-penetrating peptides, PepFects, show no evidence of toxicity and immunogenicity in vitro and in vivo. *Bioconjug. Chem.* **22,** 2255–2262 (2011).

65. McDannold, N., Vykhodtseva, N., Jolesz, F. A. & Hynynen, K. MRI Investigation of the Threshold for Thermally Induced Blood-Brain Barrier Disruption and Brain Tissue Damage in the Rabbit Brain. *Magn. Reson. Med.* **51,** 913–923 (2004).

66. Kuo, Y. C. & Kuo, C. Y. Electromagnetic interference in the permeability of saquinavir across the blood-brain barrier using nanoparticulate carriers. *Int. J. Pharm.* **351,** 271–281 (2008).

67. Reinhard, M. *et al.* Blood-brain barrier disruption by low-frequency ultrasound. *Stroke* **37,** 1546–1548 (2006).

68. Christensen DA. Ultrasonic Bioinstrumentation. 1st edition. John Wiley & Sons; 1988

69. Berg, D. & Becker, G. Perspectives of B-mode transcranial ultrasound. *Neuroimage* **15,** 463–473 (2002).

70. Lindberg, F., Öhberg, F., Brodin, L. Å. & Grönlund, C. Assessment of intramuscular activation patterns using ultrasound M-mode strain. *J. Electromyogr. Kinesiol.* **23,** 879–885 (2013).

71. Markus, H. S. Transcranial Doppler ultrasound. *Br. Med. Bull.* **56,** 378–388 (2000).

72. ter Haar, G. Therapeutic applications of ultrasound. *Progress in Biophysics and Molecular Biology* **93,** 111–129 (2007).

73. Dogra, V. S., Zhang, M. & Bhatt, S. High-Intensity Focused Ultrasound (HIFU) Therapy Applications. *Ultrasound Clinics* **4,** 307–321 (2009).

74. Yoshizawa, S. *et al.* High intensity focused ultrasound lithotripsy with cavitating microbubbles. *Med. Biol. Eng. Comput.* **47,** 851–860 (2009).

75. Zhou, Y., Cui, J. & Deng, C. X. Dynamics of sonoporation correlated with acoustic cavitation activities. *Biophysical journal* **94,** L51–L53 (2008).

76. Maxwell, A. D. *et al.* Noninvasive Thrombolysis Using Pulsed Ultrasound Cavitation Therapy - Histotripsy. *Ultrasound Med. Biol.* **35,** 1982–1994 (2009).

77. Wu, J. & Nyborg, W. L. Ultrasound, cavitation bubbles and their interaction with cells. *Advanced Drug Delivery Reviews* **60,** 1103–1116 (2008).

78. Chen, H., Li, X. & Wan, M. The inception of cavitation bubble clouds induced by high-intensity focused ultrasound. *Ultrasonics* **44,** (2006).

79. Ikeda, T. *et al.* Cloud cavitation control for lithotripsy using high intensity focused ultrasound. *Ultrasound Med. Biol.* **32,** 1383–1397 (2006).

80. Ikeda, M. *et al.* Quantitative analysis of hyperosmotic and hypothermic blood-brain barrier opening. *Acta Neurochir. Suppl.* **86,** 559–563 (2003).

81. Callahan, M. J., Kinsora, J. J., Harbaugh, R. E., Reeder, T. M. & Davis, R. E. Continuous ICV infusion of scopolamine impairs sustained attention of rhesus monkeys. *Neurobiol. Aging* **14,** 147–151 (1993).

82. Tamai, I. & Tsuji, A. Transporter-mediated permeation of drugs across the blood-brain barrier. *Journal of Pharmaceutical Sciences* **89,** 1371–1388 (2000).

83. Sheikov, N., McDannold, N., Sharma, S. & Hynynen, K. Effect of Focused Ultrasound Applied With an Ultrasound Contrast Agent on the Tight Junctional Integrity of the Brain Microvascular Endothelium. *Ultrasound Med. Biol.* **34,** 1093–1104 (2008).

84. McDannold, N., Vykhodtseva, N. & Hynynen, K. Targeted disruption of the blood-brain barrier with focused ultrasound: association with cavitation activity. *Phys. Med. Biol.* **51,** 793–807 (2006).

85. Salgaonkar, V. A., Datta, S., Holland, C. K. & Mast, T. D. Passive cavitation imaging with ultrasound arrays. *J. Acoust. Soc. Am.* **126,** 3071–3083 (2009).

86. Arvanitis, C. D., Livingstone, M. S., Vykhodtseva, N. & McDannold, N. Controlled Ultrasound-Induced Blood-Brain Barrier Disruption Using Passive Acoustic Emissions Monitoring. *PLoS One* **7,** (2012).

87. T. Kodama and Y. Tomita, "Cavitation bubble behavior and bubble-shock wave interaction near a gelatin surface as a study of in vivo bubble dynamics," *Appl. Phys. B Lasers Opt.*, vol. 70, no. 1, pp. 139–149, Jan. 2000.

88. Yang, F.-Y. *et al.* Micro-SPECT/CT-based pharmacokinetic analysis of 99mTc-diethylenetriaminepentaacetic acid in rats with blood-brain barrier disruption induced by focused ultrasound. *J. Nucl. Med.* **52,** 478–484 (2011).

89. Cho, E. E., Drazic, J., Ganguly, M., Stefanovic, B. & Hynynen, K. Two-photon fluorescence microscopy study of cerebrovascular dynamics in ultrasound-induced blood-brain barrier opening. *J. Cereb. Blood Flow Metab.* **31,** 1852–1862 (2011).

90. Ayaz, M., Boikov, A. S., Haacke, E. M., Kido, D. K. & Kirsch, W. M. Imaging cerebral microbleeds using susceptibility weighted imaging: One step toward detecting vascular dementia. *J. Magn. Reson. Imaging* **31,** 142–148 (2010).

91. Smith, a. S. *et al.* Magnetic resonance with marked T2-weighted images: Improved demonstration of brain lesions, tumor, and edema. *Am. J. Roentgenol.* **145,** 949–955 (1985).

92. Raymond, S. B. *et al.* Ultrasound enhanced delivery of molecular imaging and therapeutic agents in Alzheimer's disease mouse models. *PLoS One* **3,** (2008).

93. Liu, H.-L. *et al.* Blood-brain barrier disruption with focused ultrasound enhances delivery of chemotherapeutic drugs for glioblastoma treatment. *Radiology* **255,** 415–425 (2010).

94. Hsu, P.-H. *et al.* Noninvasive and targeted gene delivery into the brain using microbubble-facilitated focused ultrasound. *PLoS One* **8,** e57682 (2013).

95. Zeng, H.-Q., Lü, L., Wang, F., Luo, Y. & Lou, S.-F. Focused ultrasound-induced blood-brain barrier disruption enhances the delivery of cytarabine to the rat brain. *J. Chemother.* **24,** 358–63 (2012).

96. Park, E. J., Zhang, Y. Z., Vykhodtseva, N. & McDannold, N. Ultrasound-mediated blood-brain/blood-tumor barrier disruption improves outcomes with trastuzumab in a breast cancer brain metastasis model. *J. Control. Release* **163,** 277–284 (2012).

97. Kinoshita, M., McDannold, N., Jolesz, F. A. & Hynynen, K. Targeted delivery of antibodies through the blood-brain barrier by MRI-guided focused ultrasound. *Biochem. Biophys. Res. Commun.* **340,** 1085–1090 (2006).

98. Jordão, J. F. *et al.* Amyloid-β plaque reduction, endogenous antibody delivery and glial activation by brain-targeted, transcranial focused ultrasound. *Exp. Neurol.* **248,** 16–29 (2013).

99. Liu, H.-L. *et al.* In vivo MR quantification of superparamagnetic iron oxide nanoparticle leakage during low-frequency-ultrasound-induced blood-brain barrier opening in swine. *J. Magn. Reson. Imaging* **34,** 1313–24 (2011).

100. Etame, A. B. *et al.* Enhanced delivery of gold nanoparticles with therapeutic potential into the brain using MRI-guided focused ultrasound. *Nanomedicine Nanotechnology, Biol. Med.* **8,** 1133–1142 (2012).

101. Baseri, B. *et al.* Activation of signaling pathways following localized delivery of systemically administered neurotrophic factors across the blood–brain barrier using focused ultrasound and microbubbles. *Physics in Medicine and Biology* **57,** N65–N81 (2012).

102. Wang, F. *et al.* Targeted Delivery of GDNF through the Blood-Brain Barrier by MRI-Guided Focused Ultrasound. *PLoS One* **7,** (2012).

103. Burgess, A. *et al.* Targeted delivery of neural stem cells to the brain using MRI-guided focused ultrasound to disrupt the blood-brain barrier. *PLoS One* **6,** (2011).

104. McDannold, N,. *et al* Targeted, non-invasive blockade of cortical neuronal activity via ultrasound-induced blood-brain barrier disruption and intravenous GABA. *15th annual International Symposium on Therapeutic Ultrasound.* (2015)

105. Brown, L. L., Schneider, J. S. & Lidsky, T. I. Sensory and cognitive functions of the basal ganglia. *Current Opinion in Neurobiology* **7,** 157–163 (1997).

106. Graybiel, A. M., Aosaki, T., Flaherty, A. W. & Kimura, M. The basal ganglia and adaptive motor control. *Science* **265,** 1826–1831 (1994).

107. Groenewegen, H. J. The basal ganglia and motor control. *Neural Plast.* **10,** 107–120 (2003).

108. Hikosaka, O. Role of basal ganglia in control of innate movements, learned behavior and cognition – a hypothesis. *Advances in Behavioral Biology*, *41*, 589-596 (1994)

109. Meyer, J. H. *et al.* Elevated putamen D-2 receptor binding potential in major depression with motor retardation: An [C-11] raclopride positron emission tomography study. *Am. J. Psychiatry* **163,** 1594–1602 (2006).

110. Charntikov, S. *et al.* Importance of D1 and D2 receptors in the dorsal caudate-putamen for the locomotor activity and stereotyped behaviors of preweanling rats. *Neuroscience* **183,** 121–133 (2011).

111. Lauwereyns, J., Watanabe, K., Coe, B. & Hikosaka, O. A neural correlate of response bias in monkey caudate nucleus. *Nature* **418,** 413–417 (2002).

112. Seger, C. A. & Cincotta, C. M. The roles of the caudate nucleus in human classification learning. *J. Neurosci.* **25,** 2941–2951 (2005).

113. Herrero, M. T., Barcia, C. & Navarro, J. M. Functional anatomy of thalamus and basal ganglia. *Child's Nervous System* **18,** 386–404 (2002).

114. Schlag-Rey, M. & Schlag, J. Visuomotor functions of central thalamus in monkey. I. Unit activity related to spontaneous eye movements. *J. Neurophysiol.* **51,** 1149–1174 (1984).

115. Haber, S. N. & Calzavara, R. The cortico-basal ganglia integrative network: The role of the thalamus. *Brain Research Bulletin* **78,** 69–74 (2009).

116. Saalmann, Y. B. & Kastner, S. Cognitive and Perceptual Functions of the Visual Thalamus. *Neuron* **71,** 209–223 (2011).

117. Molnar, G. F., Pilliar, A., Lozano, A. M. & Dostrovsky, J. O. Differences in neuronal firing rates in pallidal and cerebellar receiving areas of thalamus in patients with Parkinson's disease, essential tremor, and pain. *J. Neurophysiol.* **93,** 3094–3101 (2005).

118. Halliday, G. M. Thalamic changes in Parkinson's disease. *Park. Relat. Disord.* **15,** (2009).

119. Hikosaka, O. Basal ganglia mechanisms of reward-oriented eye movement. in *Annals of the New York Academy of Sciences* **1104,** 229–249 (2007).

120. Lauwereyns, J. & Wisnewski, R. G. A reaction-time paradigm to measure reward-oriented bias in rats. *J. Exp. Psychol. Anim. Behav. Process.* **32,** 467–473 (2006).

121. Aspell, J. E., Tanskanen, T. & Hurlbert, A. C. Neuromagnetic correlates of visual motion coherence. *Eur. J. Neurosci.* **22,** 2937–2945 (2005).

122. De Bruyn, B. & Orban, G. A. Human velocity and direction discrimination measured with random dot patterns. *Vision Res.* **28,** 1323–1335 (1988).

123. Snowden, R. J. & Kavanagh, E. Motion perception in the ageing visual system: Minimum motion, motion coherence, and speed discrimination thresholds. *Perception* **35,** 9–24 (2006).

124. Nyberg, P., Nordberg, a., Wester, P. & Winblad, B. Dopaminergic deficiency is more pronounced in putamen than in nucleus caudatus in Parkinson's disease. *Neurochem. Pathol.* **1,** 193–202 (1983).

125. Feshitan, J. A., Chen, C. C., Kwan, J. J. & Borden, M. A. Microbubble size isolation by differential centrifugation. *J. Colloid Interface Sci.* **329,** 316–324 (2009).

126. Jenkinson, M., Beckmann, C. F., Behrens, T. E. J., Woolrich, M. W. & Smith, S. M. FSL. *NeuroImage* **62,** 782–790 (2012).

127. Hom, G.J., *et al.* Comparison of cardiovascular parameters and/or serum chemistry and hematology profiles in conscious and anesthetized rhesus monkeys (*Macaca mulatta)*. *Contemp Top Lab Anim Sci 38*(2): 60-64 (1999)

128. Pratt PW. Principles and practice of Veterinary Technology. 1st ed. Mosby INC; 1998.

129. Vlachos, F., Tung, Y.-S. & Konofagou, E. Permeability dependence study of the focused ultrasound-induced blood-brain barrier opening at distinct pressures and microbubble diameters using DCE-MRI. *Magn. Reson. Med.* **66,** 821–830 (2011).

130. Cheng, A. L. *et al.* Susceptibility-weighted imaging is more reliable than T2*-weighted gradient-recalled echo mri for detecting microbleeds. *Stroke* **44,** 2782–2786 (2013).

131. Ding, L. & Gold, J. I. Separate, Causal Roles of the Caudate in Saccadic Choice and Execution in a Perceptual Decision Task. *Neuron* **75,** 865–874 (2012).

132. Whishaw, I. Q., O'Connor, W. T. & Dunnett, S. B. The contributions of motor cortex, nigrostriatal dopamine and caudate-putamen to skilled forelimb use in the rat. *Brain* **109 (Pt 5,** 805–843 (1986).

133. Lonsdorf, E. V & Hopkins, W. D. Wild chimpanzees show population-level handedness for tool use. *Proc. Natl. Acad. Sci. U. S. A.* **102,** 12634–12638 (2005).

134. Shen, Y.-C. & Franz, E. A. Hemispheric competition in left-handers on bimanual reaction time tasks. *J. Mot. Behav.* **37,** 3–9 (2005).

135. Wenzlaff, H., Bauer, M., Maess, B. & Heekeren, H. R. Neural characterization of the speed-accuracy tradeoff in a perceptual decision-making task. *J. Neurosci.* **31,** 1254–1266 (2011).

136. Tagliabue, M., Ferrigno, G. & Horak, F. Effects of Parkinson's disease on proprioceptive control of posture and reaching while standing. *Neuroscience* **158,** 1206–1214 (2009).

137. Bogacz, R. & Gurney, K. The basal ganglia and cortex implement optimal decision making between alternative actions. *Neural computation* **19,** 442–477 (2007).

138. Bogacz, R. in *Handbook of Reward and Decision Making* 373–397 (2009). doi:10.1016/B978-0-12-374620-7.00018-2

139. Gold, J. I. & Shadlen, M. N. The neural basis of decision making. *Annu. Rev. Neurosci.* **30,** 535–574 (2007).

140. Britten, K. H., Shadlen, M. N., Newsome, W. T. & Movshon, J. A. The analysis of visual motion: a comparison of neuronal and psychophysical performance. *J. Neurosci.* **12,** 4745–4765 (1992).

141. Pardridge, W. CNS drug design based on principles of blood-brain barrier transport. *J. Neurochem.* **70,** 1781–1792 (1998).

142. Reinke, A. *et al.* Haloperidol and clozapine, but not olanzapine, induces oxidative stress in rat brain. *Neurosci. Lett.* **372,** 157–160 (2004).

143. Barbui, C. & Saraceno, B. Low-dose neuroleptic therapy and extrapyramidal side effects in schizophrenia: An effect size analysis. *Eur. Psychiatry* **11,** 412–415 (1996).

144. Roy-Desruisseaux, J. *et al.* Domperidone-induced tardive dyskinesia and withdrawal psychosis in an elderly woman with dementia. *Ann. Pharmacother.* **45,** (2011).

145. Joshi, G. *et al.* Free radical mediated oxidative stress and toxic side effects in brain induced by the anti cancer drug adriamycin: insight into chemobrain. *Free Radic. Res.* **39,** 1147–1154 (2005).

146. Hornykiewicz, O. A brief history of levodopa. in *Journal of Neurology* **257,** (2010).

147. Contin, M. & Martinelli, P. Pharmacokinetics of levodopa. in *Journal of Neurology* **257,** (2010).

148. Jankovic, J. Management of motor side effects of chronic levodopa therapy. *Clin. Neuropharmacol.* **5 Suppl 1,** S19–S28 (1982).

149. Barone, J. A. Domperidone: A peripherally acting dopamine2-receptor antagonist. *Annals of Pharmacotherapy* **33,** 429–440 (1999).

150. Vella-Brincat, J. & Macleod, A. D. Haloperidol in palliative care. *Palliat. Med.* **18,** 195–201 (2004).

151. Freeze, B. S., Kravitz, A. V, Hammack, N., Berke, J. D. & Kreitzer, A. C. Control of basal ganglia output by direct and indirect pathway projection neurons. *J. Neurosci.* **33,** 18531–9 (2013).

152. Krafft, P. R. *et al.* Correlation between subacute sensorimotor deficits and brain edema in two mouse models of intracerebral hemorrhage. *Behav. Brain Res.* **264,** 151–160 (2014).

153. Charntikov, S., *et al*. Importance of D1 and D2 receptors in the dorsal caudate-putamen for the locomotor activity and stereotyped behaviors of preweanling rats. *Neuroscience*, *183*, 121–133. (2011).

154. Karakatsani, M.E., *et al.* Targeting effects on the volume and gray-to-white-matter ratio of the focused ultrasound induced blood-brain-barrier opening in non-human primates in vivo. *15th Annual International Symposium on Therapeutic Ultrasound* (2015)

155. Nordström, A. L., Farde, L. & Halldin, C. Time course of D2-dopamine receptor occupancy examined by PET after single oral doses of haloperidol. *Psychopharmacology (Berl).* **106,** 433–438 (1992).

156. Kreitzer, A. C. & Malenka, R. C. Striatal Plasticity and Basal Ganglia Circuit Function. *Neuron* **60,** 543–554 (2008).

157. McOmish, C. E., Lira, A., Hanks, J. B. & Gingrich, J. A. Clozapine-Induced Locomotor Suppression is Mediated by 5-HT2A Receptors in the Forebrain. *Neuropsychopharmacology* (2012). doi:10.1038/npp.2012.139

158. Wise, R. A. & Carlezon, W. A. Attenuation of the locomotor-sensitizing effects of the D2 dopamine agonist bromocriptine by either the D1 antagonist SCH 23390 or the D2 antagonist raclopride. *Synapse* **17,** 155–159 (1994).

159. Correa, M. *et al.* The adenosine A2A antagonist KF17837 reverses the locomotor suppression and tremulous jaw movements induced by haloperidol in rats: Possible relevance to parkinsonism. *Behav. Brain Res.* **148,** 47–54 (2004).

160. Zvezdochkina, N. V. *et al.* Locomotor responses and neuron excitability in conditions of haloperidol blockade of dopamine in invertebrates and vertebrates. *Neurosci. Behav. Physiol.* **36,** 21–27 (2006).

161. Wickelgren, W. A. Speed-accuracy tradeoff and information processing dynamics. *Acta Psychologica* **41,** 67–85 (1977).

162. Bogacz, R., Wagenmakers, E. J., Forstmann, B. U. & Nieuwenhuis, S. The neural basis of the speed-accuracy tradeoff. *Trends in Neurosciences* **33,** 10–16 (2010).

163. Conceição, I. M. & Frussa-Filho, R. Effects of microgram doses of haloperidol on open-field behavior in mice. *Pharmacol. Biochem. Behav.* **53,** 833–838 (1996).

164. Laduron, P. M. & Leysen, J. E. Domperidone, a specific in vitro dopamine antagonist, devoid of in vivo central dopaminergic activity. *Biochem. Pharmacol.* **28,** 2161–2165 (1979).

165. Goikolea, J. M. *et al.* Faster onset of antimanic action with haloperidol compared to second-generation antipsychotics. A meta-analysis of randomized clinical trials in acute mania. *Eur. Neuropsychopharmacol.* **23,** 305–316 (2013).

166. Valentim, A. M., Alves, H. C., Olsson, I. A. S. & Antunes, L. M. The effects of depth of isoflurane anesthesia on the performance of mice in a simple spatial learning task. *J. Am. Assoc. Lab. Anim. Sci.* **47,** 16–19 (2008).

167. Wiklund, A. *et al.* Sevoflurane anesthesia alters exploratory and anxiety-like behavior in mice lacking the beta2 nicotinic acetylcholine receptor subunit. *Anesthesiology* **109,** 790–798 (2008).

168. Schwinn, D. A., McIntyre, R. W. & Reves, J. G. Isoflurane-induced vasodilation: role of the alpha-adrenergic nervous system. *Anesth. Analg.* **71,** 451–459 (1990).

169. Gelman, S., Fowler, K. C. & Smith, L. R. Regional blood flow during isoflurane and halothane anesthesia. *Anesth. Analg.* **63,** 557–565 (1984).

170. Weber, B., Keller, A. L., Reichold, J. & Logothetis, N. K. The microvascular system of the striate and extrastriate visual cortex of the macaque. *Cereb. Cortex* **18,** 2318–2330 (2008).

171. Li, C. X., Patel, S., Auerbach, E. J. & Zhang, X. Dose-dependent effect of isoflurane on regional cerebral blood flow in anesthetized macaque monkeys. *Neurosci. Lett.* **541,** 58–62 (2013).

172. Li, C.X., Patel, S., Wang, D.J.J., Zhang, Z., Effects of high dose isoflurane on cerebral blood flow in macaque monkeys. *Magnetic Resonance Imaging* **32,** 956-960 (2014).

173. Nyborg, W. L. Biological effects of ultrasound: Development of safety guidelines. Part II: General review. *Ultrasound Med. Biol.* **27,** 301–333 (2001).

174. Tung, Y. S., Choi, J. J., Baseri, B. & Konofagou, E. E. Identifying the inertial cavitation threshold and skull effects in a vessel phantom using focused ultrasound and microbubbles. *Ultrasound Med. Biol.* **36,** 840–852 (2010).

175. Chen, H. & Konofagou, E. E. The size of blood-brain barrier opening induced by focused ultrasound is dictated by the acoustic pressure. *J. Cereb. blood flow Metab.* **34,** 1197–204 (2014).

176. Liu, H.-L. *et al.* Hemorrhage detection during focused-ultrasound induced blood-brain-barrier opening by using susceptibility-weighted magnetic resonance imaging. *Ultrasound Med. Biol.* **34,** 598–606 (2008).

177. Itani, M. & Mattrey, R. F. The effect of inhaled gases on ultrasound contrast agent longevity in vivo. *Mol. Imaging Biol.* **14,** 40–46 (2012).

178. De Luca, C. J. The use of surface electromyography in biomechanics. in *Journal of Applied Biomechanics* **13,** 135–163 (1997).

179. Gordon, J., Ghilardi, M. F. & Ghez, C. Impairments of reaching movements in patients without proprioception. I. Spatial errors. *J. Neurophysiol.* **73,** 347–360 (1995).

Appendix 1: List of Publications and Conference Presentations/Proceedings

Publications

1. **Downs, M. E.** *et al.* Blood-Brain Barrier Opening in Behaving Non-Human Primates via Focused Ultrasound with Systemically Administered Microbubbles. *Scientific Reports* (submitted).
2. **Downs, M. E.** *et al.* Long-Term Safety of Repeated Blood-Brain Barrier Opening via Focused Ultrasound with Microbubbles in Non-Human Primates Performing a Cognitive Task. *PLoS One* **10,** e0125911 (2015).
3. Wu, S. Y., Tung, Y-S., Marquet, F., **Downs M.E.,** *et al* Transcranial cavitation detection in primates during blood-brain barrier opening-a performance assessment study. *IEEE Trans. Ultrason. Ferroelectr. Freq. Control* **61,** 966–978 (2014).
4. Marquet, F., Teichert, T.*, Wu, S-Y., Tung, Y-S., **Downs M.E.** *et al.* Real-time, transcranial monitoring of safe blood-brain barrier opening in non-human primates. *PLoS One* **9,** (2014).
5. Sunagawa, T., Tanahashi, A., **Downs, M. E**., Hess, H. & Nitta, T. In silico evolution of guiding track designs for molecular shuttles powered by kinesin motors. *Lab Chip* **13,** 2827–33 (2013).
6. Young, Y. N., **Downs, M.** & Jacobs, C. R. Dynamics of the primary cilium in shear flow. *Biophys. J.* **103,** 629–639 (2012).

7. **Downs, M. E.**, Nguyen, A. M., Herzog, F. A., Hoey, D. A. & Jacobs, C. R. An experimental and computational analysis of primary cilia deflection under fluid flow. *Computer Methods in Biomechanics and Biomedical Engineering* 1–9 (2012). doi:10.1080/10255842.2011.653784
8. Hoey, D. A., **Downs, M. E.** & Jacobs, C. R. The mechanics of the primary cilium: An intricate structure with complex function. *Journal of Biomechanics* **45,** 17–26 (2012).
9. Luria, I., Crenshaw, J., **Downs M.E.,** *et al.* Microtubule nanospool formation by active self-assembly is not initiated by thermal activation. *Soft Matter* **7,** 3108 (2011).

Selected Conference Presentations / Proceedings

1. Non-Invasive Focused Ultrasound Mediated Blood-Brain Barrier Opening in Awake Non-Human Primates. **Matthew E. Downs**, Amanda M. Buch, Marilena E. Karakatsani, Elisa E. Konofagou, Vincent P. Ferrera. 15th International Symposium on Therapeutic Ultrasound (Utrecht, Netherlands), April 15 to 18, 2015. Outstanding Presentation and Student Travel Award Recipient.

2. Non-invasive focused ultrasound blood-brain barrier opening in awake non-human primates. **Matthew E. Downs**, Amanda M. Buch, Marilena E. Karakatsani, Vincent P. Ferrera, Elisa E. Konofagou. Cold Spring Harbor Laboratory Meeting: The Blood-Brain Barrier (Cold Spring Harbor, NY, USA), December 10 to 13, 2014

3. Behavioral effects of targeted drug delivery via non-invasive microbubble enhanced focused ultrasound blood brain barrier opening in non-human primates. **Matthew E. Downs**, Amanda M. Buch, Marilena E. Karakatsani, Carlos J. Sierra Sánchez, Shangshang Chen, Vincent P. Ferrera, Elisa E. Konofagou. 4th

International Symposium on Focused Ultrasound (Washington, DC, USA), October 12 to 16, 2014. Student Travel Award Recipient.

4. Behavioral Effects of Targeted Drug Delivery via Non-Invasive Focused Ultrasound Blood Brain Barrier Opening in Non-Human Primates. **Matthew E. Downs**, Amanda M. Buch, Carlos J. Sierra Sánchez, Marilena E. Karakatsani, Shangshang Chen, Elisa E. Konofagou, Vincent P. Ferrera. 14th International Symposium on Therapeutic Ultrasound (Las Vegas, NV, USA), April 2 to 5, 2014

5. Minimally invasive ultrasound based drug delivery in the non-human primate. **Matthew E. Downs**, Tobias Teichert, Vincent P. Ferrera, Shih-Ying Wu, Elisa E. Konofagou. Neuroscience (San Diego, CA, USA) November 9 – 13 2013